Guilherme Mota Horta Morais

Licenciado em Ciências da Engenharia Química e Bioquímica

Dry powder formulations for antibiotic pulmonary delivery

Dissertação para obtenção do Grau de Mestre em
Engenharia Química e Bioquímica

Orientadora: Prof. Doutora Ana Aguiar Ricardo, FCT-UNL
Co-orientadora: Doutora Susana Gaudêncio, FCT-UNL

Júri:

Presidente: Prof. Doutor Mário Fernando José Eusébio
Arguente: Prof. Doutora Susana Felipe Barreiros
Vogal: Prof. Doutora Ana Isabel Nobre Martins Aguiar de Oliveira

FACULDADE DE CIÊNCIAS E TECNOLOGIA
UNIVERSIDADE NOVA DE LISBOA

Abril 2018

Dry powder formulations for antibiotic pulmonary delivery

Acknowledgments

I would thank very much to my supervisor Prof. Doctor Ana Aguiar-Ricardo for the opportunity to work in Polymer Synthesis and Processing laboratory and for all the guidance and support given throughout this year. Likewise, I would thank my co-supervisor Doctor Susana Gaudêncio for the opportunity to learn and work in natural products and for all the support given throughout this year.

I want to thank Prof. Paula Branco for the provision and support for helping me accomplish the organic synthesis, that without it I would not have completed the thesis. I also thank Dr. Vasco Bonifácio by provision and support at the beginning of this synthesis.

Dr. Teresa Casimiro for help when the SASD had problems and for give enlightening ideas that contributed to my work.

Prof. Rita Sobral and Dr. Inês Grilo for the help and availability to perform the antimicrobial assays.

To Ana Teresa from the NMR service, Luz Fernandes and Nuno Costa from Chemical Analyses Lab thank you for your help and assistance.

I want to thank Mrs. Maria José Carapinha, Mrs. Maria Isabel Rodrigues and Mrs. Maria Amália for assistance.

A very special thanks to three people who helped me throughout this work: first, Olesia Shapovalova thank you for guidance, support, kindness and availability whenever I needed help; Clarinda Costa thank you for guidance, support and for the enormous patience that you had with me in most difficult or most crazy days; and finally to Miguel Mateus thank you very much for your support, your knowledge in organic chemistry and for the most hilarious moments.

To all the staff at the lab. 508/510: Sofia Messias, Raquel Viveiros, Gosia Zakrzewska, Maria Romeu, Catarina Melo, Ana Inês Paninho and Filipa Santos. Not forgetting also, the other people who have worked in this lab: Sílvia Rebocho, Rita Gameiro and Javier Fernández.

To all friends, in and outside of the University campus, tanks for every moment that I shared during the five last years. In particular, Marta Faria, Marta Marques, Duarte Rente and Catarina Araújo who shared the same lab with me; Gonçalo Policarpo, André Ribeiro, Mónica Cunha, and Margarida Pinto for your friendship.

Lastly, I have to thank my parents, my brother, my grandmother, my uncle, my aunt and my cousins for the help and support you over these years. I dedicate my work to all of you. I love you all!!!

This work was supported by funding from FCT, through grants PTDC/QUIQUI/119116/2010, IF/00700/2014, UID/QUI/ 50006/2013 (LAQV) and UID/Multi/04378/2013 (UCIBIO), and co-financed by the FEDER under the PT2020 partnership agreement POCI-01-0145-FEDER-007265 and POCI-01-0145-FEDER-007728. The NMR spectrometers are part of The National NMR Facility, supported by FCT (RECI/BBB-BQB/0230/2012).

Abstract

In this work, dry powder formulations (DPFs) containing fusidic acid were produced for the purpose of studying the pulmonary delivery of this drug. As fusidic acid is poorly soluble in aqueous media, this drug was conjugated with two different hydrophilic polymers to increase the bioavailability of the drug. The two hydrophilic polymers used were methoxypolyethylene glycol amine, a commercial product, and poly(2-ethyl-2-oxazoline), that was synthesized by supercritical-assisted CO_2 polymerization and then end-capped with ethylenediamine. The conjugation compounds were synthesized in one-pot reaction and in inert atmosphere conditions. The compounds were characterized in relation to their physical-chemical properties (NMR, MS) and their antibacterial properties (against methicillin-resistant *Staphylococcus aureus*, MRSA JE2, and methicillin-sensitive *S. aureus*, MSSA ATCC 25923 and UAMS-1, strains). The biological test results indicate that both conjugated compounds have antimicrobial activity, but the fusidic acid has the lower values of minimum inhibitory concentration in all the tested pathogens. Trehalose-leucine dry powders were produced through the Supercritical CO_2 Assisted Spray-Drying (SASD) technique, testing different operating conditions such as temperature, pressure and CO_2/solution flow ratio. After finding the optimal operation conditions, three trehalose-leucine DPFs were prepared, containing fusidic or one of two conjugated compounds. All DPFs were characterized in relation to their morphology (Morphologi G3, SEM), to their physical-chemical properties (FT-IR, Water Content, Quantification of fusidic acid) and aerodynamic performance (Andersen Cascade Impactor measurements - to obtain data such as the fine particle fraction (FPF), emitted fraction (EF) and the mass median aerodynamic diameter (MMAD)). The resulting microparticles showed aerodynamics diameters between 1 and 7 μm, yields up to 67% and FPF up to 62%, making them suitable for pulmonary delivery.

Keywords: fusidic acid, conjugation reaction, dry powders, supercritical assisted spray-drying

Resumo

Neste trabalho, foram produzidas formulações de pó seco contendo ácido fusídico com a finalidade de estudar formulações para a administração pulmonar deste fármaco. Como o ácido fusídico é pouco solúvel em meio aquoso, o fármaco foi conjugado com dois polímeros hidrofílicos diferentes para aumentar a biodisponibilidade do fármaco. Usaram-se dois polímeros hidrofílicos: o metoxilo de polietileno de glicol amina, um produto comercial e poli(2-etil-2-oxazolina), que foi sintetizado por polimerização em CO_2 supercrítico e depois terminada com etilenodiamina. Os compostos de conjugação foram sintetizados em reação "one-pot" e em condições de atmosfera inerte. Os compostos foram caracterizados em relação às suas propriedades físico-químicas (NMR, MS) e suas propriedades antibacterianas (contra estirpes de *Staphylococcus aureus* resistente à meticilina, MRSA JE2, e *S. aureus* sensível à meticilina, MSSA ATCC 25923 e UAMS-1). Os resultados dos testes biológicos indicam que ambos os compostos conjugados possuem atividade antimicrobiana, mas o ácido fusídico possui os valores mais baixos de concentração inibitória mínima (MIC) em todos os patógenios testados. Os pós secos de trealose-leucina foram produzidos através da técnica de secagem assistida por CO_2 supercrítico (SASD), testando diferentes condições operacionais tais como a temperatura, a pressão e rácio de caudal de CO_2/solução. Depois de encontrar as condições ideais de operação, três formulações de pós secos de trealose-leucina foram preparadas, contendo ácido fusídico ou um dos dois compostos conjugados. Todas as formulações de pós secos foram caracterizadas em relação à sua morfologia (Morphologi G3, SEM), às suas propriedades físico-químicas (FT-IR, teor de água, quantificação do ácido fusídico) e ao desempenho aerodinâmico (medições de Andersen Cascade Impactor - para obter dados como a fração de partículas finas (FPF), a fração emitida (EF) e o diâmetro aerodinâmico massa mediano (MMAD)). As micropartículas resultantes mostraram diâmetros aerodinâmicos entre 1 e 7 μm, rendimentos até 67% e FPF até 62%, tornando-os adequadas para administração pulmonar.

Palavras-chave: ácido fusídico, reação de conjugação, pós secos, secagem assistida por fluidos supercríticos

Contents

Index of Figures

Index of Tables

List of Abbreviations

^{13}C NMR: Carbon-13 nuclear magnetic resonance

^{1}H NMR: Proton nuclear magnetic resonance

ACI: Andersen cascade impactor

ACN: Acetonitrile

API: Active pharmaceutical ingredient

CFC: Chlorofluorocarbon

CO_2: Carbon dioxide

COPD: Chronic obstructive pulmonary disease

CROP: Cationic ring-opening polymerization

DCC: N,N'-dicyclohexylcarbodiimide

DCM: Dichloromethane

DCU: Dicyclohexylurea

DMAP: 4-dimethylaminopyridine

DMAPP: Dimethylallyl diphosphate

DMF: Dimethylformamide

DMSO: Dimethyl sulfoxide

DPF: Dry powder formulation

DPI: Dry powder inhaler

DUSA: Dosage Unit Sampling Apparatus

EF-G: Elongation factor G

EtOx: 2-ethyl-2-oxazoline

FA-BzNH_2: Fusidic acid conjugated with benzylamine

FA: Fusidic acid

FDA: Food and Drug Administration

FPF: Fine particle fraction

FPP: Farnesyl diphosphate

FT-IR: Fourier Transform Infrared

GGPP: Geranylgeranyl diphosphate

GPP: Geranyl diphosphate

GSD: Geometric standard deviation

HFA: Hydrofluoroalkane

HMBC: Heteronuclear Multiple Bond Correlation

HPLC: High Performance Liquid Chromatography

HSQC: Heteronuclear Single Quantum Coherence

IPP: Isopentenyl diphosphate

KF: Karl-Fisher

LADME: Liberation, absorption, distribution, metabolism and excretion

MeOx: 2-methyl-2-oxazoline

MEP: Methylerythritol phosphate pathway

MEV: Mevalonate pathway

MIC: Minimum Inhibitory Concentration

MMAD: Mass median aerodynamic diameter

MRSA: Methicillin-resistant *Staphylococcus aureus*

MS: Mass spectrum

MSSA: Methicillin-sensitive *Staphylococcus aureus*

NCE: New chemical entity

NHS: N-hydroxysuccinimide

NMR: Nuclear magnetic resonance

OD: Optical density

PEG-FA: Fusidic acid conjugated with methoxypolyethylene glycol amine

PEG-NH_2: Methoxypolyethylene glycol amine

PEG: Poly(ethylene glycol)

PEtOx-FA: Fusidic acid conjugated with poly(2-ethyl-2-oxazoline) end-capped ethylenediamine

PEtOx-NH_2: Poly(2-ethyl-2-oxazoline) end-capped ethylenediamine

PEtOx: Poly(2-ethyl-2-oxazoline)

PGSS: Particles from gas saturated solutions

PMeOx: Poly(2-methyl-2-oxazoline)

pMID: Pressurized metered dose inhaler

PS: Particle size

PSD: Particle size distribution

RESS: Rapid expansion of supercritical solutions

SAA: Supercritical assisted atomization

SAR: Structure-activity relationship

SAS: Supercritical antisolvent

SASD: Supercritical assisted spray drying

scCO_2: Supercritical carbon dioxide

SEM: Scanning Electron Microscopy

SF: Supercritical fluids

TEA: Triethylamine

TFA: Trifluoroacetic acid

T_g: Glass transition temperature

TL: Trehalose-Leucine

TLFA: Trehalose-Leucine-Fusidic acid

TLPEtOx-FA: Trehalose-Leucine- Fusidic acid conjugated with methoxypolyethylene glycol amine

TLPEtOx-FA: Trehalose-Leucine- Fusidic acid conjugated with poly(2-ethyl-2-oxazoline) end-capped ethylenediamine

VLE: Vapor-liquid equilibria

1. Introduction

In recent years, lung diseases are a major cause of mortality in the world. Lower respiratory infections (like influenza and pneumonia), chronic pulmonary diseases (like asthma, chronic obstructive pulmonary disease (COPD) and sarcoidosis), and trachea, bronchus, and lung cancer represented 8,7 million death, in 2013.[1] The lower respiratory infection is the second disease with high mortality in 2013, however, asthma and COPD are both the diseases that most affect the global population (329 millions for COPD and 242 millions for asthma, in 2013).[2]

There are several ways to treat diseases, depending on the type of route of administration of the drug. The oral route is the simplest and common of all known routes of administration, however, it has a risk of drug degradation due to pH variations in the digestive system. The transdermal route is also simple but generally has a low adsorption efficiency. The injection method has a high adsorption efficiency, an early effect of injected drugs' pharmacological actions, and no risk of drug decomposition by digestive organs because the injections' spot can be in the skin (subcutaneous-SC), muscular tissue (intramuscular-IM) or bloodstream (intravenous-IV). Despite being a very effective method, it is also an invasive method and provokes pain and discomfort to patients.[3,4]

The best route of administration of the drug to treat lung diseases like asthma and COPD is through pulmonary delivery. The lungs are, in fact, an efficient port of entry for drugs to the bloodstream due to large and highly vascularized absorptive surface area (80-100 m^2), the thin alveolar-capillary membrane (0.1-0.5 μm) and the elevated blood flow (5l/min). In addition, the physiological environment of the lungs, such as physiological pH, allows a low metabolic activity, and it is not subject to first-pass metabolism, which is important to drugs that are sensitive to degradation by enzymes. All this makes the pulmonary delivery an easy administration route showing early effects of drugs' pharmacological actions and no risk of drug decomposition.[5–7]

One disadvantage of inhalation therapy is the short duration of drug action.[7] Therefore, the development of pulmonary controlled release formulations would be highly beneficial for patients suffering from lung diseases. Controlled drug release systems composed of polymeric materials with particular characteristics, such as biocompatibility and degradability, have been shown to improve the pharmacokinetic (evaluation of the effects of drug administration) and pharmacodynamic (evaluation of the pharmacological and physiological effects of the drugs on the body) profiles of encapsulated drugs in the lung.[4,7,8]

The inhalation technology has two main areas: development of new inhalation devices with enhanced efficiency and improvement of the existing inhalation formulations.[9] In recent research, the use of dry powders as drug delivery systems has been increasingly considered as a treatment option, even though it brings out concerns related to respiratory tract anatomy, breathing pattern and particle size.[10] The ideal characteristics of the dry powders must be high dispersibility, drug stability, narrow size distribution and sustained release. Also, the particles must have a physical stability in order to prevent solid-state transitions during the drug deposition. Also, there is the need to control both size and morphology of the particles that will affect the drug deposition.[3]

1.1. Dry Powder Inhalers

A good inhaler device should generate an aerosol of a suitable size (1–5 μm) and provide reproducible drug dosing that ensure the protection of the physical and chemical stability of the drug formulation. Moreover, this device must be simple, easy to use, inexpensive and portable.[6]

The nebulizers were the first inhalers that appeared on the market. The nebulizers use a large volume of drug solution (the drug is dissolved in a polar liquid). They have high delivery efficiency, however, there are some drawbacks such as low efficiency and reproducibility, the required time to the administration was 30 minutes and their use was confined to hospitals or home, given that they were not portable.[5,6]

To overcome these issues, the pressurized metered dose inhalers (pMDIs) were developed. They have high efficiency and reproducibility, they are portable and are faster to use than the nebulizers. Despite that, there is a major disadvantage: they require the use of compressed volatile liquids as propellants, like chlorofluorocarbon (CFC) and hydrofluoroalkane (HFA), making them environmentally unfriendly.[11]

In order to overpass these problems, the inhalers were improved, and dry powder inhalers (DPIs) appeared. They are easy to use, portable and propellant-free, therefore environmentally friendly. Also, since the aerosols are in a dry state they assure the stability of the drug, needing no special condition for storage neither for distribution.[12] However, they are expensive, complex to develop and the uniformity of the doses depends on the patient's inspiratory flow since it is what set the particles in motion, provoking turbulence and shear in order to generate the aerosol. These devices are divided in "single-dose" DPIs, which use a

single dose capsule, in “multiple unit dose” DPIs, which contains small doses separated in several capsules or blisters and in “multidose” DPIs that contain an amount of powder that is then delivered in several metered doses.[13]

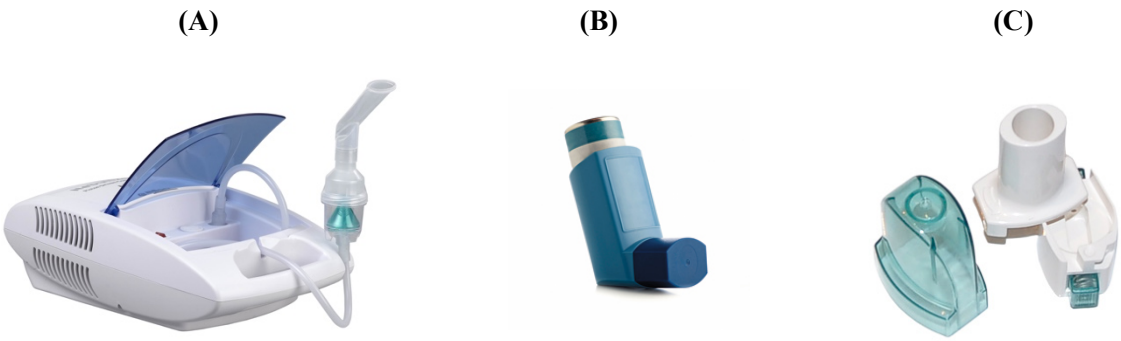

Figure 1 – Example of inhalers: (A) nebulizer, (B) pMID and (C) DPI

1.2. Drug Excipients

Excipients are a group of materials which exhibit unique properties and that are used in most of all therapeutic products. Excipients are derived from natural sources or are synthesized chemically and they range from simple, usually highly characterized, organic, or inorganic molecules to highly complex materials that are difficult to fully characterize.[14,15]

Excipients have multiple functions in the drug products, serving as chemical or physical stabilizers, preservatives and buffers, and some of these are included in the majority of drug formulations. Excipients are used in tablets and also serve as diluents, solvents, wetting agents, emulsifiers, preservatives, absorption enhancers, colouring agents, binders, disintegrants, lubricants, glidants, surfactants, dye, flavoring agents, controlled release agents, carriers and propellants in inhalation products, which allows the efficient manufacturing of the compressed tablets, affect the physical and chemical characteristics of the active drug ingredients and their bioavailability.[15,16]

They are critical components in the formulation of most inhaled drug products, including dry powder formulations. In this type of formulation, most of the excipients work as a carrier and have four primary functions: modification of the bulk powder properties via control of surface forces, improvement of physical and/or chemical stability, modification of the pharmacokinetics and/or pharmacodynamics of the drug substance, and serving as a bulking agent to enable accurate metering of potent drugs.[17]

There are many significant physicochemical properties of interactive carrier particle

systems that affect the aerosol dispersion of interactive carrier-based formulations and their influence on inter-particulate forces (van der Waals, electrostatics, capillary, and gravitational): drug properties (charge, surface, size, concentration and stability), carriers properties (size, shape and type), surface roughness, electrostatic charge, particle engineering, hygroscopicity and crystallinity/polymorphs.[18]

There are several types of carriers, such as carbohydrates (fructose, galactose, sucrose, trehalose, raffinose and melezitose), alditols (mannitol and xylitol), maltodextrins, dextrans, cyclodextrins, amino acids (glycine, arginine, lysine, aspartic acid and glutamic acid), and proteins (human serum albumin and gelatin).[13]

1.2.1. Carbohydrates

Carbohydrates are a large class of chemical compounds that includes sugars, starches and cellulose. These compounds are naturally produced by plants from carbon dioxide and water and are important as food: they supply energy and are used in the production of fats. There are three main classes of carbohydrates: sugars, which includes monosaccharides (fructose and glucose), disaccharides (lactose, trehalose, maltose, and sucrose), and polyols (mannitol, and sorbitol); oligosaccharides, carbohydrate polymer with small number of monosaccharides (raffinose and maltodextrins); and polysaccharides (cellulose, dextrin, and starch).[19] One negative aspect of the use of sugar-carrier particles, particularly for antimicrobial drug therapy, is the potential for microbes to use sugars as substrates for growth.[14,18]

Lactose (Figure 2) is the most used in dry powder formulation[6] since it is approved by government regulatory agencies in the US and Europe. It has many benefits: a well-established safety profile, low cost, and wide availability. The physicochemical properties of lactose are also excellent from a DPI formulation point of view: smooth surfaces, crystalline, and moderate flow properties. However, lactose may not be suitable for some active compounds because of its sugar reducing function.[14,18]

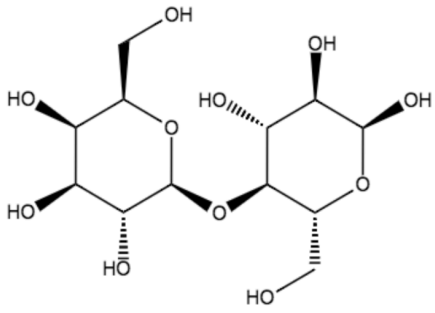

Figure 2 - Chemical structure of lactose

Trehalose is a disaccharide composed of two glucose molecules bound by an α, α-1, 1 linkage. It is known to be one of the sources of energy in most living organisms and can be found in many organisms, including bacteria, fungi, insects, plants, and invertebrates. It has many advantages over other excipients, such as low hygroscopicity, high glass transition temperature (T_g), which is about 124 ºC, low chemical reactivity, an absence of internal hydrogen bonds that allows more flexible formation of hydrogen bonds with drugs, it not susceptible to the Millard reactions and it is not metabolized by bacteria. Trehalose dihydrate is commonly used in drug formulations (Figure 3).[20–23]

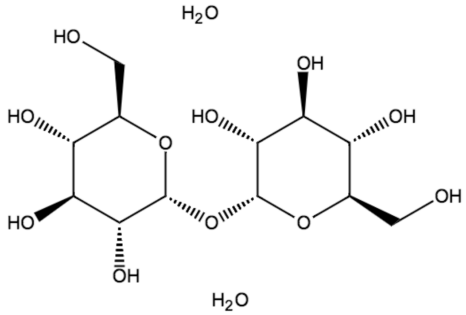

Figure 3 - Chemical structure of trehalose dihydrate

Chitosan (Figure 4) is a semi-crystalline polysaccharide composed of (1-4)-2-acetamido-2-deoxy-b-D-glucan (N-acetyl D-glucosamine) and (1-4)-2-amino-2-deoxyb-D-glucan (D-glucosamine) units available in different grades depending upon the degree of acetylated moieties and is the second most abundant natural polymer obtained from the shells of crabs and shrimp. Chitosan is a biodegradable natural polymer with an excellent potential for pharmaceutical applications due to its biocompatibility, high charge density, non-toxicity, and anti-inflammatory and mucoadhesive properties. Also, it has a low cytotoxicity with cell lines of human origin from the airways and the alveolar regions of the pulmonary tract.[24,25]

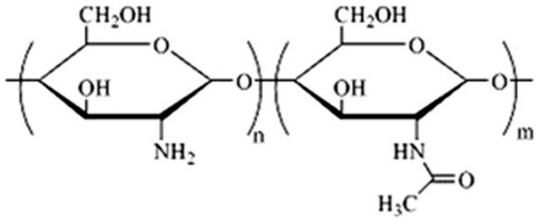

Figure 4 - Chemical structure of chitosan (n – represents the number of d-glucosamine momoner and m – represents the number of N-acetyl-d-glucosamine monomer), adapted from Dash *et al*[24]

1.2.2. Polymers

Polymers have been employed to stabilize aerosol drug formulations, modify the particle morphology, density and drug release characteristics, and reduce the adhesion/cohesion force between particles. There are three class of materials of polymers: natural polymers (albumin, carrageenan, chitosan, hyaluronic acid); synthetic polymers (poly(lactic acid), oligo(lactic acid), poly(vinyl alcohol), acrylic acid derivatives); and synthetic block copolymers (PLGA, poly(lactic acid)-poly(ethylene glycol)-poly(lactic acid)).[17,26]

Poly(ethylene glycol) (PEG) (Figure 5) is one of the most important and widely used polymers in the field of polymer-based drug delivery. It has many advantages such as, a wide range of molecular weight (between 200 and 300000 g/mol), low hygroscopicity, low melting point (<65 °C), good solubility in aqueous and organic solvents, high biocompatibility, low toxicity, and shielding effect. PEG has many applications: it is used as an excipient for parenteral, topical, nasal, and ocular applications and as the active principle in laxatives, and it used in cosmetics applications, such as tooth paste, shampoo, and after shave lotion. However, there are some disadvantages: its non-biodegradability, easy degradation when exposition to oxygen, and the side products formed during PEG synthesis may have some toxicity.[27–29]

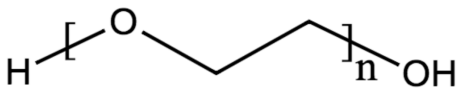

Figure 5 - Chemical structure of poly(ethylene glycol)

Oxazoline-based polymers have been proposed as alternative polymers to PEG-based materials, in particular, poly(2-methyl-2-oxazoline) (PMeOx) and poly(2-ethyl-2-oxazoline) (PEtOx) (Figure 6) because of their low toxicity and immunogenicity. Oxazoline-based polymers are non-toxic, water soluble, biodegradable and has many applications, such as smart

materials, membrane structures, drug carriers, synthetic vectors for DNA or RNA delivery and antimicrobial agents.[30] Polyoxazolines (POx) are obtained through living polymerization reactions and controlled manner via cationic ring-opening polymerization (CROP). This type of reaction allows the tuning of final polymer properties (such as hydrophilic, hydrophobic, fluorophilic) as it enables copolymerization with a variety of monomers and polymer chain end-capping. When the reaction is performed in $scCO_2$, oligo-oxazolines (OOx) are obtained.[30,31]

Figure 6 - Chemical structure of PMeOx (left) and PEtOx (right)

1.2.3. Amino Acids

Amino acids are endogenous substances (natural compounds) which may have fewer safety concerns for delivery to the respiratory tract and are well-known stabilizers for biomolecule formulations. Among all amino acids, leucine and trileucine are the most used for dry powder aerosol formulations (Figure 7).[26]

Leucine act as a lubricant, dispersion enhancer and/or coating for inhalable powders. When leucine is used in particle process, the resulting particles have corrugated surfaces due to a formation of leucine shell. Such particles would have reduced inter-particulate contact points, hence lower cohesive or adhesive forces than the smooth ones. The leucine shell may protect the amorphous particles against moistures, temperatures, and inhibit crystallization of other components in the formulation, which will improve the inhalable amorphous powder stability, and dispersibility/flowability and aerosolizing performance. Leucine has a major disadvantage: the solubility both in water and in ethanol are low, which can lead the leucine to reach the supersaturation stage early in the process of drying, resulting in crystallization.[26,32,33]

Another amino acid for dry powder formulation is trileucine, which has a relatively high T_g (104 °C), which imparts physical stability to the powder. It has a higher surface activity, a very low solubility in water compared with leucine, and microparticles of trileucine do not crystallize during spray drying process.[26,32]

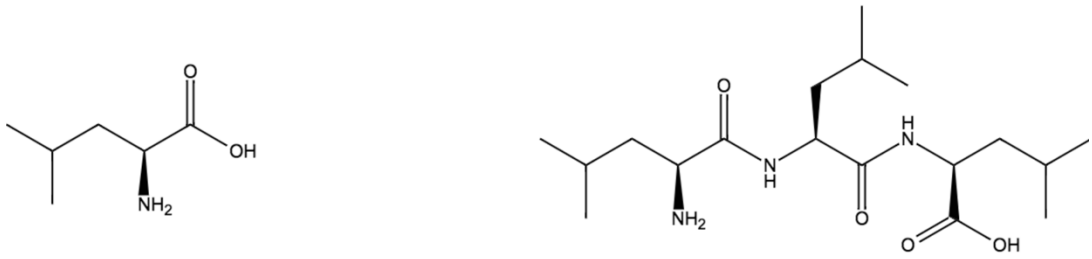

Figure 7 - Chemical structure of leucine (left) and trileucine (right)

1.3. Particle Production

There are several known methods to produce particles for inhalation and those can be divided into two groups: the top-down (large particles are mechanically broken down to smaller ones) and the bottom-up (particles are formed from the molecular level).[17]

The top-down methods are based on the grinding of crystallized particles into small ones by using mechanical forces such as pressure, friction, attraction, impact or shear. There are three types of mills that can be used to produce particles for inhalation, fluid-energy mills (jet-milling), high-peripheral-speed mills (pin-mill) and ball mills. The jet-milling is the most used technique where high pressure nitrogen is used to provoke the collisions between solid particles with each other at sonic velocity, causing the fracture of particles down to 1μm. Despite being a low cost technique, it is inadequate when it comes to particle production since the control of size distribution is limited. Also, the process might change the physicochemical properties of the material, turning the surface of fractured crystals amorphous.[17]

The bottom-up processes tend to be more sophisticated and complex and produce particles with a better control of its characteristics from a diversity of starting materials. In this case, the manufacturing methods involve the use of an antisolvent or are based on solvent evaporation as is spray-drying, the most used and studied solvent evaporation technique.[34] Spray drying is very rapid, convenient and it is suitable for industrial scalable processing and it also provides stability and biological activity for the active pharmaceutical ingredient (API). In this process, drug/protein/peptide loaded microspheres are prepared by atomization of the feed solution into a spray, which later enters in contact with heated air in a drying chamber forming a dry powder. The nature of the solvent used, temperature of the solvent evaporation and feed rate are some parameters that will affect the morphology of the microspheres. The disadvantages of this process are the adhesion of the microparticles to the inner walls of the spray-dryer, turning the yields insufficient, and the possible degradation of heat-sensitive drugs.[17,35]

One important class of particle production techniques are the ones that use supercritical

fluids. Supercritical Fluids (SF) are the substances that behave simultaneously like a gas and a liquid when above their critical temperature and pressure. They have the density of a liquid, showing good solvation power and negligible surface tension, while on the other hand, they have the viscosity of a gas with an associated high diffusivity. Since these aspects are very changeable near the critical point, it is easy to control both of them by a slight change in pressure/temperature.[36,37]

The carbon dioxide (CO_2) is the most used gas as a SF since it is non-toxic, non-flammable, inexpensive, inert nature and readily available in high purity from a variety of sources. Also, it has a low critical point (31.1 °C/73.8 bar), which is ideal to use with heat-sensitive materials and can reduce manufacturing complexity and energy (Figure 8).[9] The use of supercritical CO_2 ($scCO_2$) in particle production has major advantage comparing the conventional methods, which is the minimization or elimination of organic solvents since $scCO_2$ has a high affinity for them. A rapid expansion of the CO_2 using a pressure drop leads to the clustering of CO_2 molecules inside the liquid polymer, expanding it and inducing pore formation, making the system suitable for drug delivery.[38,39] Moreover, the morphology and porosity can be easily altered by changing operation parameters such as pressure, temperature and gas release rate.[40]

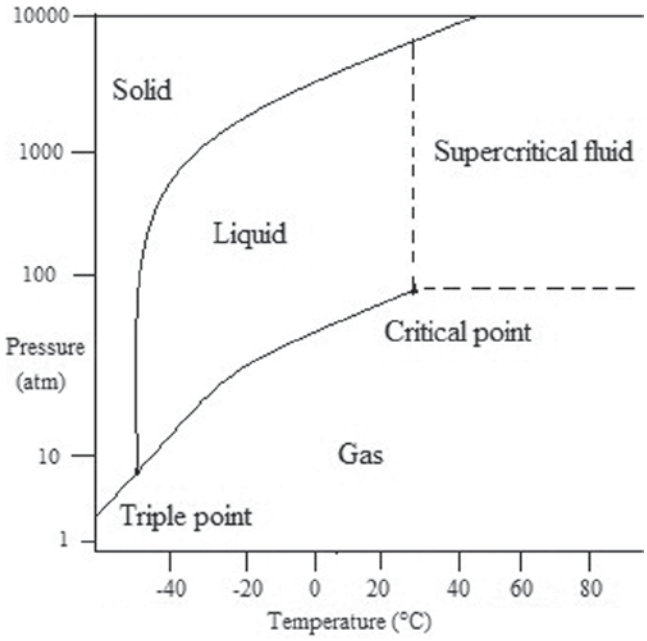

Figure 8 - Phase diagram of CO_2, adapted from P. Girotra *et al*[35]

Several supercritical CO_2-assisted methods for particle production have been reported: i) rapid expansion of supercritical solutions (RESS)[41] where the solid material is dissolved in $scCO_2$ and the solution is expanded by depressurization, leading to a fast decrease of temperature that will induce supersaturation and consequently microparticle formation; ii) supercritical antisolvent process (SAS),[37] where the solid material is dissolved in a liquid solvent and the resulting solution is sprayed in a chamber containing supercritical fluid as the antisolvent; iii) particles from gas saturated solutions (PGSS)[37,42] where the supercritical fluid acts as the solute and is dissolved in a solution (or suspension) of the drug in a solvent, which is followed by rapid depressurization of this mixture through a nozzle; iv) supercritical assisted atomization (SAA)[43] or as recently coined supercritical CO_2-assisted spray drying (SASD) that is based on the solubilization of controlled quantities of supercritical CO_2 in liquid solutions containing a solid solute and on the subsequent atomization of the ternary solution through a nozzle. This last $scCO_2$-assisted technique has been largely applied for production of dry powders and will be described in detail in the next subchapter.

1.3.1. Supercritical Assisted Spray-Drying (SASD)

Supercritical Assisted Spray-Drying (SASD) is a process similar to the one patented by E. Reverchon in US 7276190B2, based on the solubilization of controlled quantities of $scCO_2$ in liquid solutions. SASD offers many advantages over conventional methods, the possibility of operating in a continuous method in mild operating conditions and being able to use both organic and inorganic solvents while at the same time providing a good control over particle size and distribution.[44]

The SASD apparatus mainly consists of a saturator, a precipitator, a condenser and two pumps (one to deliver liquid CO_2 and other the liquid solution). The pumps are used to deliver the liquid solution and the liquid CO_2, which was previously cooled through a cryostat, to the saturator. The liquid CO_2 is then heated and the pressure is increased until supercritical conditions are reached. The mixing takes place in a saturator containing high-surface packing and ensuring long residence times in order to achieve near-equilibrium conditions. When the mixture reaches the nozzle, it will be atomized by a two-step atomization process: first primary droplets are obtained due to pneumatic atomization at the nozzle exit; then a secondary atomization process takes place by decompressive atomization due to CO_2 expansion from inside the primary droplets (Figure 9). This implies that the smallest particle size that can be achieved is the size of the smallest droplet achieved during the first atomization. The droplet size is determined by viscosity, surface tension and the amount of $scCO_2$ dissolved in the liquid solution, while temperature and chemical characteristics of the solute determine whether the

particle is crystalline or amorphous.[45,46]

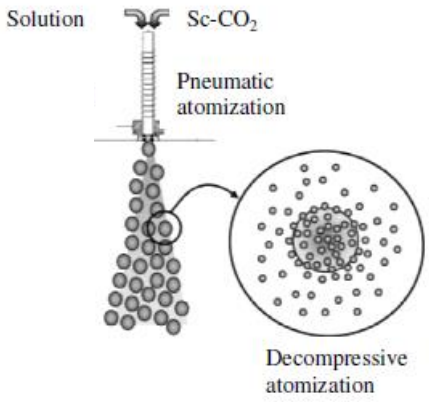

Figure 9 - Representation of the atomization mechanism, adapted from E.Reverchonet *et al*[44]

One important factor in this process is the solubility of $scCO_2$ in liquid solutions, which depends on the properties of the solvent and on the operating temperature and pressure since it is related to high-pressure vapour-liquid equilibria (VLEs) of the system. In addition, the presence of the solute might induce some modifications, because in order to have a successful atomization a single-phase should be formed in the saturator. However, when one is working with a ternary blend complicated it is well known that by means of high pressure and temperature, it becomes easier to avoid a two-phase behaviour. The use of aqueous solutions in this process is complicated due to the low solubilization of CO_2 in water, but that can be resolved with the use of an organic solvent and the reduction of water percentage to a minimum.[46–48]

1.4. Natural Products

A large part of the marketed pharmaceuticals products and other chemical compounds with biological activity comes from natural or semi-synthetic sources. From the 974 small molecule new chemical entities developed between 1981 and 2006, around 63% were natural derived or semisynthetic derivatives of natural products.[49]

Natural products are chemical substances produced by living organisms, like prokaryotic bacteria, eukaryotic microorganisms, fungi, plants and animals. These compounds

are produced by the pathways of primary or secondary metabolism from living organisms.[50] The primary metabolites (amino acids, nucleotides, fatty acids, vitamins and carbohydrates) are common in all biological systems, since they are the main basic building blocks of life.[50,51] The secondary metabolites are chemical compounds that have a broad range of functions, such as competitive weapons (venoms and toxins), metal transporting agents, agents of symbiosis between microorganism and microorganisms, and hormones or pheromones. They have low molecular weight (MW<3000) and exhibits a wide range of biological activities.[50,52]

Since the detection of the antibiotic properties of penicillin by Alexander Fleming in 1928 until our present day, about 15000 natural products derived from microbial sources were discovered.[50] The oceans, that covering more than 70% of the Earth's surface, contains an exceptional biological diversity, accounting for more than 95% of the whole biosphere, and most importantly, they have a highly complex microbiological environment with typical microbial abundances of 10^6 and 10^9 per ml in seawater and ocean-bottom sediments, respectively. By applying the methods of sequencing DNA in marine microbial ecology, the microorganisms are unique and highly adapted to the environment around them. Natural products are indeed a very important source of new chemical diversity and an integral constituent of pharmaceutical's field.[53,54]

1.5. Terpenoids

Terpenoids (or isoprenoids) are a large and ubiquitous class of metabolites that provide diverse functions in both primary and secondary metabolism and they are assembled from five-carbon isoprene subunits into a wide assortment of structures that generally range from monoterpenes (two isoprene units) to triterpenes (six isoprene units) and sometimes to polyterpenes (seven or more isoprene units). Terpenoids are common in plants, insects, fungi, mammals, and some marine invertebrates, such as soft corals and they are known as the largest single family of natural products, with more than 23000 known compounds, such as flavors, antibiotics, and plant hormones.[55–57]

Isoprenoids may be synthesized throught two ways: the mevalonate pathway (MEV) which is used in eukaryotes, archaea, and the cytoplasm of plants, and the methylerythritol phosphate pathway (MEP) is used in prokaryotes and the chloroplasts of plants.[58] It is synthesized by consecutive condensations of two types of C_5 precursors, isopentenyl diphosphate (IPP) and dimethylallyl diphosphate (DMAPP).[59] All isoprenoid chains are constructed using DMAPP as the initiator and IPP as the monomer. The chain length and

stereochemistry of the resulting prenyl diphosphate are specified by the corresponding prenyltransferases: in this case, the production of geranyl diphosphate (GPP), farnesyl diphosphate (FPP) and geranylgeranyl diphosphate (GGPP) are controlled by the GPP synthase, FPP synthase and GGPP synthase, respectively.[58]

1.6. Fusidic acid

Fusidic acid (FA) is a tetracyclic triterpenoid derived from the fungus *Fusidium coccineum* which was initially isolated from monkey faeces in 1960. Later, it is found in bacteria sources such as *Acremonium fusidioides*, *Calcarisporium arbuscula*, *Cephalosporium lamellaecula*, *C. acremonium*, *Epidermophyton floccosum*, *Gabarnaudia tholispora*, *Mucor ramannianus*, and *Paecilomyces fusidioides*.[60–62]

The molecular formula of FA is $C_{31}H_{48}O_6$, which contains one acetoxyl, one carboxylic and two hydroxyl groups (Figure 10) is found in the form of a white hygroscopic powder that is insoluble in water, ether, and hexane and soluble in ethanol, acetone, chloroform, pyridine, dioxane, and acetonitrile. It is also a weak acid with pKa of 5.7 and is available in ionized form in plasma and tissue at the physiological pH of 7.4.[60,61]

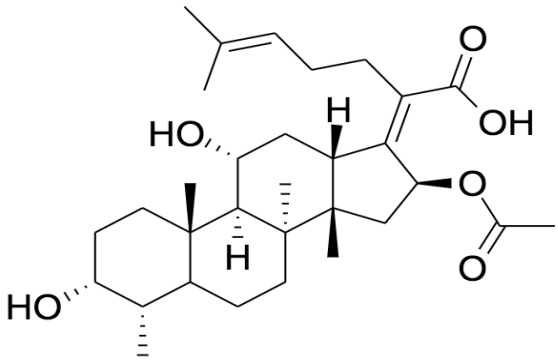

Figure 10 - Chemical struture of fusidic acid

FA is an antimicrobial agent with a bacteriostatic action (it inhibits the growth and reproduction of bacteria) and at high concentrations, it has a bactericidal action (kills the bacteria). In vitro, it uses against various strains of staphylococci including Methicillin susceptible, resistant variety of *Staphylococcus aureus* (for example, methicillin-resistant *Staphylococcus aureus* and methicillin-sensitive *Staphylococcus aureus* – MRSA and MSSA, respectively), and coagulase-negative *Staphylococcus* strains, *Clostridia*, *Moraxella*, *Peptococcus*, *Peptrococcus* and *Neisseria* species.[60,62,63]

In terms of medical application, FA it uses to treat bacterial conjunctivitis, colitis, cystic fibrosis, respiratory infections (such as, asthma, COPD, pneumonia), leprosy, bone and joint infections, and skin infections (such as, boils, anthrax, acne).[61,64] It comes in different formulations such as, oral tablets, oral suspension, intravenous formulation, topical administration (most common, in cream and ointment), and inhalation formulation.[60,61,64,65] It is available in the European and Australian market for more than 40 years, but, in United States it is not available, due to unknown seeking license from FDA.[61,62,66]

1.7. Thesis Layout

Chapter 1 is a review of literature related to the work performed in this thesis and on the existing technology, with special attention on the production of dry powders for inhalation. Chapter 2 describes the materials and the protocol for each laboratory experiment. Chapter 3 describes the results and discussion of the laboratory work which is divided in seven subchapters: the first two are related with chemical and biochemical synthesis to obtain polymers and conjugate compounds; the third is about the bioassays of product obtained in the preceding subchapters; and the last four are about dry powders formulation and characterization of those dry powders – morphology, aerodynamics and physical-chemical properties. Chapter 4 presents the general conclusions obtained in this work and provides some recommendations for further research and work.

The original purpose of this work was to use a natural antimicrobial product isolated from the marine actinomycete strain PTM-029[67] as the main bioactive agent to incorporate in the dry powders formulations and then characterize in order to compare them in certain properties. However, the mass of the isolated natural product, an antimicrobial napyradiomycin-derivative (PTM-029, F4, F39), was very low and insufficient to perform our work and for this reason, the fusidic acid was selected as a model drug in this study. All the materials, experimental protocols and main results of the natural product isolation are in Annex 1.

2. Experimental Section

2.1 Materials

Boron triflouride diethyl etherate, methoxypolyethylene glycol amine 2000, N-hydroxysuccinimide (99%), L-leucine (98%), triethylamine (99.0%) and 2-ethyl-2-oxazoline (99%) were purchased from Sigma–Aldrich. Ethylenediamine (99.5%) was purchased from Fluka. Dimethyl sulfoxide (99.7%), acetonitrile (99.9%), dimethylformamide (99.9%), propanol (99.5%), benzylamine (99%), methanol (99.9%), ethanol absolute anhydrous and 4-dimethylaminopyridine were purchased from Carlo Erba Reagents. Acetone was purchased from LabChem. Fusidic acid was purchased from Carbosynth. N,N'-dicyclohexylcarbodiimide (99%) was purchased from Alfa-Aesar. Dichloromethane (99.9 %) was purchased from Honeywell. Trehalose dihydrate (99.0%) was purchased from Calbiochem. Carbon dioxide (99.998%) was purchased Air Liquid. D-chloroform was purchased from Cambridge Isotope Laboratories, Inc.

2.2. Synthesis of Poly(2-ethyl-2-oxazoline) End-capped with Ethylenediamine in $scCO_2$

The synthesis of living polyoxazolines followed the reported protocol in Veiga de Macedo, C. *et al*[31]. The polymerization reactions were carried out in an 11 ml stainless-steel reactor that was loaded with 1 ml of 2-ethyl-2-oxazoline (EtOx) – monomer, and 100 µl of boron triflouride diethyl etherate ($BF_3.OEt_2$) – initiator, under stirring conditions. The reactor was closed with two sapphires (one of steel and the other of glass) in both tops with Teflon rings, connected to the CO_2 line charged with 10 bar and placed in a hot water bath at 61 ºC to assure control and to avoid gas leakage from the reactor. After that, the pressure was increased to 160 bar to ensure that the substrates were solubilized under a homogenous supercritical phase during at least 24 hours.

After 24 hours, the reactor was slowly depressurized with a schlenk tube, and cooled to room temperature, and then ethylenediamine, an end-capping agent, is added onto reactor and was left to stirred for 16 to 24 hours. After that, the dialyses process starts by put the liquid in the dialysis membrane with cut-off of 500 g/mol and then placed in water at room temperature and stirred for 2 days. The liquid obtained in the membranes was placed in round-bottomed flask and evaporated to dryness to remove the excess of water and then, it was placed in the

vacuum line for drying. The final yellow oil product was further analysed by NMR.

2.3. Conjugation of Fusidic Acid with Polymers

2.3.1. Activation of Fusidic Acid

2.3.1.1. First Attempt

Following a reported procedure from literature[68], the activation of fusidic acid was carried out in a small round-bottomed flask with 0.782 g (1.51 mmol) of fusidic acid (FA), 0.349 g (3.03 mmol) of N-hydroxysuccinimide (NHS), 0.42 ml (3.02 mmol) of trimethylamine (TEA), 0.343 g (1.66 mmol) of N,N'-dicyclohexylcarbodiimide (DCC), and 8 ml of dimethyl sulfoxide (DMSO), under stirring conditions at room temperature, leaving the mixture for overnight. Afterwards, water was added to the mixture and then placed in the dialysis membrane with cut-off of 500 g/mol and later placed in water at room temperature and stirred for at least 2 days. The liquid obtained in the membranes was placed in round-bottomed flask and evaporated to dryness. Later, the mixture was filtered under vacuum conditions with hot methanol to remove the impurities. The organic solution collected in the Kitasato flask was evaporated on the dryness in a rotary evaporator and then was dried in the vacuum line. The final white powder product was further analysed by NMR and FTIR.

2.3.1.2. Second Attempt

The activation of fusidic acid was performed under the same conditions as the reaction in DMSO, but instead of using DMSO, 7.5 ml of chloroform was used in this reaction. Afterwards, 10 ml of cold acetone was added to the mixture and then was set aside in the fridge or in an ice bath at least 2 hours. Later, the mixture was filtered under vacuum conditions. The organic solution collected in the Kitasato flask was evaporated to dryness in the rotary evaporator and then was dried in the vacuum line. The final white powder product was further analysed by NMR.

2.3.1.3. Third Attempt

The activation of fusidic acid was performed under the same conditions as the reaction in DMSO, but instead of using DMSO, acetonitrile (ACN) and dimethylformamide (DMF) was used in this reaction. The volume used was 7 ml of ACN and 1.5 ml of DMF. Afterwards, the

mixture was set aside in the fridge or in an ice bath at least 3 hours. Later, the precipitated in the mixture was filtered under vacuum conditions. The organic solution collected in the Kitasato flask was evaporated to dryness in the rotary evaporator to remove the ACN. A liquid-liquid extraction was performed: 10 ml of ethyl acetate was added into the mixture in the separation funnel and then 10 ml of distilled water was added five times. The organic phase was collected in a round-bottomed flask, where was dried first in the rotary evaporator and then in the vacuum line. The final white powder product was further analysed by NMR.

2.3.2. Conjugation with Poly(2-etlhyl-2-oxazoline) end-capped ethylenediamine

In small round-bottomed flask, 0.200 g (0.105 mmol) of PEtOx-NH_2 was dissolved in 13 ml of DMSO and then, 44.0 µl (0.316 mmol) of TEA was added to the mixture and was left in stirring for 30 minutes. After that, 0.185 g (0.316 mmol) of fusidic acid activated (FA-NHS) from the 1st attempt was added to mixture, and left stirring at 60 ºC overnight. Then, the mixture was placed in the dialysis membrane with cut-off of 500 g/mol and later placed in water at room temperature and stirred for at least 2 days. The liquid obtained in the membranes was evaporate to remove the excess of water. Later, the mixture was filtered under vacuum conditions with hot methanol. The organic solution collected was evaporated in the rotary evaporator and then dried in the vacuum line. The final white powder product was further analysed by NMR.

2.3.3. Conjugation with Metoxypolyethylene glycol amine

In small round-bottomed flask, 0.200 g (0.100 mmol) of PEG-NH_2 was dissolved in 13 ml of DMSO and then, 41.8 µl (0.300 mmol) of TEA was added to mixture and was left in stirring for 30 minutes. After that, 0.176 g (0.300 mmol) of fusidic acid activated (FA-NHS) from the 1st attempt was added to mixture and left stirring at 60 ºC overnight. Then, the mixture was placed in the dialysis membrane with cut-off of 500 g/mol and later placed in water at room temperature and stirred for at least 2 days. The liquid obtained in the membranes was evaporate to remove the excess of water. Later, the mixture was filtered under vacuum conditions with hot methanol. The organic solution collected was evaporated in the rotary evaporator and then dried in the vacuum line. The final white powder product was further analysed by NMR.

2.3.4. Conjugation in One-pot Reaction

2.3.4.1. Conjugation with Benzylamine

In a two necked round-bottomed flask, 0.100 g (0.194 mmol) of FA, 0.040 g (0.194 mmol) of DCC and 5 ml of dichloromethane (DCM) were placed under agitation and under inert atmosphere environment during 30 minutes. Then, 0.005 g (0.04 mmol) of dimethylaminopyridine (DMAP) dissolved in 1 ml of DCM and 0.025 ml (0.232 mol) of benzylamine were added to the mixture and left under stirring for overnight. The mixture was filtered, then evaporated to dryness in a rotary evaporator and after that was placed in the vacuum line for few hours. The final white powder product was further analysed by NMR.

2.3.4.2. Conjugation with Poly(2-ethyl-2-oxazoline) end-capped ethylenediamine

In a two necked round-bottomed flask, 0.782 g (1.51 mmol) of FA, 0.343 g (1.66 mmol) of DCC and 15 ml of DCM were placed under agitation and under inert atmosphere environment during 30 minutes. Then, 0.023 g (0.188 mmol) of DMAP dissolved in 2 ml of DCM and 0.728 g (0.383 mmol) of PEtOx-NH_2 dissolved in 5 ml of DCM were added to the mixture, and left under stirring for overnight. The mixture was filtered, then evaporated to dryness in a rotary evaporator and after that was placed in the vacuum line for few hours. Propanol (5 ml) were added to the mixture then was placed in one dialysis membrane and then put in a small flask with propanol and left for at least 2 days. The solution inside the membrane was evaporated to dryness in to the rotary evaporator and then put in the vacuum line for few hours. The final yellow powder product was further analysed by NMR.

2.3.4.3. Conjugation with Metoxypolyethylene glycol amine

In a two necked round-bottomed flask, 0.207 g (0.400 mmol) of FA, 0.082 g (0.400 mmol) of DCC and 5 ml of DCM were placed under agitation and under inert atmosphere environment during 30 minutes. Then, 0.010 g (0.188 mmol) of DMAP and 0.200 g (0.10 mmol) of PEG-NH_2 dissolved in 1 ml of DCM were added to the mixture and left under stirring for overnight. The mixture was filtered, then evaporated to dryness in a rotary evaporator and after that was placed in the vacuum line for few hours. The same dialysis procedure as mention in **2.2.4.2.** was also here performed. The final light yellow oil product was further analysed by NMR.

2.4. Microparticles Production

2.4.1. Microparticles Preparation

To produce trehalose-leucine microparticles with or without fusidic acid or the conjugated compounds, eleven solutions with 2% (w/v) total of solids concentration were prepared. Trehalose was dissolved in distilled water, while leucine, fusidic acid and the conjugated compounds were dissolved in ethanol.

Table 1 - Composition of casting solutions used for the preparation of trehalose-leucine microparticles

Assay	Total of solids concentrations	Solution components	Solvents of the solution	Code
1	2% (w/v)	1.6% (w/v) Trehalose 0.4% (w/v) Leucine	80% (v/v) Water 20% (v/v) Ethanol	**TL**
2				
3				
4				
5				
6		1.5952% (w/v) Trehalose 0.3988% (w/v) Leucine 0.0060% (w/v) FA		**TLFA**
7				
8		1.5836% (w/v) Trehalose 0.3960% (w/v) Leucine 0.0204% (w/v) PEtOx-FA		**TLPEtOx-FA**
9				
10		1.5766% (w/v) Trehalose 0.3924% (w/v) Leucine 0.0292% (w/v) PEG-FA		**TLPEG-FA**
11				

FA: fusidic acid; PEtOx-FA: fusidic acid conjugated with poly(2-ethyl-2-oxazoline) end-capping ethylenediamine; PEG-FA: fusidic acid conjugated with methoxypolyethylene glycol amine

TL: trehalose – leucine; TLFA: trehalose – leucine – fusidic acid; TLPEtOx-FA: trehalose – leucine – fusidic acid conjugated with PEtOx-NH_2 ; TLPEG-FA: trehalose – leucine – fusidic acid conjugated with PEG-NH_2

2.4.2. SASD Apparatus

The laboratory scale SASD apparatus (Figure 11) consists of two high-pressure pumps to deliver the liquid solution (Smartline pump 1000, Knauer) and the CO_2 (HPLC pump K-501, Knauer) to the static mixer. The CO_2 pump is suitable for liquid solutions, so the CO_2 is liquefied in a cryogenic bath (by using monoethylene glycol at -20 ºC). Before entering the static mixer, the CO_2 is heated in an oil bath at 79 ºC. The static mixer (3/16 model 37-03-075 Chemieer) is a high-pressure vessel with a 4.8 mm diameter, 191 mm length and 27 helical mixing elements that allows the solubilization of the CO_2 into the liquid solution due to its high surface packing. In order to control the temperature of the mixture, the static mixer is enrolled by heating tapes controlled by a shinko FCS-13A temperature controller (0.2 ºC resolution). The obtained mixture is then atomized into the precipitator in the form of a spray by the passage through a nozzle with an internal diameter of 150 μm. At the same time, a flow of previously heated compressed air enters the precipitator to evaporate the liquid solvent. The precipitator is a plastic vessel that operates at near-atmospheric conditions. After the precipitator there is a short plastic tube connected to a high-efficiency cyclone to make sure the flow remains at high temperatures, thus avoiding heat losses and consequent solvent condensation. The high-efficiency cyclone will help the separation between the particles and the CO_2-solvent flow, to collect the microparticles in a glass flak which is placed after the cyclone.

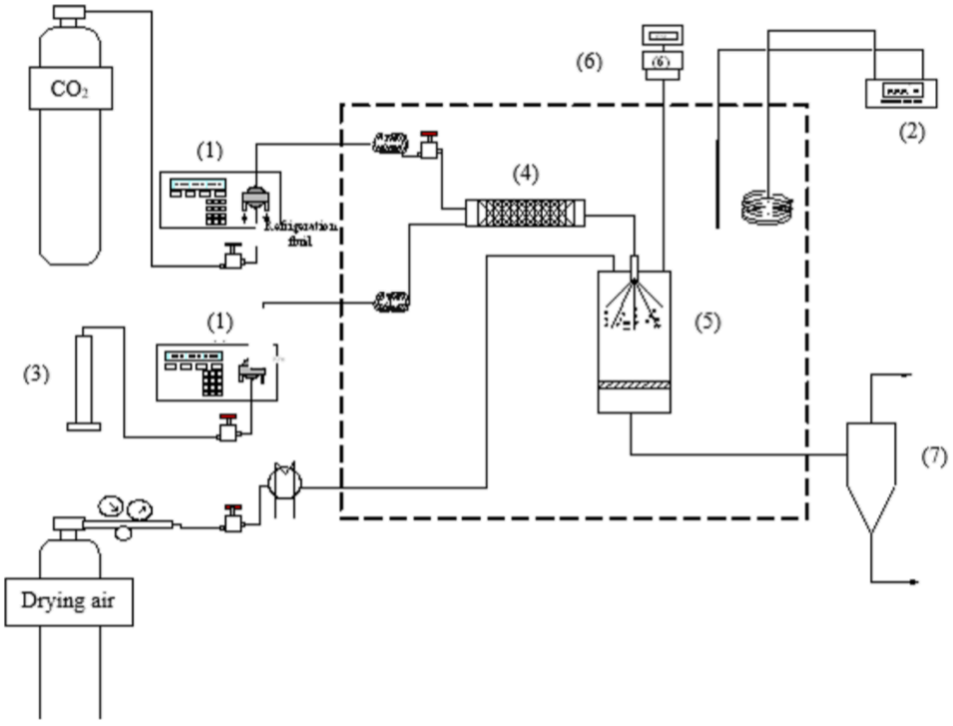

Figure 11 - Schematic of the supercritical CO_2-assisted spray drying (SASD) apparatus: (1) HPLC pump; (2) temperature controller; (3) container with liquid solution; (4) saturator; (5) precipitator; (6) manometer; (7) high efficienct cyclone

2.5. Microparticles Characterization

2.5.1. Particles Morphology

The morphology of the produced particles was studied by Scanning Electron Microscopy (SEM) equipment from Hitachi, S-2400 instrument, with an accelerating voltage set to 15kV and at magnifications of 5K and 10K. All the samples were dispersed on carbon tape previously attached to an aluminum stub and were coated with gold before analysis.

The particle size (PS) and the particle size distribution (PSD) were measured by a Morphologi G3 essentials, a particle analyzer system. In each particle size calculation around 30000 particles were considered. Also the span was calculated, a measure of the width of particle distribution, and it considers the $d_{v,10}$, $d_{v,50}$ and $d_{v,90}$ (particle diameter in volume corresponding to 10, 50 and 90% of the population) as represented in equation 1:

$$(1) \qquad Span = \frac{d_{v,90} - d_{v,10}}{d_{v,50}}$$

2.5.2. Fourier Transform Infrared (FT-IR)

FT-IR spectra was carried out on a Perkin Elmer Sepectrum Two equipped with a PerkinElmer Universal ATR (UATR), and coupled with a PerkinElmer Sepectrum Software.

2.5.3. Water Content Determination

Karl Fischer coulometric titration was used for the determination of water content on the samples. An aliquot of the samples was transferred into the titration vessel and titrated with Karl Fischer reagent (hydranal), which reacts quantitatively and selectively with water. The instrument was composed by the 831 KF Coulometer, 728 Stirrer, double Pt-wire electrode, generator electrode with diaphragm, KF adsorber tube, and KF titration vessel, all from Metrohm.

2.5.4. Aerodynamics Properties

To determine the shot weight, which is the amount of powder that is released from the capsules, the Dosage Unit Sampling Apparatus (DUSA) is used (Figure 12). The air is drawn by a High Controller Pump model HCP5 (Copley) that simulates inhalation and air flow was regulated in a Critical Flow Controller model TPK (Copley) until the P1 pressure achieves the 4kPa. The air flow (Q_{air}) was measured with a flow meter model DFM3 (Copley) in order to calculate the run time of each capsule using the equation 2:

$$(2) \qquad t(s) = \frac{4(L) \times 60\ (min/s)}{Q_{air}\ (L/min)}$$

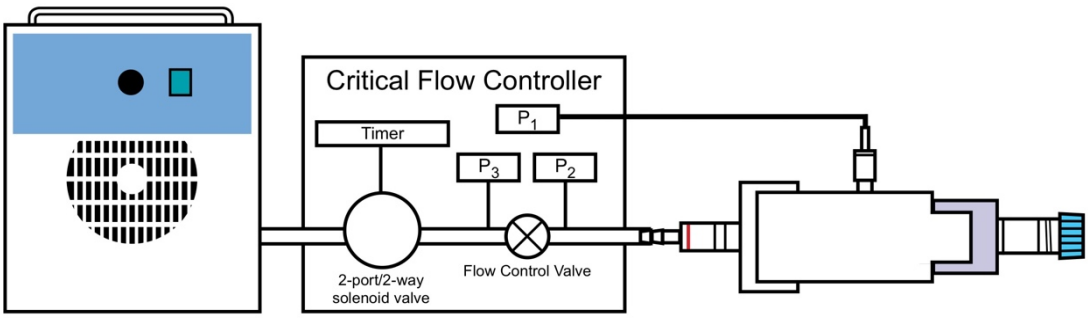

Figure 12 - Schematic representation of the DUSA, adapted from Copley Scientific

Also, there is a need to ensure that P3/P2 ≤ 0.5 in order to guarantee the critical flow. The assay consists on the release of 3 capsules (HPMC capsules nº3 Aerovaus) with 30±2 mg of powder each from a dry powder inhaler (Plastique 60LPM – Mode 7) and it is performed in triplicate as reported in the European Pharmacopeia. The emitted fraction (EF) or emitted dose (ED) (%) corresponds to the total loaded powder exiting the capsule and is calculated by using the weights (mg) of the capsule before and after the assay (m_{full} and m_{empty}, respectively) and the weight of the powder placed initially inside of the capsule (m_{powder}) as represented in equation 3:

$$(3) \qquad EF(\%) = \frac{m_{full} - m_{empty}}{m_{powder}} \times 100\%$$

The aerodynamic properties of fine particles were carried out using an aluminium Andersen Cascade Impactor apparatus (ACI) from Copley (Figure 13). The assay is performed with the same instruments as the emitted fraction test, being the capsules prepared equally and the run time calculated using the same European Pharmacopeia protocol.

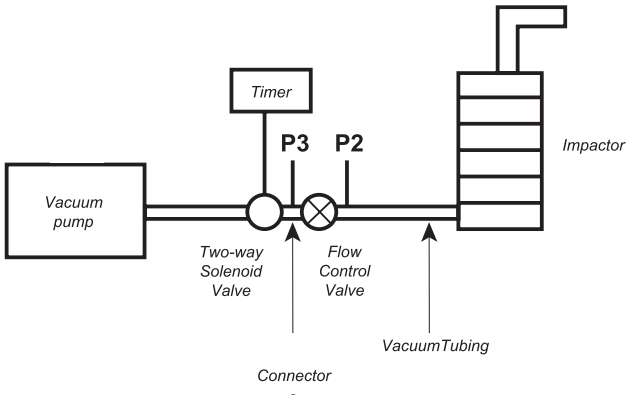

Figure 13 - Experimental set-up to perform ACI, adapted from European Pharmacopeia

The assays were performed gravimetrically, so glass microfiber filters (80mm, Filter Lab) were placed in all the stages and were weighted before and after the capsules release. Each capsule was drawn through the induction port into the ACI at a flow rate of 60±1 L/min for 4.0±0.1 seconds. The effective cut-off aerodynamic diameter for each stage of the ACI were: stage 0, 8.6 µm; stage 1, 6.5 µm; stage 2, 4.4 µm; stage 3, 3.2 µm; stage 4, 1.9 µm; stage 5, 1.2 µm; stage 6, 0.55 µm; stage 7, 0.26 µm.

The fine particle fraction (FPF) was determined by the interpolation of the percentage of the particles containing less than 5 µm. The Mass Median Aerodynamic Diameter (MMAD) was determined as the particle diameter corresponding to 50% of the cumulative distribution. The Geometric Standard Deviation (GSD) was determined using the values of d_{84} and d_{16}, which represent the diameters of 84% and 16% of the cumulative distribution as in equation 4:

$$(4) \qquad GSD = \sqrt{\frac{d_{84}}{d_{16}}}$$

2.6. Antimicrobial Activity Evaluation

The antimicrobial activity was evaluated within an established collaboration with Professor Rita Sobral from the Department of Life Sciences.

The test compounds, that were previously dissolved in ethanol, were added to the first row of a sterile tissue-culture treated 96-well assay plates at a concentration of 12.5 μg/ml (for fusidic acid) and serially diluted two-fold into the following rows, nine times. Three different strains of Staphylococcus aureus were diluted to an OD of 0.005 tryptone soy broth (TSB) and then added to the top row of a 96-well microtiter plate. The cultures were incubated at 37ºC for 24 hours without shaking. Following the incubation period, the growth was assessed by determining the OD, using a microplate reader. Optical density (OD) was measured at 600 nm.

2.7. Quantitation of Fusidic Acid

The process of quantitation of the fusidic acid contained in the dry powders was performed using High Performance Liquid Chromatography (HPLC). The HPLC analyses were performed by Nuno Costa from the Chemical Analysis Lab.

The HPLC equipment used was an Agilent Infinity 1100 with a Thermo Kromasil C18 column (250 × 4.6 mm, 5 μm). The tested samples were eluted at flow rate of 0.7 ml/ min with various gradients of H_2O/ACN (0,1% formic acid). All analyses were made at 30ºC and volume of solution injected onto the column was 50 μl. The UV-vis detector was set at 240 nm.

Three sample were tested: fusidic acid, as standard sample and the dry powders TLFA. For the standard samples, eight solutions containing fusidic acid with different concentrations (0, 1.0128, 5.064, 10.128, 20.256, 30.384, 40.512, and 50.64 mg/l) were prepared with ACN:H_2O 75%:25% (v/v). For the dry powders samples, four solutions (duplicates for each powder) with the same concentration (2,016 g/l) were prepared in 25 ml of ACN:H_2O 10%:90% (v/v).

3. Results and Discussion

3.1. Synthesis of Polymers in $scCO_2$

The polymerization of 2-ethyl-2-oxazoline begins with a nucleophilic attack of a pair of electrons of the oxazoline ring, which reacts with a Lewis acid catalyst, $BF_3.OEt_2$, to form an oxazoline ring open chains by cleavage of the C-O bond promoted by another molecule of oxazoline. As there are no chain-transfer or termination reactions, the polymer continues to grow until all the monomers are consumed or when a terminating agent is added, which usually is a good nucleophile. Ethylenediamine is an excellent terminating agent since it is a molecule with low steric effect and has two amides on the ends that act as Lewis bases. Figure 14 represents the reaction of polymerization of 2-ethyl-2-oxazoline at high temperature and pressure with end-capped with ethylenediamine.

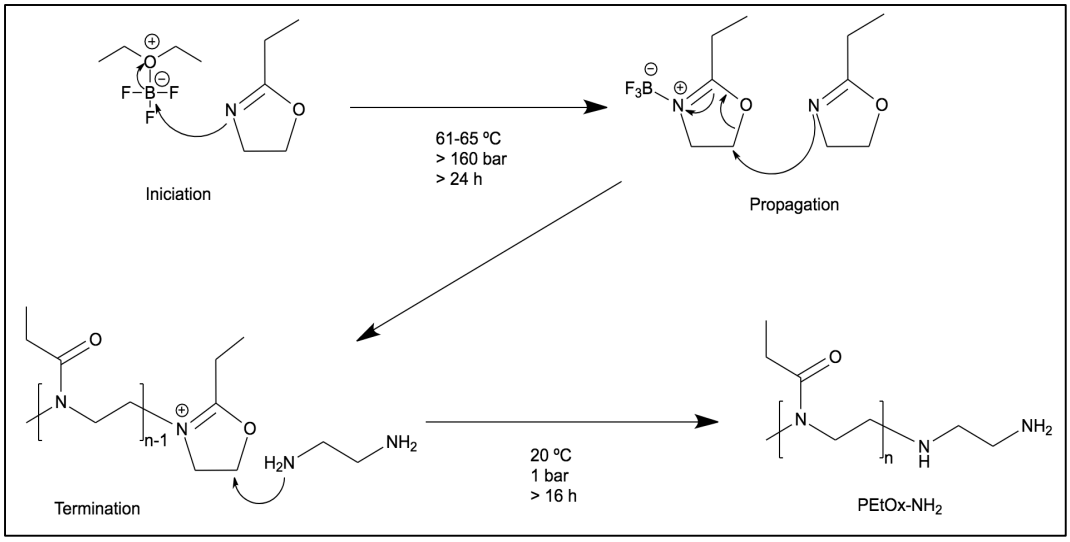

Figure 14 - Proposal for reaction mechanism of polymerization of 2-ethyl-2-oxazoline end-capped ethylenediamine ($PEtOx\text{-}NH_2$)

Through the analysis of ^{1}H and ^{13}C NMR spectra (Figure 15 and Figure 16, respectively), it was possible to confirm the characteristic peaks of the poly(2-ethyl-2-oxazoline) and the ethylenediamine that linked to the polymer.

$PEtOx\text{-}NH_2$ (yellow oil): ^{1}H NMR (400 MHz, $CDCl_3$): δ 3.43 (bs, 68H), 2.82-2.68 (bs, 4H), 2.38-2.16 (bs, 46H), 1.10 (bs, 55H) ppm**; ^{13}C NMR (400 MHz, $CDCl_3$):** δ 174.87, 174.06, 70.58, 53.53, 41.75, 45.56, 43.92, 38.54, 29.71, 29.51, 26.07, 9.85, 9.55, 9.44, 1.09 ppm.

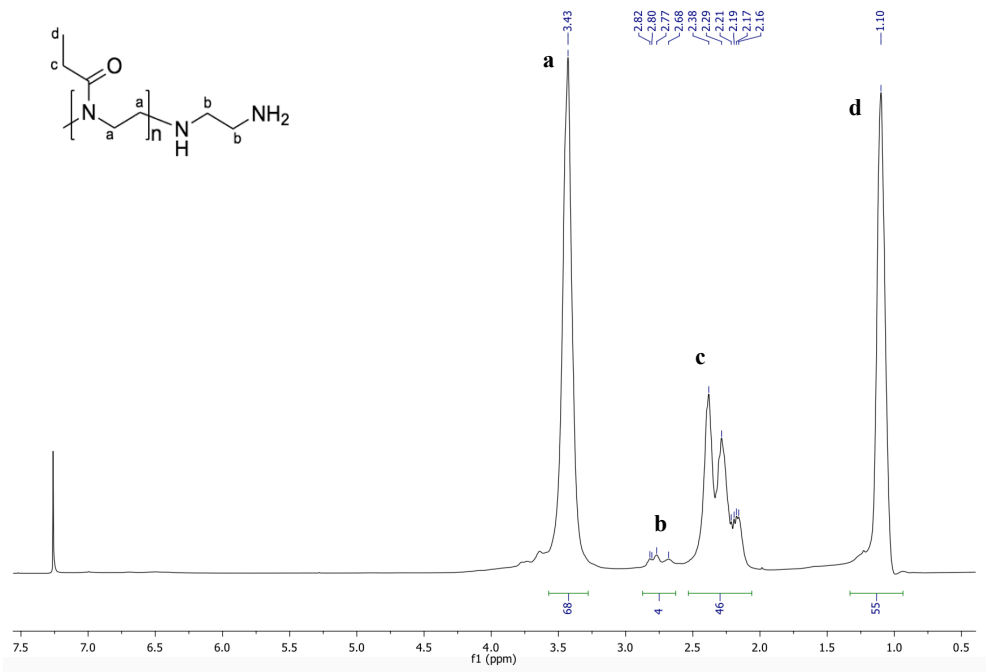

Figure 15 - ^{1}H NMR spectrum of PEtOx-NH_2 in $CDCl_3$

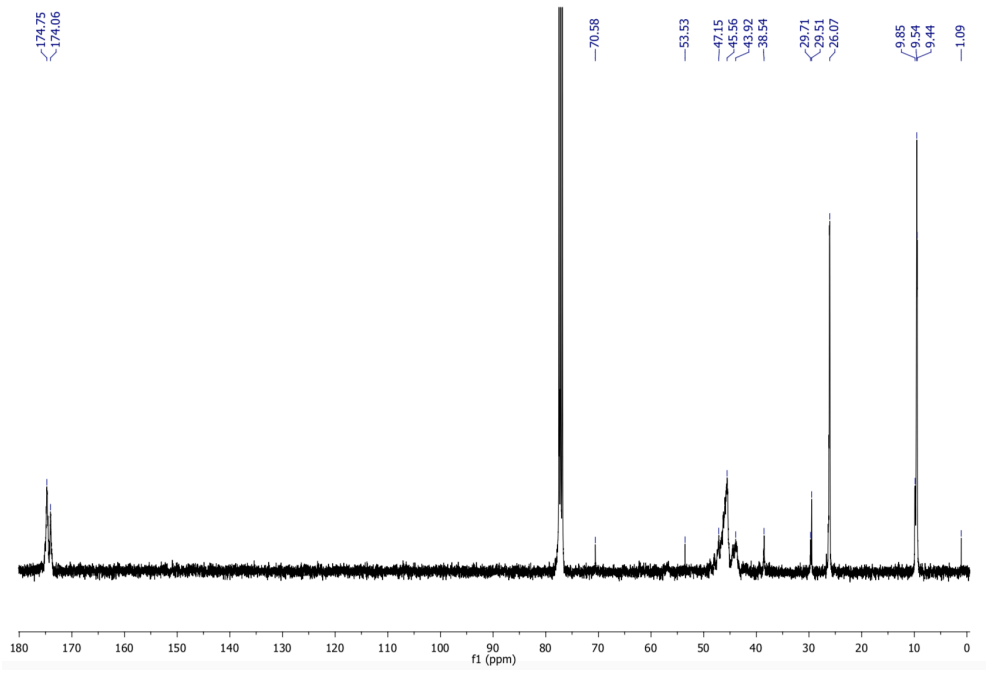

Figure 16 - ^{13}C NMR spectrum of PEtOx-NH_2 in $CDCl_3$

3.2. Conjugation Compounds

3.2.1. Conjugation of Activated Fusidic Acid with Polymers

To form a polymer bound with fusidic acid, it is required a compound that reacts with the FA, to facilitate the conjugation reactions with polymers, because the FA is very stable. The compound that reacts with the FA must have two important characteristics: activate the FA to react with the polymer without disrupting the FA structure and allowing to maintain their antimicrobial properties, i.e. protecting the carboxylic group and ensure that it is transformed in a good leaving group. The NHS will react with the carboxylic group of FA, which will activate the carboxylic group, namely, protecting this group to prevent the biological deactivation of fusidic acid, and forming the compound fusidic-NHS (FA-NHS) (Figure 17). But, for the reaction to occur with NHS it is necessary to activate the carboxylic acid, which is ensured with the *N*,*N*'-dicyclohexylcarbodiimide (DCC) and using triethylamine (TEA) as a base that will deprotonate the hydroxyl group of NHS to form an ester bond.

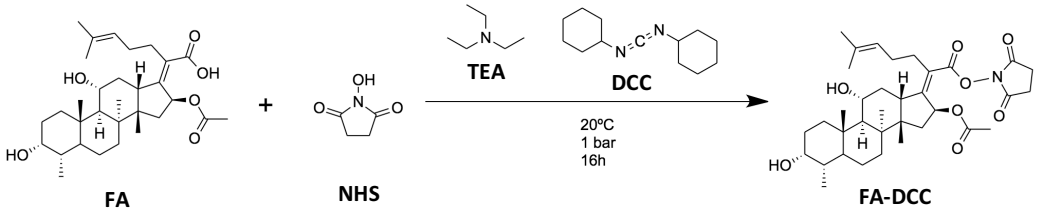

Figure 17 - Syntetic methodology adopted for activation of fusidic acid (FA-NHS)

The results of the ^{1}H NMR spectrum (Figure 18) of the first attempt indicates that the product has undesired impurities, such as remains of unreacted NHS (2.75 ppm) and dicyclohexylurea (DCU) (5.63-5.60 ppm), a by-product of the reaction with DCC and free fusidic acid (5.88 ppm). The presence of these impurities leads to two conclusions: there was no reaction or the purification steps were not effective. The presence of DCU could be related with bad vacuum filtration. The fusidic acid molecular mass is slightly higher than the cut-off of the membrane (516.71 g/mol), since the cut-off size of membrane is limited (500 g/mol), it may be the reason why it is present in the reaction products. Another problem that may have occurred is related to the work up of the reaction, since the ester FA-NHS is very unstable and reactive. Indeed, extractions or dialysis with water may have provoked FA-NHS hydrolysis to the FA. The presence of FA was clearly identified on the ^{1}H NMR by the duplet at 5.88 ppm from H-16. Another important fact to this unsuccessful attempt is the use of DMSO, because it is very hard to remove: first, to evaporate DMSO it was required a high temperature (189° C) and in second, DMSO destroyed the dialysis membranes and to prevent this event it was necessary to put considerable quantities of water, making the process inefficient.

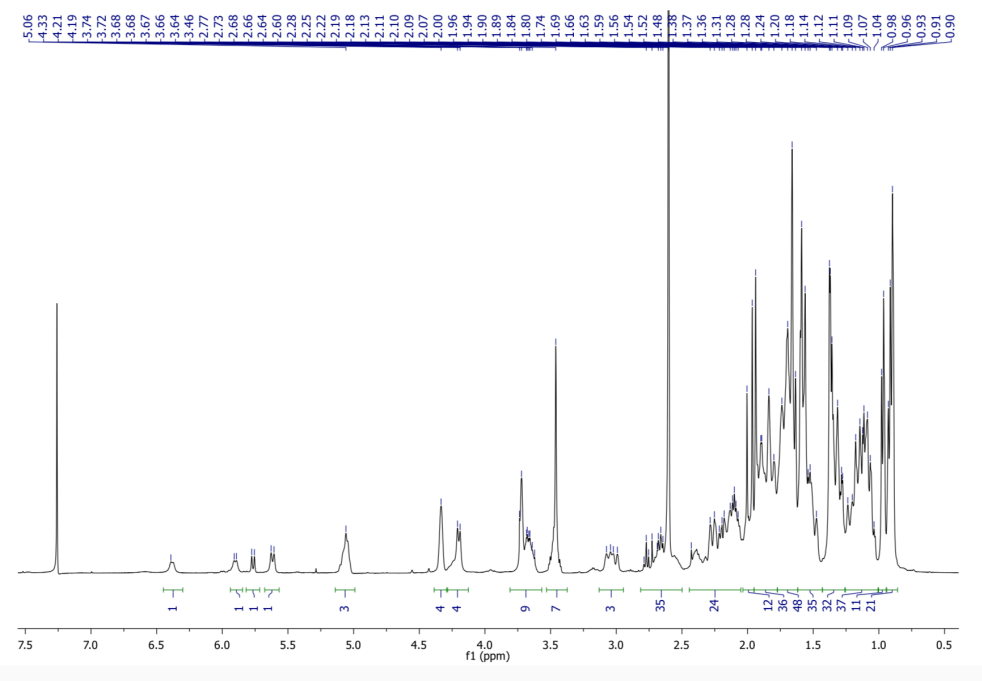

Figure 18 - ^{1}H NMR spectrum of FA-NHS (1st attempt) in $CDCl_3$

In order to solve the DMSO solvent removal issues, a 2nd and 3rd attempts were performed. The use of solvents like chloroform, acetonitrile and DMF are easier to remove. To remove DMF in the 3rd attempt, a liquid-liquid extraction was performed using water and ethyl acetate allowing to separate the product (in the organic phase) from DMF (in the aqueous phase). Comparing the ^{1}H NMR spectrum of the last attempt with the 2nd and 3rd attempts (Figure 19 and 20, respectively), it showed that the 2nd and 3rd attempts were slightly cleaner than the 1st attempt. However, there issues of the 1st attempt persisted: NHS, DCU, FA presence's and also some residues of solvents used in reactions, like ethyl acetate (4.16 – 4.08 ppm) and DMF (8.00, 2.95 and 2.87 ppm) in the 3rd attempt. So, it was not possible to determine the characteristic peaks of the activated product ester bond or any other relevant NMR chemical shift that confirms the presence of activated fusidic acid.

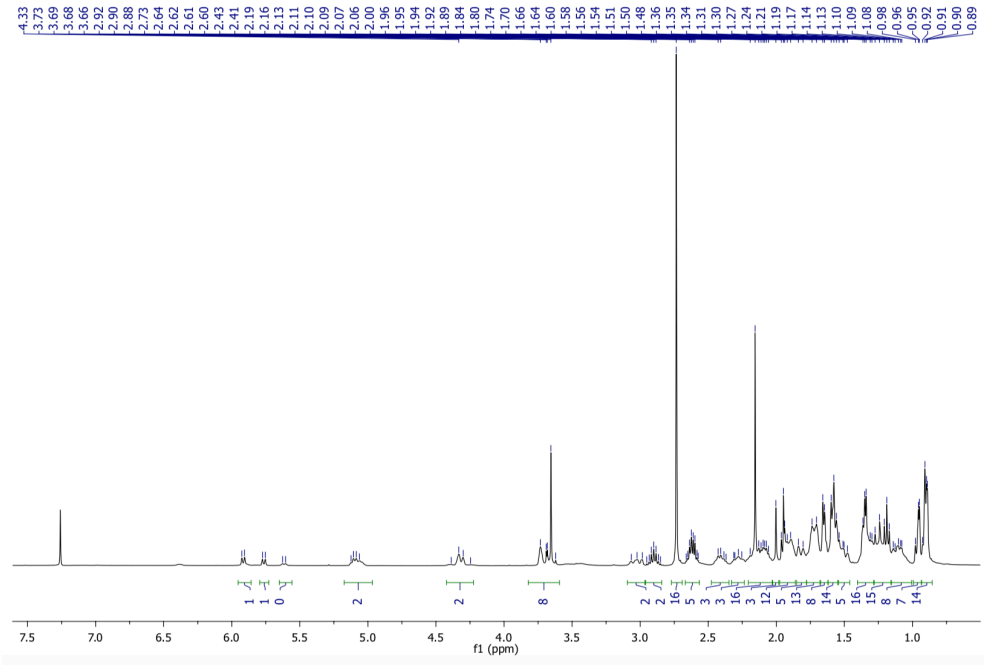

Figure 19 - ^{1}H NMR spectrum of FA-NHS (2nd attempt) in $CDCl_3$

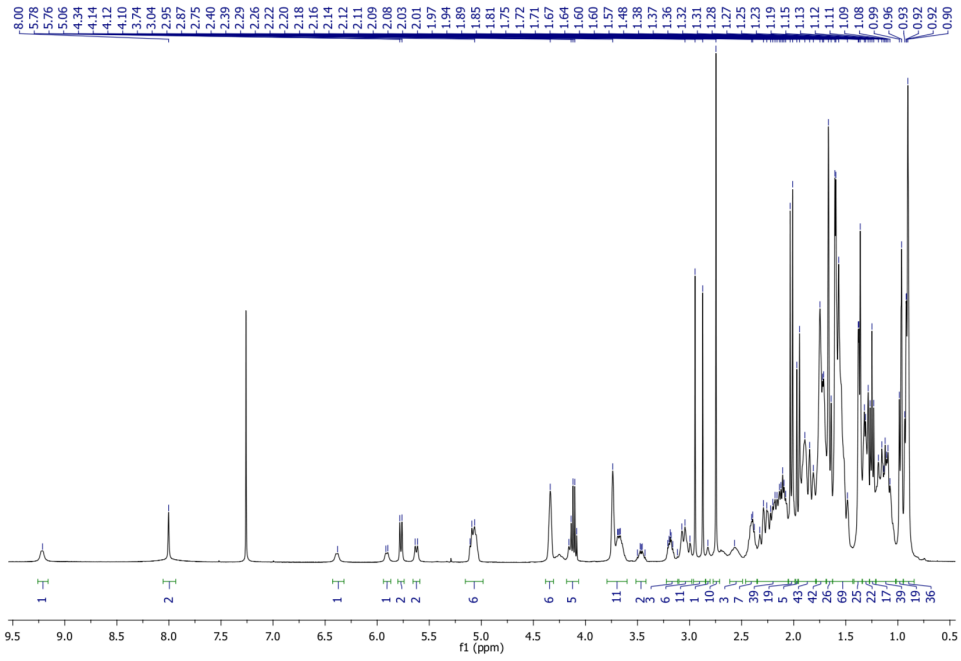

Figure 20 - ^{1}H NMR spectrum of FA-NHS (3nd attempt) in $CDCl_3$

Despite the results, the obtained reaction products were mixed with the PEtOx-NH_2 and the PEG-NH_2, respectively, in order to determine if the reaction occurred, assuming that there was some activated fusidic acid. The mechanism of this reaction is similar to the fusidic acid activation reaction, where the end-capped amine group of the polymers will replace the protective acid group by attacking the ester bond and forming an amide bond (Figure 21).

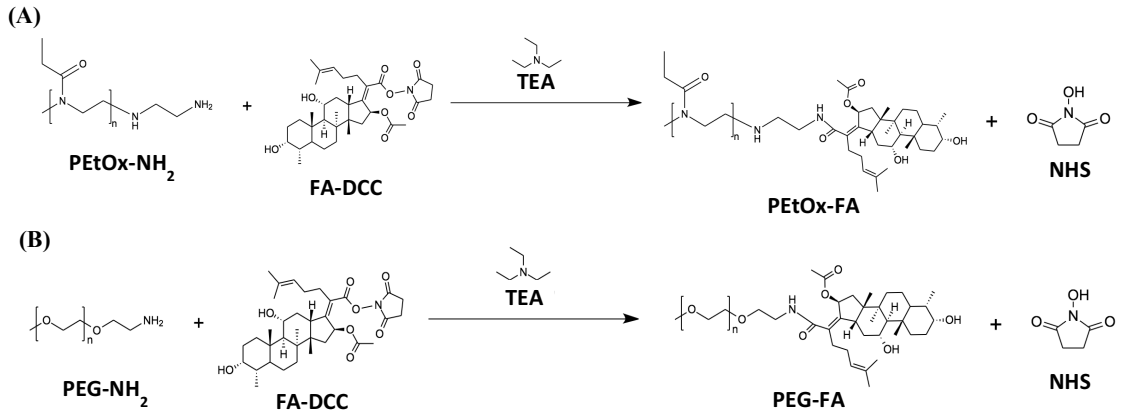

Figure 21 - Reaction between polymers with FA-NHS: (A) PEtOx-NH_2; (B) PEG-NH_2

Both ^{1}H and ^{13}C NMR spectra of the reaction with PEtOx-NH_2 and with PEG-NH_2 (Figure 22 and 23, respectively for ^{1}H, Annex 2 for ^{13}C) showed the characteristics chemical shifts of the polymers and the fusidic acid, but similar to the previous process, there is no evidence of conjugation of the fusidic acid, either with PEtOx-NH_2 or PEG-NH_2. In addition, it had the same problems from the activation reaction: the presence of NHS and DCU. In conclusion, the reaction of fusidic acid conjugation did not occur. As mentioned before, the presence of water during the work up of the FA-NHS preparation was the cause of reaction failure: water destroys the connection of activated fusidic acid (FA-NHS), hence explaining the presence of huge NHS peak in ^{1}H NMR spectra.

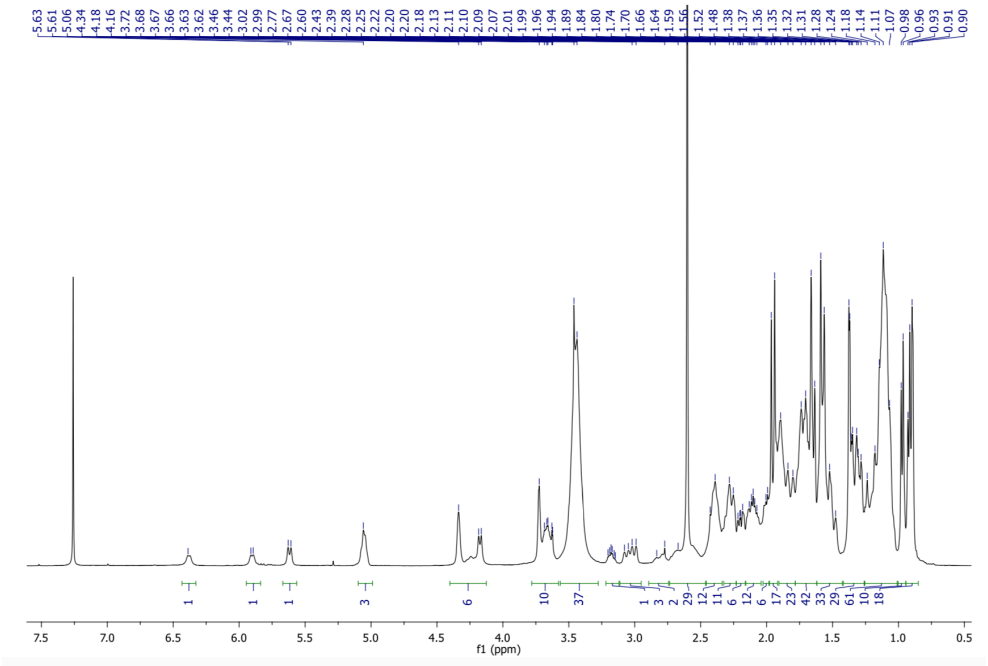

Figure 22 - ^{1}H NMR spectrum of conjugation reaction with PEtOx-NH_2 in $CDCl_3$

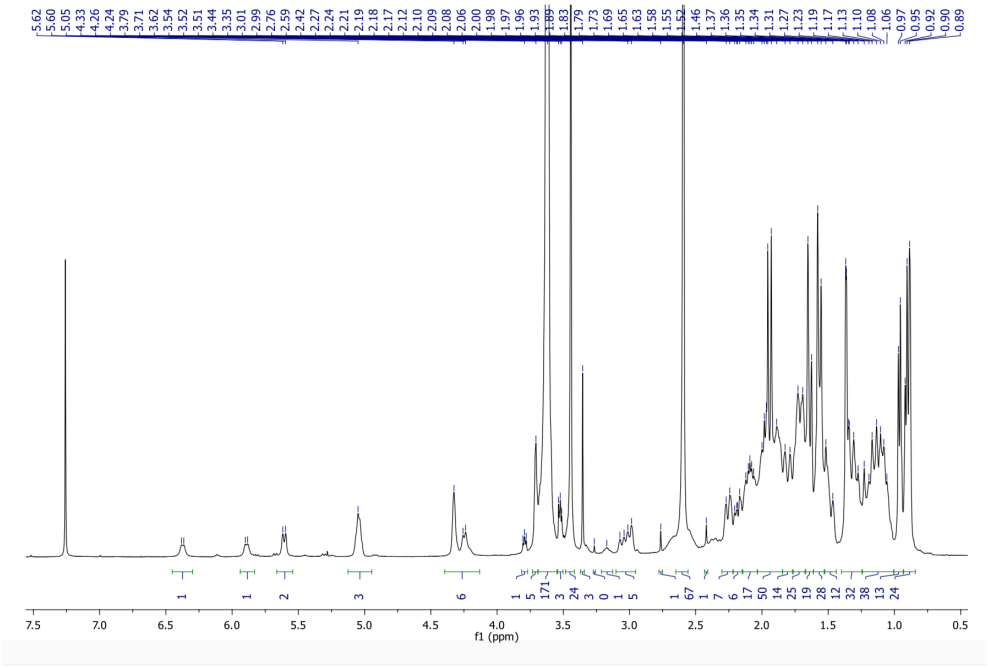

Figure 23 - ^{1}H NMR spectrum of conjugation reaction with PEG-NH_2 in $CDCl_3$

3.2.2. Conjugation in One-pot Reaction

Since the previous synthetic methodologies, which involved the isolation of the activated FA were not successful, it was decided to make the conjugation reactions in one-pot procedure and in inert atmosphere environment following a reported procedure from literature[69]. In these conditions, it was possible to avoid some of the problems in terms of purification, such as the use of DCC as a good leaving group instead of the NHS and the removal of the DCU that precipitate from DCM. Additionally, working in nitrogen environment prevents the presence of water, which can destroy the reaction intermediate.

The first step of this reaction began with the formation of an intermediary with fusidic acid and DCC linked by an ester bond (Fig. 24A). Then in the presence of a catalytic amount of DMAP, which will attack the carbon from ester bond, allowed to form a new intermediary product between fusidic acid and DMAP (FA-DMAP) and DCU (it precipitates in the reaction medium) (Fig. 24B). The final step was the conjugation with poly(2-ethyl-2-oxazoline) end-capped ethylenediamine (PEtOx-NH_2) (Fig. 24C) or with methoxypolyethylene glycol amine (PEG-NH_2) (Fig. 24D), where the terminal amine of the polymers attacks the intermediate FA-DMAP with liberation of DMAP that can activate another FA molecule.

Both 1D and 2D NMR spectra of PEtOx-FA and PEG-FA were analysed in conjunction with ^{1}H and ^{13}C NMR spectra of PEtOx-NH_2 (see chapter 3.1), FA (Annex 3) and PEG-NH_2 (Annex 4).

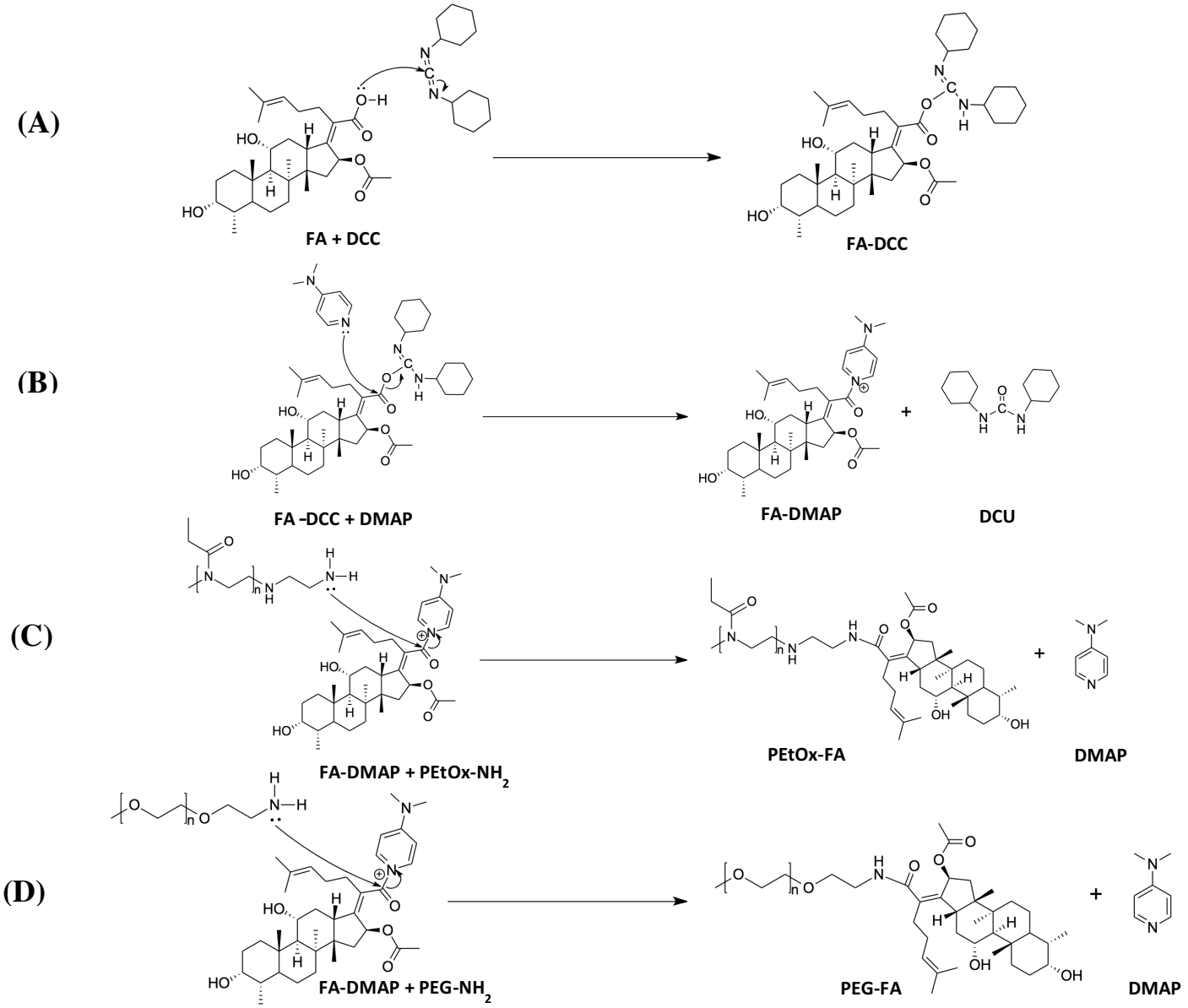

Figure 24 - Mechanism of conjugation reactions with the formation of: (A) FA-DCC; (B) FA-DMAP and DCU; (C) PEtOx-FA and (D) PEG-FA

3.2.2.1. Fusidic Acid – Benzylamine

To verify that this new method works, it was necessary to confirm that a bond between a carboxylic group of FA and an amine group allows to form an amide bond. So, a conjugation reaction was performed using as nucleophile, the primary amine, benzylamine. Similar to the reaction mechanism of polymer conjugation, the amine group attacked the connection between fusidic acid and the DMAP (Figure 25) giving origin to the conjugated compound FA-$BzNH_2$.

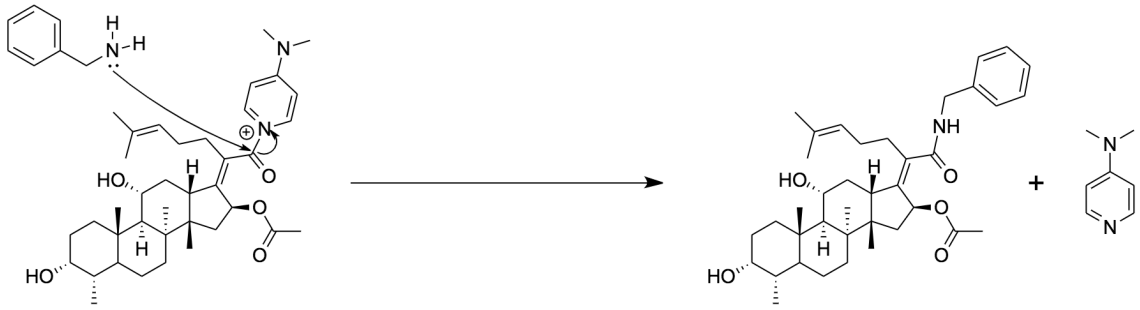

Figure 25 - Mechanism of conjugation reaction between benzylamine and fusidic acid (last part)

Through the analysis of the ^1H NMR Spectrum (Annex 5), are identified the signals of the protons of the phenyl group between 7.49 and 7.28 ppm as well as the signals of the methylene group at 4.3 ppm. This last signal integrates for 3 protons because at this field it is also present the signal of the proton H-11 of the fusidic acid (see Annex 3). The signals at 2 ppm and 1.96 pm are also singlet signals corresponding to two acetyl groups. In this reaction, besides the product of combination with benzylamine was also identified another secondary reaction product from the fusidic acid showing signs at 4.61 ppm possibly due the proton H-11. The hydroxyl group in this position must have attacked another molecule of fusidic acid forming an ester linkage. Through the mass spectra in both negative and positive ionization modes, the presence of the conjugate fusidic acid-benzylamine (FA-$BzNH_2$) and of the ester form with two molecules of fusidic acid (Figure 26) were confirmed.

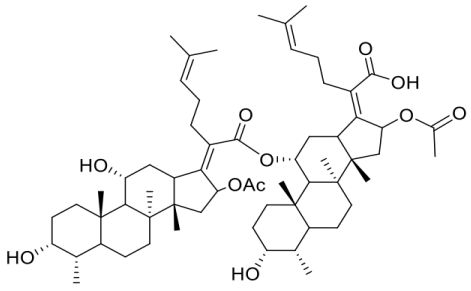

Figure 26 - Ester of two molecules of fusidic acid

In the mass spectrum (positive mode), the two values of apparent molecular masses were 314.2 and 431.3 Da, while in negative mode, the values were 540.2 and 657.3 Da. Figure 27 represents the mass spectra in the positive and negative ionization modes with the fragmentation patterns found in each of the compounds that are representatives of the conjugation reaction with the benzylamine.

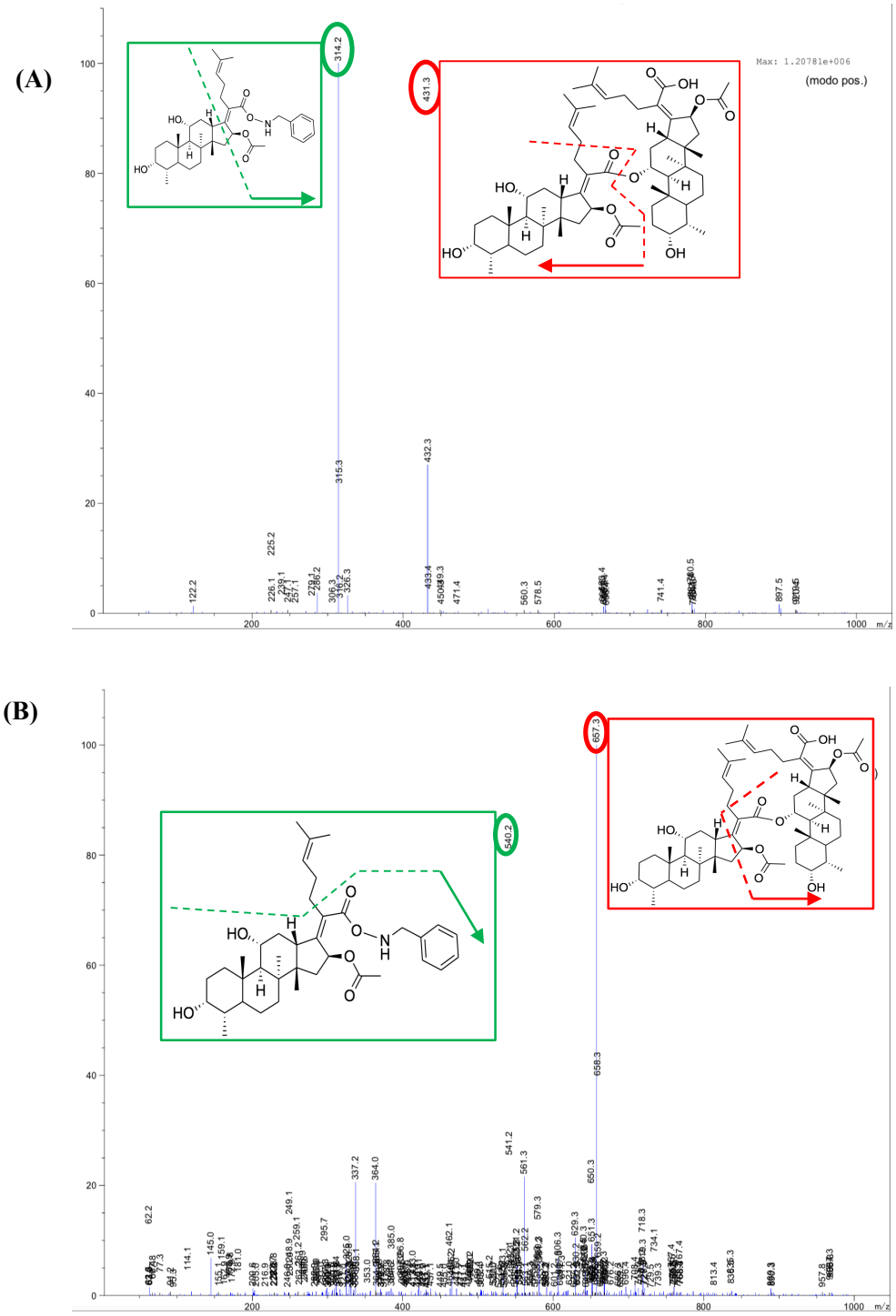

Figure 27 – Mass spectra of benzylamine-fusidic acid (A) positive and (B) negative mode (green - benzylamine-fusidic acid; red - ester of two molecules of fusidic acid)

The molecular ions of FA-BzNH_2 and ester of FA were not visible in both mass spectra. In the positive mode, verify the existence of mass fragments of both products, but in the negative mode, matched to mass fragments with less a molecule of water in both products. With these results, it could be concluded that the conjugated compound was successfully obtained. However, the formation of other secondary products like the fusidic acid conjugation with itself also occurred. It is also noted that there was only a single step of purification in this product.

3.2.2.1. PEtOx-FA

First, in the ^{13}C NMR spectrum of PEtOx-FA showed an isolated chemical shift at 172.8 ppm that indicated the presence of an α, β-unsaturated amide of the conjugated product. Second, in the HMBC (Heteronuclear Multiple Bond Correlation) spectrum, there was a correlation between the H-22 protons from the fusidic acid at 2.4 ppm and the carbon at 172.8 ppm (from the new formed amide) and also a correlation between the protons from the polymer terminals at 3.4 ppm and the carbon at 172.8 ppm. Both correlations indicate that there was a new bond formed between the polymer and fusidic acid. Finally, the protons at 2.7 ppm in the polymer disappeared, which means that those protons were more unshielded in the conjugated product and were shifted in to the broad signal at 3.4 ppm. Figure 28 shows the chemical structure of the compound with the signs and correlations found in the HMBC NMR spectrum. The mass spectrum did not present the characteristic Gaussian distribution of masses for a polymer which may be due to an inefficient ionization of the compound. The ^{1}H ,^{13}C, HSQC and HMBC NMR full spectra are in Annex 6. Through detailed analysis of the NMR data of PEtOx-FA and comparing with NMR data of FA and PEtOx-NH_2, it was possible to conclude that conjugation of fusidic acid with polyoxazoline was successful (Figure 29).

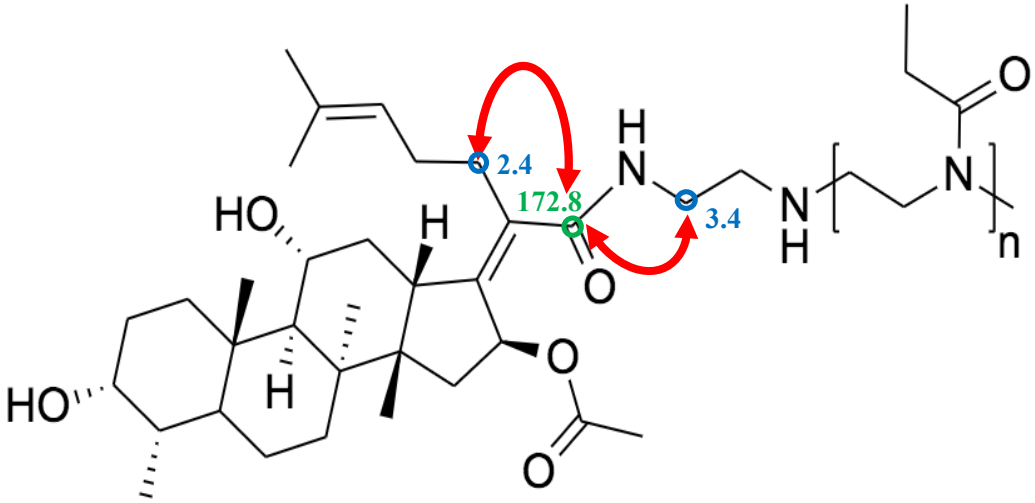

Figure 28 – Chemical structure of PEtOx-FA with NMR peaks (blue – ^{1}H; green – ^{13}C) and HMBC correlations (red)

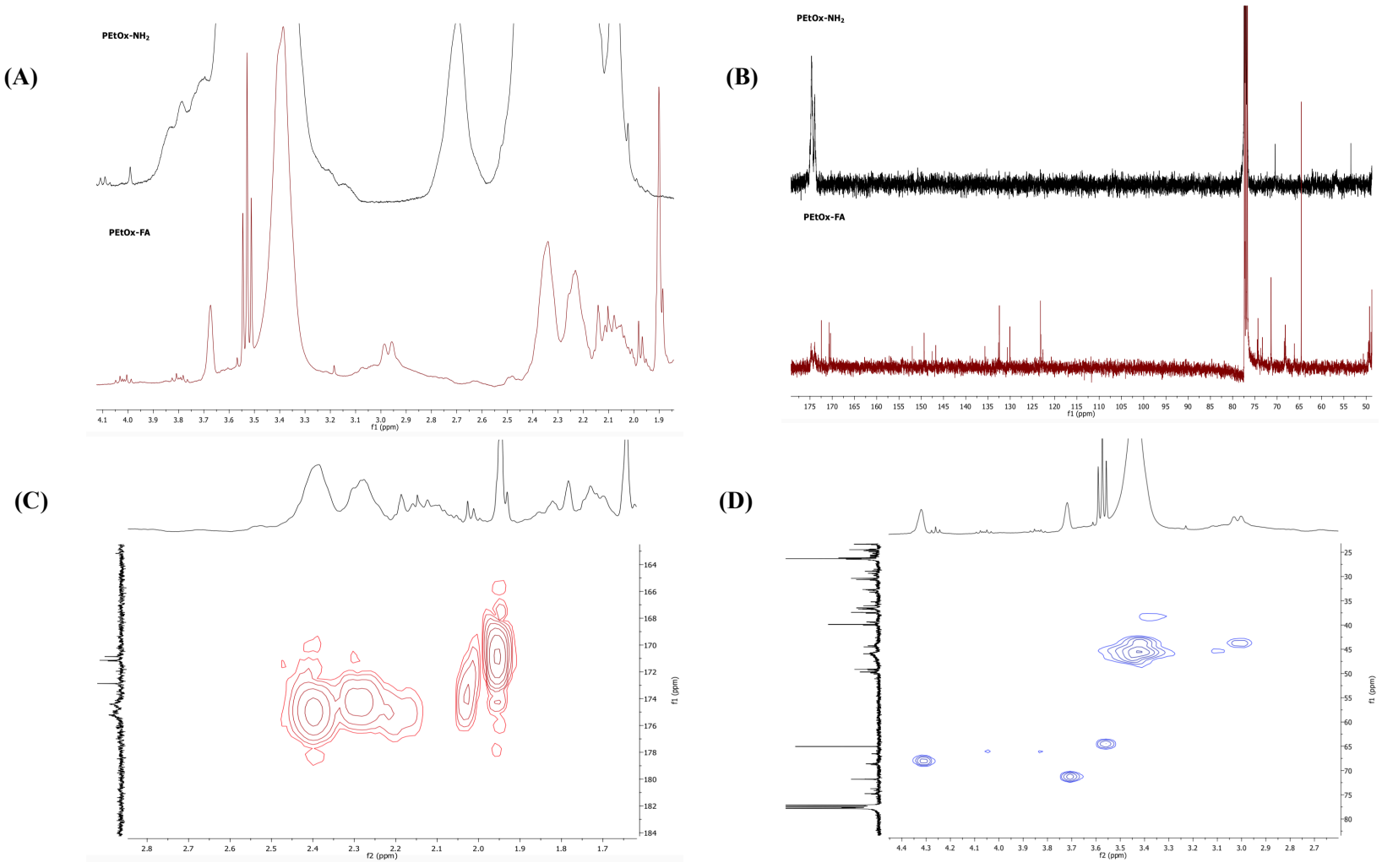

Figure 29 - (A) ^{1}H NMR and (B) ^{13}C NMR spectra comparison of PEtOx-NH_2 and PEtOx-FA; (C) HSQC and (D) HMBC expanded of PEtOx-FA

3.2.2.2. PEG-FA

By comparing the ^{1}H and ^{13}C spectra of PEG-NH_2 and PEG-FA, there was evidence that the PEG was conjugated with the fusidic acid: the protons next to the amine group disappear in the ^{1}H and ^{13}C spectra of the polymers at 2.8 ppm and 41.8 ppm, respectively. The ^{1}H and ^{13}C spectra of the conjugated FA with PEG showed downfield as expected, at 3.03 ppm and 44.0 ppm, respectively. The ^{13}C spectrum of PEG-FA had a new sign at 172.6 ppm that suggested formation of a new carbonyl group the in the conjunction product. The 2D spectrum did not give any relevant information. Figure 30 shows the chemical structure of the compound and highlights the chemical shifts found in the ^{1}H NMR spectra. As for the mass data, both the PEG-NH_2 and PEG-FA spectra presented the characteristic Gaussian distribution of masses with mono and double charged fragments. Moreover, the PEG-FA spectrum showed a mass increment of 498 Da in relation to PEG-NH_2. The ^{1}H, ^{13}C, HSQC and HMBC NMR spectra are in Annex 7. Through detailed analysis of the NMR data of PEG-FA, FA and PEG-NH_2, it was possible to conclude that the conjugation of fusidic acid with polyethylene glycol was successful (Figure 31).

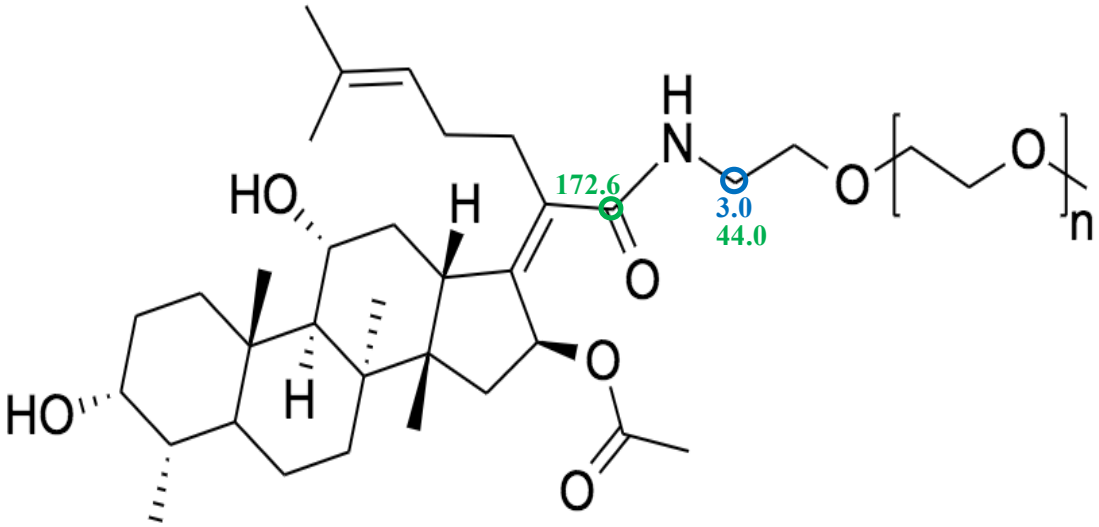

Figure 30 - Chemical structure of PEG-FA with NMR peaks (blue – ^{1}H; green – ^{13}C)

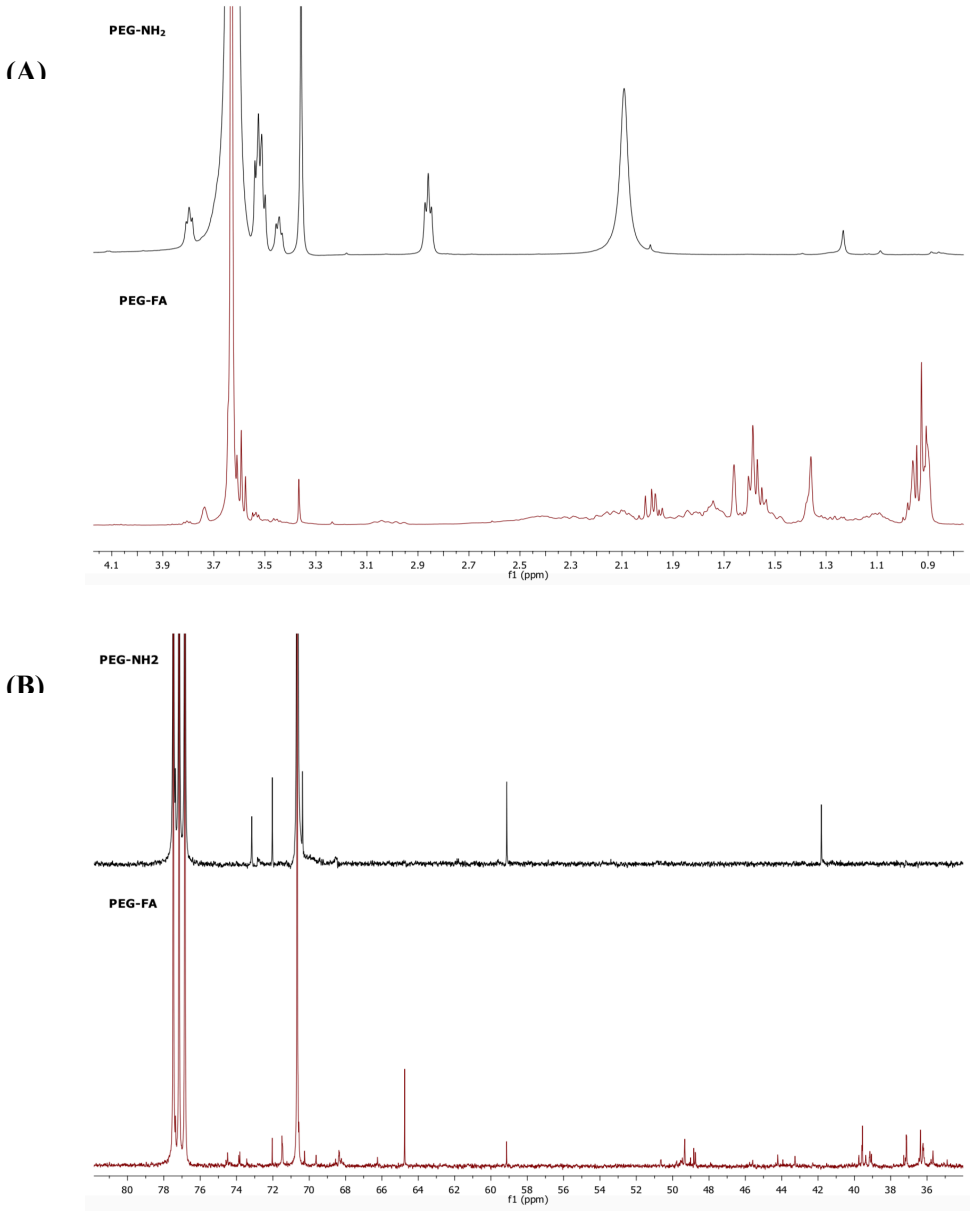

Figure 31 - (A) ^{1}H NMR and (B) ^{13}C NMR spectra comparison of PEG-NH_2 and PEG-FA

3.3. Antimicrobial activity evaluation

The microbial assays were performed to determine the minimum inhibitory concentration (MIC) of five different test compounds against three different strains of *Staphylococcus aureus*. The tested compounds were fusidic acid, PEtOx-NH_2, PEtOx-FA, PEG-NH_2 and PEG-FA. The tested *S. aureus* strains were: ATCC 25923, a control MSSA strain; JE2, a derivative of MRSA strain LAC; and UAMS-1, MSSA strain.

Analysing the results, Table 2, the MIC values of the polymers (PEtOx-NH_2 and PEG-

NH_2) indicated that both polymers did not exhibit any antimicrobial activity at low concentrations. The MIC values of the conjugated compounds, PEtOx-FA and PEG-FA, demonstrated antimicrobial activity but revealed higher MICs than the non-conjugated FA, meaning that fusidic acid when conjugated with any of the polymers lost antimicrobial activity.

Table 2 - MIC values of fusidic acid, polymers and conjugate compounds in MSSA (ATCC 25923, UAMS-1) and MRSA (JE2) strains

	FA (µg/ml)	**PEtOx-NH_2 (µg/ml)**	**PEtOx-FA (µg/ml)**	**PEG-NH_2 (µg/ml)**	**PEG-FA (µg/ml)**
ATCC 25923	0.78	> 12.5	6.25	> 12.5	3.125
JE2	0.195	> 12.5	3.125	> 12.5	1.5625
UAMS-1	0.195	> 12.5	3.125	> 12.5	3.125

3.4. Microparticles Formulation

There are four types of dry powder formulations in this work: trehalose – leucine (TL), trehalose – leucine – fusidic acid (TLFA), trehalose – leucine – fusidic acid conjugated with PEtOx-NH_2 (TLPEtOx-FA) and trehalose – leucine – fusidic acid conjugated with PEG-NH_2 (TLPEG-FA). All these formulations were dissolved in water to dissolve the trehalose and in ethanol to dissolve leucine, fusidic acid, PEtOx-FA and PEG-FA. For each formulation, the first step for atomization was to find the best operating conditions by establishing the temperature in the static mixer, temperature of air, the pressure in the static mixer and gas to liquid ratio.

Temperature is a very important parameter to control due to the melting temperature of trehalose dehydrate (97-99 ºC) and also has a tendency to caramelize, which can cause clog in the nozzle. Thus, the temperature used in the static mixer was 80° C for one only reason: prevent the caramelisation of trehalose. The temperature of air to drying the particles in the precipitator need to be well efficient because of water and ethanol' boiling temperature (78ºC and 100ºC, respectively). The best drying temperature is between 115ºC to 140ºC. Below this range of temperatures, the drying efficiency decreases, but above this range, it has the risk of caramelize and degrade the trehalose. The used pressure was 103.3 bar and 120.4 bar and the used gas to liquid ratio, which was calculated using the volumetric flows, was 4.55 and 7.14. These changes in these two parameters were used to see the different characteristics of the

microparticles, such as morphological and aerodynamic properties.

Table 3 summarizes the operation conditions for each assay. The yields obtained in the second and fourth assays were lower, due to clogging of the nozzle problems caused by powder accumulation and/or the broken O-ring of the nozzle caused by sudden rise of air temperature. The yields of the ninth and eleventh assays decreased in relation to the eighth and tenth assays respectively, because of small leak in the precipitator. The TLFA, TLPEtOx-FA and TLPEG-FA assays showed improvements in terms of yields compared with the TL assays.

Table 3 - Operating parameters of the assays and the respective yields

Assay	**DPF**	**DPF Code**	**Tsm (ºC)**	**TscCO_2 (ºC)**	**Tair (ºC)**	**Pressure (bar)**	**QCO_2 / Qsolution**	**Yield (%)**
1	TL	**TL1**	80	80	115	103.3	4.55	62.3
2		**TL2**	80	80	140	120.4	7.14	26.4
3		**TL3**	80	80	140	120.4	7.14	50.8
4		**TL4**	80	80	140	120.4	7.14	28.8
5		**TL5**	80	80	140	120.4	7.14	50.8
6	TLFA	**TLFA1**	80	80	140	120.4	7.14	55.8
7		**TLFA2**	80	80	140	120.4	7.14	62.0
8	TLPEtOx-FA	**TLPEtOx-FA1**	80	80	140	120.4	7.14	67.4
9		**TLPEtOx-FA2**	80	80	140	120.4	7.14	47,6
10	TLPEG-FA	**TLPEG-FA1**	80	80	140	120.4	7.14	61.6
11		**TLPEG-FA2**	80	80	140	120.4	7.14	42.6

Tsm – Temperature of static mixer; TscCO_2 – Temperature of supercritical CO_2; Tair – Temperature of compressed dry air; QCO_2 / Qsolution - ratio of the CO_2 volumetric flow rate over the solution flow rate.

3.5. Morphology

Analysing the Table 4, the $D_{v,50}$ in all the dry powders have values between 13 and 19 μm, when comparing the geometric and numeric diameters, $D_{n,50}$, which have a range between 2 and 7 μm, showing the existence of large agglomerates. The span values show two different result sets: span values between 1 and 2 indicate that the microparticles are more homogenous, while the span values greater than 2 indicate that microparticles are more heterogeneous. The TLFA1 microparticles is the best dry powder in morphological terms, due it lowest $D_{v,50}$ value and low span value.

Table 4 - Size properties of the DPFs microparticles

Assay	**DPF**	**$D_{n,50}$ (μm)**	**$D_{v,50}$ (μm)**	**Span**
1	TL	3.93	12.24	2.79
2		6.93	17.68	1.65
3		3.83	12.50	3.83
4		2.92	15.40	2.47
5		2.28	14.42	2.17
6	TLFA	2.52	11.65	1.34
7		3.17	13.84	1.27
8	TLPEtOx-FA	4.71	16.86	1.27
9		4.63	18.13	1.21
10	TLPEG-FA	2.85	17.88	1.29
11		6.51	22.16	1.43

In Figure 32, the images showed the microparticles are mainly spherical and also confirmed the presence of agglomerates in the formulations.

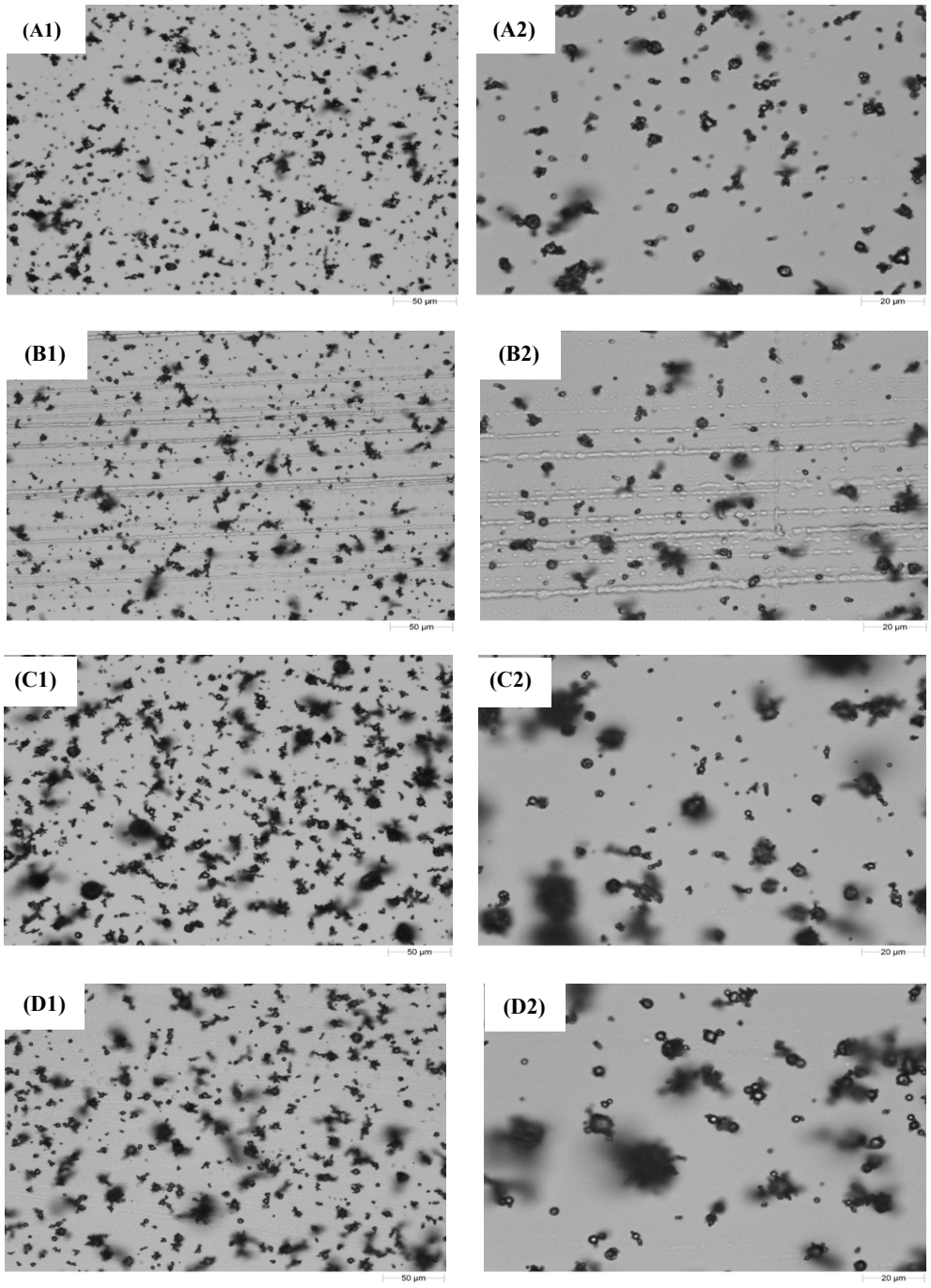

Figure 32 - Morphologi G3 images of the TL microparticles (A1) 20x and (A2) 50x; TLFA microparticles (B1) 20x and (B2) 50x; TLPEtOx-FA microparticles (C1) 20x and (C2) 50x; TLPEG-FA microparticles (D1) 20x and (D2) 50x

The images of SEM in Figure 33, confirmed that the microparticles are spherical and have a smooth texture, presenting agglomerates, as it was observed in the images obtained using Morphologi G3.

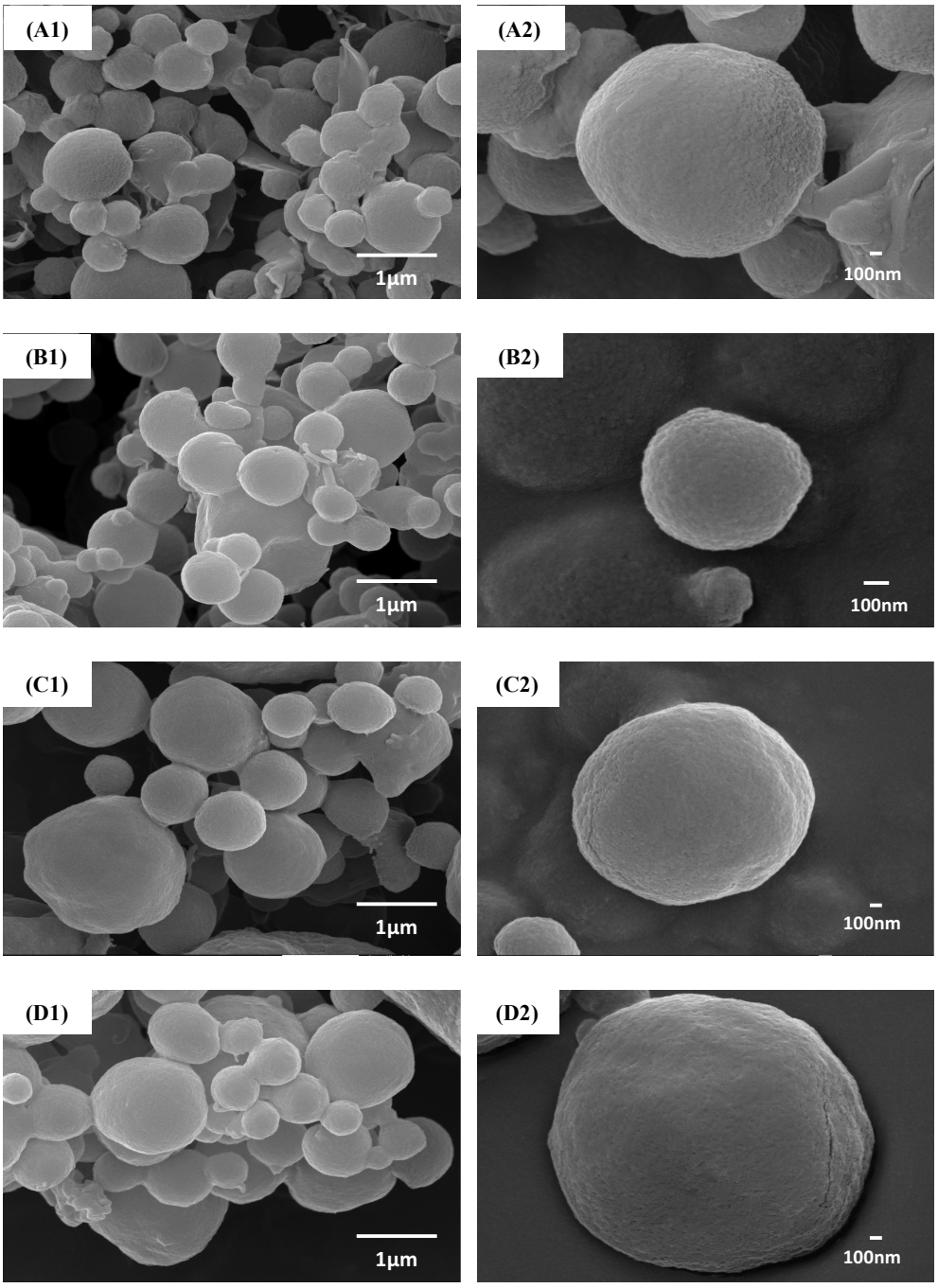

Figure 33 - SEM images of the TL microparticles (A1) 20000x and (A2) 35000x; TLFA microparticles (B1) 20000x and (B2) 60000x; TLPEtOx-FA microparticles (C1) 20000x and (C2) 35000x; TLPEG-FA microparticles (D1) 20000x and (D2) 35000x

3.6. Aerodynamic Properties

The microparticles were analysed by ACI measurements and the DPFs presenting the best aerosolization behaviour are shown in Figure 34. All other the results obtained through ACI measurements are in Annex 8. In general, most of the dry powders were retained in the induction port, which represents the upper airways, because of the presence of aggregates and the formation of turbulent eddies in the curving zone of the tube, that cause aggregates impaction. Excluding the induction port, most of the dry powder deposited between stage 1 and stage 5, which means that a portion of the dry powder reaches the deep lung.

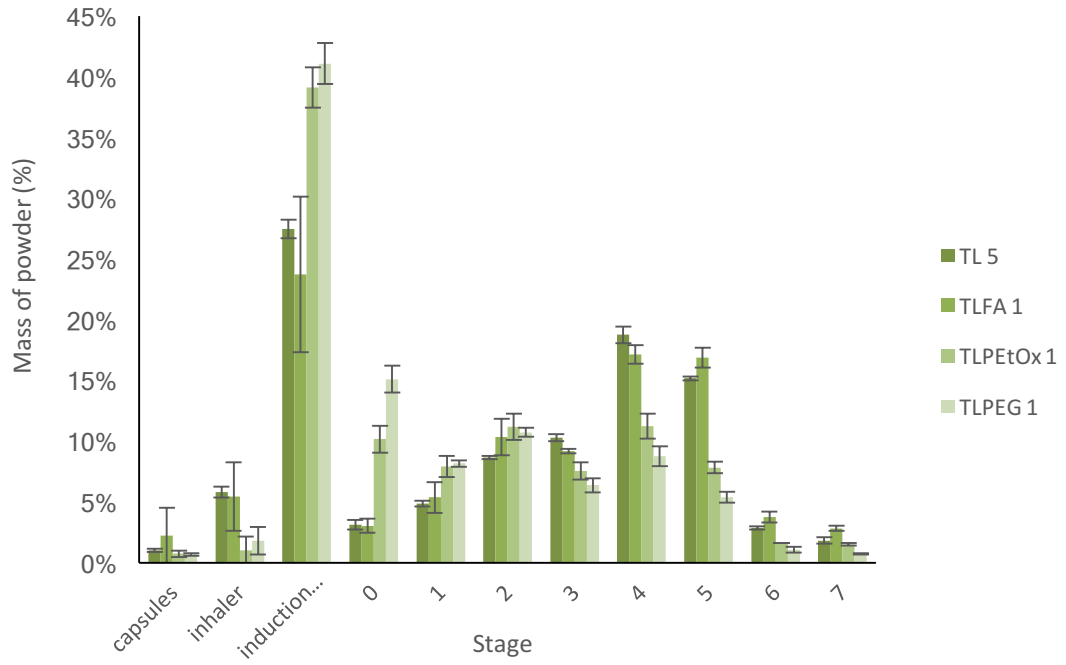

Figure 34 - Graphical representation of the powder distribution in the ACI menauments of DPFs with higher FPF

The FPF, EF, MMAD and GSD values of the best DPFs are summarized in Table 5. The powders presented aerodynamic diameters between 1 and 5µm, which are desired values to ensure the microparticles deposition in the deep lungs. The EF values are also excellent, since there is almost no powder left in the capsule. The FPF of the TL5 and TLFA1 have values above 50%, which means that have less aggregates than the DPF with the conjugate compound (TLPEtOx-FA and TLPEG-FA). With these results, it possible to concluded that the DPFs TL5 and TLFA1 are aerodynamically more suitable for inhalation than DPFs TLPEtOx-FA1 and TLPEG-FA1.

Table 5 - Aerodynamic properties of DPF with higher FPF, determined by ACI and DUSA

DPF	FPF (%)	EF (%)	MMAD (µm)	GSD
TL5	59 ± 1	99.0 ± 0.1	1.48 ± 0.38	2.25 ± 0.01
TLFA1	61.7 ± 0.2	97.8 ± 2.3	1.64 ± 0.09	2.38 ± 0.02
TLPEtOx-FA1	43 ± 4	99.3 ± 0.3	3.15 ± 0.13	2.48 ± 0.06
TLPEG-F1	35 ± 2	99.3 ± 0.1	3.85 ± 0.05	2.34 ± 0.02

3.7. Physical-Chemical Properties

FT-IR spectra of TL microparticles allows checking the presence of trehalose and leucine bands. The FTIR analysis from Figure 35 confirms the presence of trehalose' characteristics absorption bands, which are 3288 cm^{-1} (O-H stretching of the hydroxyls groups) and 1028/ 993 cm^{-1} (C-O stretching) and the leucine' characteristics absorption bands: 2932 cm^{-1} (C-H stretching of methyl group), 1580 cm^{-1} (N-H bending of amine group) and 1407 cm^{-1} (C-N stretching).

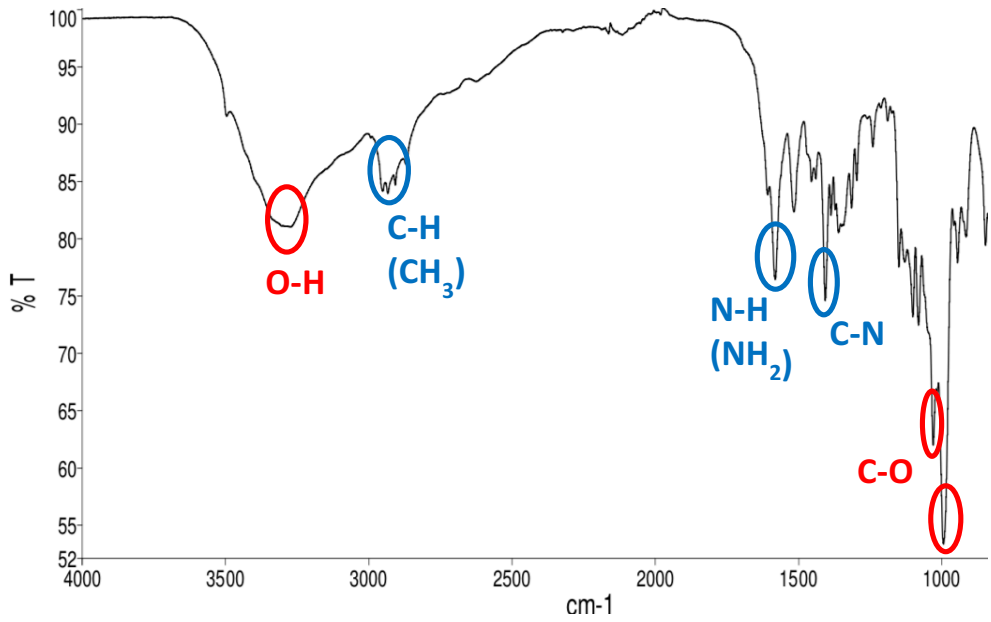

Figure 35 – FT-IR of TL microparticles (red represents the functional groups of trehalose and blue represents the functional groups of leucine)

Comparing the FT-IR of each dry powder with FA, PEtOx-FA, or PEG-FA, the Figure 36 does not indicate any characteristic band of the fusidic acid and of the polymers, just indicates trehalose and leucine. The main reason was the reduced quantities of FA, PEtOx-FA and PEG-FA used for the SASD assays.

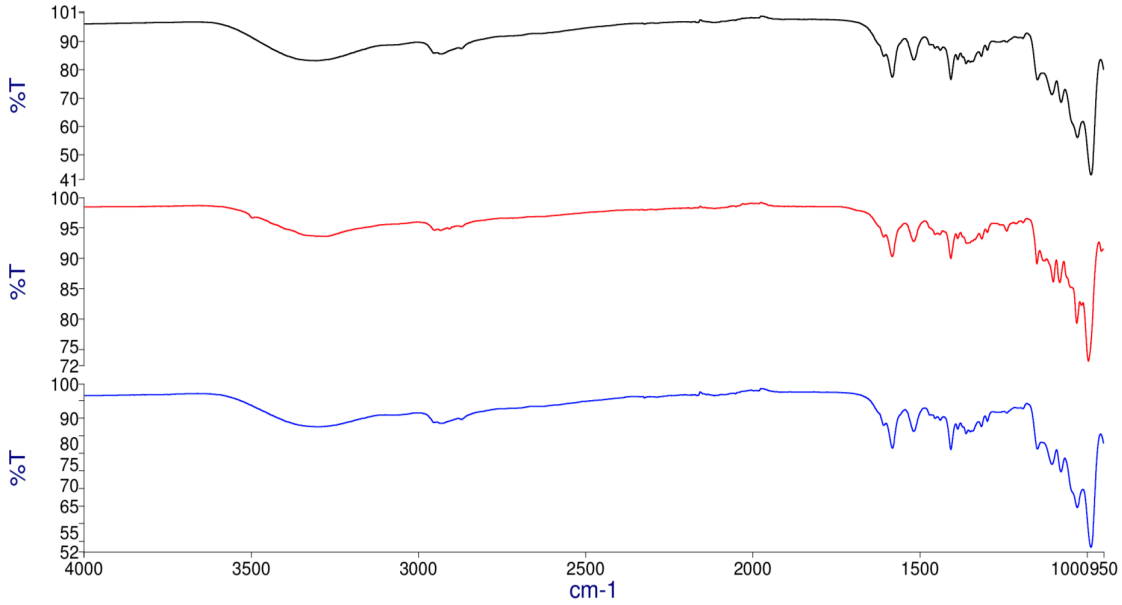

Figure 36 - FT-IR of TLFA (black), TLPEtOx-FA (red) and TLPEG-FA (blue)

The water content for all microparticles are presented in Table 6, showing that the microparticles retained low amounts of water. The lowest values of water content, 3% to 7%, were obtained for trehalose-leucine formulations meaning that the drying efficiency in these assays was very good. The TLFA microparticles have the lowest values of water content, due to its hydrophobic behaviour and TLPEtOx-FA and TLPEG-FA microparticles have higher values then TLFA microparticles, because of the more hydrophilic behaviour of both conjugated polymers.

Table 6 - Water content values for DPFs

Assay	DPF	Water content (%)
1	TL	6.4 ± 0.5
2		7.0 ± 0.4
3		4.2 ± 0.4
4		4.8 ± 0.2
5		5.6 ± 0.3
6	TLFA	3.5 ± 0.2
7		3.6 ± 0.5
8	TLPEtOx-FA	5.1 ± 0.4
9		4.00 ± 0.08
10	TLPEG-FA	4.7 ± 0.3
11		6.8 ± 0.2

3.8. Quantitation of fusidic acid in the dry powders

Through the chromatograms obtained for each of the eight fusidic acid solutions (Annex 10), it was determined that the retention time of the FA is about 20.12 minutes. The values of peak area specific of the FA was used to make a calibration line (Figure 37). The values of the peak area and the retention time for each solution containing FA is found in Table 12 (Annex 10).

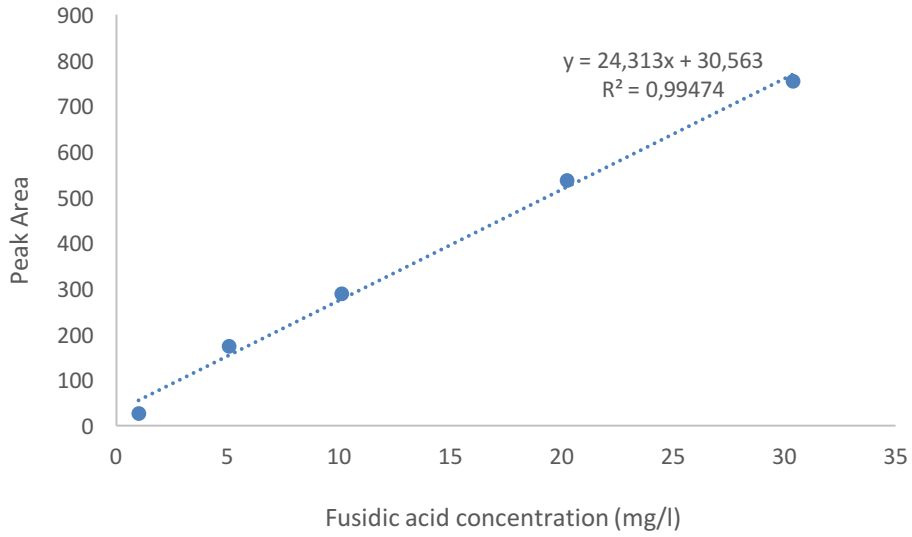

Figure 37 - Fusidic acid calibration line

The equation of the calibration line allowed to calculate the concentration of fusidic acid contained in the dry powders:

$$(5) \qquad C\ (mg/l) = \frac{PA - ordinate\ intersect}{slope}$$

Where C is the concentration of fusidic acid in the sample and PA is the peak area fusidic acid in the sample. To calculate the mass of fusidic acid in the sample (volume of solution used in each sample was 25 ml):

$$(6) \qquad m\ (mg) = C\ (mg/l) \times V_{solution}(l)$$

The results from Table 7 showed that quantity values of fusidic acid contained in the dry powder samples were between 0.112 mg and 0.127 mg. By comparing these values with the MIC values from the antimicrobial activity evaluation, the amount of FA in the powder is more than enough to perform antimicrobial assays.

Table 7 - Determination of the quantity of fusidic acid loaded in the dry powders formulation samples

Sample of DPF	Concentration of FA (mg/l)	Mass of FA (mg)
TLFA1	4.95	0.124
TLFA1 (B)	4.46	0.112
TLFA2	5.08	0.127
TLFA2 (B)	4.58	0.115

With these results it was possible to make three estimates: i) the total amount of FA in the dry powder; ii) the atomization yield of the FA; and iii) the amount of the FA per capsule (30 mg). By analysing Table 8, it showed that a part of the FA was lost during the atomization process in the SASD.

Table 8 - Estimative of the total quantity of the fusidic acid in the dry powders

DPF	Estimate of total mass of the FA in the dry powder (mg)	Estimate of mass of the FA per capsule (mg)	Estimate the yield of atomization of the FA (%)
TLFA1	6.2 – 6.9	0.066 – 0.074	41 – 46
TLFA2	7.1 – 7.8	0.068 – 0.076	47 – 52

4. Conclusion

The conjugation of fusidic acid with two different polymers (poly(2-ethyl-2-oxazoline) and poly(ethylene glycol)) is successful with one-pot reaction process, while the two steps reaction process (activation and conjugation) does not work, due to product purification and water hydrolyses issues.

The SASD apparatus is capable of producing trehalose-leucine dry powder microparticles suitable for inhalation. However, in light of the results obtained, it is possible to conclude that the microparticles production process had some associated issues, such as the difficulty of finding the ideal properties of the dry powders within the optimal conditions of operation of the SASD. The use of an active pharmaceutical ingredient can improve some of proprieties of the dry powders, which means that can solve some of these problems.

Overall, by adding fusidic acid or one of the two conjugated compounds to the trehalose-leucine microparticles, these tended to improve the aerodynamic properties. However, the dry powders with fusidic acid presented to be more suitable for pulmonary delivery, due to better aerodynamic and morphologic properties in relation to the conjugated compounds. The main reason is that fusidic acid has a hydrophobic behaviour, while conjugated products tend to be more hydrophilic and because of this, the conjugated products have more agglomerates.

It is possible to conclude that the best formulation for pulmonary delivery was the first assay of trehalose-leucine-fusidic acid microparticles (TLFA1) with a MMAD of 1.64 μm, a FPF of 62 %, and a yield of 56 %, which present fully adequate characteristics for inhalation. As for the conjugated compounds, the best of both is the first assay of trehalose-leucine-fusidic acid conjugated with poly(2-ethyl-2-oxazoline) (TLPEtOx-FA1) with a MMAD of 3.15 μm, a FPF of 43 %, and a yield of 67 %, which is also good for pulmonary delivery.

For future work, it is suggested the study and optimisation of one-pot reaction conditions to achieve higher yields and better quality of the product, and also to improve the methods for purification of the products. One possibility would be using dialysis membranes with cut-off 1000 g/mol, as the conjugated polymers has a molecular weight greater than 1000 g/mol, or the use of a Sephadex column (chromatography). Also it is suggested to perform antimicrobial assays with these compounds against other pathogens such as *Streptococcus pneumoniae* or *Streptococcus pyogenes*.

It is important to find new strategies to optimize the characteristics of dry powders in order to overcome some problems associated with aggregation and yield, such as improvement of the formulation with different concentrated initial solutions or search for new excipients

and/or dispersability enhancer. It would be interest to perform antimicrobial assays with dry powders to verify the antimicrobial activity of the fusidic and the conjugated products encapsulated in microparticles. It is suggested to perform quantification assays of the conjugate compounds to determine the quantity of loaded conjugated compound in the dry powder. Also, it is suggested to perform pharmacodynamics and/or pharmacokinetics studies of the conjugated compounds, for example, *in vitro* assays using a line of primary culture of lung cells to understand the effects of the conjugated compounds on the lung cells.

5. Reference

1. Naghavi, M. *et al.* Global, regional, and national age-sex specific all-cause and cause-specific mortality for 240 causes of death, 1990-2013: A systematic analysis for the Global Burden of Disease Study 2013. *Lancet* **385,** 117–171 (2015).

2. Vos, T. *et al.* Global, regional, and national incidence, prevalence, and years lived with disability for 301 acute and chronic diseases and injuries in 188 countries, 1990-2013: A systematic analysis for the Global Burden of Disease Study 2013. *Lancet* **386,** 743–800 (2015).

3. Buttini, F., Colombo, P., Rossi, A., Sonvico, F. & Colombo, G. Particles and powders: Tools of innovation for non-invasive drug administration. *J. Control. Release* **161,** 693–702 (2012).

4. Takami, T. & Murakami, Y. Development of PEG-PLA/PLGA microparticles for pulmonary drug delivery prepared by a novel emulsification technique assisted with amphiphilic block copolymers. *Colloids Surfaces B Biointerfaces* **87,** 433–438 (2011).

5. Sung, J. C., Pulliam, B. L. & Edwards, D. A. Nanoparticles for drug delivery to the lungs. *Trends Biotechnol.* **25,** 563–570 (2007).

6. Pilcer, G. & Amighi, K. Formulation strategy and use of excipients in pulmonary drug delivery. *Int. J. Pharm.* **392,** 1–19 (2010).

7. Beck-Broichsitter, M. *et al.* Characterization of novel spray-dried polymeric particles for controlled pulmonary drug delivery. *J. Control. Release* **158,** 329–335 (2012).

8. Shah, A. K. & Agnihotri, S. A. Recent advances and novel strategies in pre-clinical formulation development : An overview. *J. Control. Release* **156,** 281–296 (2011).

9. Chow, A. H. L., Tong, H. H. Y., Chattopadhyay, P. & Shekunov, B. Y. Particle engineering for pulmonary drug delivery. *Pharm. Res.* **24,** 411–437 (2007).

10. Geiser, M. *et al.* Cellular uptake and localization of inhaled gold nanoparticles in lungs of mice with chronic obstructive pulmonary disease. *Part. Fibre Toxicol.* **10,** 19 (2013).

11. Newman, S. P. & Busse, W. W. Evolution of dry powder inhaler design, formulation, and performance. *Respir. Med.* **96,** 293–304 (2002).

12. Shoyele, S. A. & Slowey, A. Prospects of formulating proteins/peptides as aerosols for pulmonary drug delivery. *Int. J. Pharm.* **314,** 1–8 (2006).

13. Malcolmson, R. J. & Embleton, J. K. Dry powder formulations for pulmonary delivery. *Pharm. Sci. Technol. Today* **1,** 394–398 (1998).

14. Katdare, A. *Excipient Development for Pharmaceutical, Biotechnology, and Drug Delivery Systems*. *Informa Healthcare USA, Inc* (2006).

15. Edge, S., Mueller, S., Price, R. & Shur, J. Factors affecting defining the quality and functionality of excipients used in the manufacture of dry powder inhaler products. *Drug Dev. Ind. Pharm.* **34,** 966–73 (2008).

16. Kalász, H. & Antal, I. Drug excipients. *Curr Med Chem* **13,** 2535–2563 (2006).

17. Weers, J. G. & Miller, D. P. Formulation Design of Dry Powders for Inhalation. *J. Pharm. Sci.* **104,** 3259–3288 (2015).

18. Smyth, Hugh D C; Hickey, A. J. Carriers in Drug Powder Delivery. *J. Drug Deliv.* **3,** 117–132 (2005).

19. *Carbohydrate*. (Columbia Electronic Encyclopedia, 2017).

20. Higashiyama, T. Novel functions and applications of trehalose. *Pure Appl. Chem.* **74,** 1263–1269 (2002).

21. López-Díez, E. C. & Bone, S. The interaction of trypsin with trehalose: An investigation of protein preservation mechanisms. *Biochim. Biophys. Acta - Gen. Subj.* **1673,** 139–148 (2004).

22. Li, X. & Mansour, H. M. Physicochemical Characterization and Water Vapor Sorption of Organic Solution Advanced Spray-Dried Inhalable Trehalose Microparticles and Nanoparticles for Targeted Dry Powder Pulmonary Inhalation Delivery. *AAPS PharmSciTech* **12,** 1420–1430 (2011).

23. Ógáin, O. N., Li, J., Tajber, L., Corrigan, O. I. & Healy, A. M. Particle engineering of materials for oral inhalation by dry powder inhalers. i - Particles of sugar excipients (trehalose and raffinose) for protein delivery. *Int. J. Pharm.* **405,** 23–35 (2011).

24. Ahmad, M. I., Ungphaiboon, S. & Srichana, T. The development of dimple-shaped chitosan carrier for ethambutol dihydrochloride dry powder inhaler. *Drug Dev. Ind. Pharm.* **41,** 791–800 (2015).

25. Dash, M., Chiellini, F., Ottenbrite, R. M. & Chiellini, E. Chitosan - A versatile semi-synthetic polymer in biomedical applications. *Prog. Polym. Sci.* **36,** 981–1014 (2011).

26. Chen, L., Okuda, T., Lu, X. Y. & Chan, H. K. Amorphous powders for inhalation drug delivery. *Adv. Drug Deliv. Rev.* **100,** 102–115 (2016).

27. Grigoletto, A. *et al.* Drug and protein delivery by polymer conjugation. *J. Drug Deliv. Sci. Technol.* **32,** 132–141 (2016).

28. Knop, K., Hoogenboom, R., Fischer, D. & Schubert, U. S. Poly(ethylene glycol) in drug delivery: Pros and cons as well as potential alternatives. *Angew. Chemie - Int. Ed.* **49,** 6288–6308 (2010).

29. Singh, A. & Van den Mooter, G. Spray drying formulation of amorphous solid dispersions. *Adv. Drug Deliv. Rev.* **100,** 27–50 (2016).

30. A. Aguiar-Ricardo, V.D.B. Bonifacio, T. Casimiro, V. G. C. Supercritical carbon dioxide design strategies: from drug carriers to soft killers. *Phil. Trans. R. Soc. A* **A 373.2057,** 20150009 (2015).

31. de Macedo, C. V., da Silva, M. S., Casimiro, T., Cabrita, E. J. & Aguiar-Ricardo, A. Boron trifluoride catalyzed polymerisation of 2-substituted-2-oxazolines in supercritical carbon dioxide. *Green Chem.* **9,** 948–953 (2007).

32. Vehring, R. Pharmaceutical particle engineering via spray drying. *Pharm. Res.* **25,** 999–1022 (2008).

33. Nieto-Orellana, A. *et al.* Dry-powder formulations of non-covalent protein complexes

with linear or miktoarm copolymers for pulmonary delivery. *Int. J. Pharm.* **540,** 78–88 (2018).

34. Zhang, J., Wu, L., Chan, H. K. & Watanabe, W. Formation, characterization, and fate of inhaled drug nanoparticles. *Adv. Drug Deliv. Rev.* **63,** 441–455 (2011).

35. Marco, G. I. L., Vicente, J. & Gaspar, F. Scale-up methodology for pharmaceutical spray drying. *Chim. Oggi* **28,** 18–22 (2010).

36. Tong, H. H. Y. & Chow, A. H. L. Control of Physical Forms of Drug Particles for Pulmonary Delivery by Spray Dr ying and Supercritical Fluid Processing. *KONA Powder Part. J.* **24,** 27–40 (2006).

37. Girotra, P., Singh, S. K. & Nagpal, K. Supercritical fluid technology: a promising approach in pharmaceutical research. *Pharm. Dev. Technol.* **18,** 22–38 (2013).

38. Makadia, H. K. & Siegel, S. J. Poly Lactic-co-Glycolic Acid (PLGA) as biodegradable controlled drug delivery carrier. *Polymers (Basel).* **3,** 1377–1397 (2011).

39. Koushik, K. & Kompella, U. B. Preparation of large porous deslorelin-PLGA microparticles with reduced residual solvent and cellular uptake using a supercritical carbon dioxide process. *Pharm. Res.* **21,** 524–535 (2004).

40. Nie, H., Lee, L. Y., Tong, H. & Wang, C. H. PLGA/chitosan composites from a combination of spray drying and supercritical fluid foaming techniques: New carriers for DNA delivery. *J. Control. Release* **129,** 207–214 (2008).

41. Cocero, M. J., Martín, Á., Mattea, F. & Varona, S. Encapsulation and co-precipitation processes with supercritical fluids: Fundamentals and applications. *J. Supercrit. Fluids* **47,** 546–555 (2009).

42. Martín, Á., Pham, H. M., Kilzer, A., Kareth, S. & Weidner, E. Micronization of polyethylene glycol by PGSS (Particles from Gas Saturated Solutions)-drying of aqueous solutions. *Chem. Eng. Process. Process Intensif.* **49,** 1259–1266 (2010).

43. Reverchon, E. Supercritical-Assisted Atomization To Produce Micro- and/or Nanoparticles of Controlled Size and Distribution. *Ind. Eng. Chem. Res.* **41,** 2405–2411 (2002).

44. Reverchon, E., Adami, R. & Caputo, G. Supercritical assisted atomization: Performance comparison between laboratory and pilot scale. *J. Supercrit. Fluids* **37,** 298–306 (2006).

45. Casettari, L. *et al.* Surface characterisation of bioadhesive PLGA/chitosan microparticles produced by supercritical fluid technology. *Pharm. Res.* **28,** 1668–1682 (2011).

46. Porta, G. Della & Reverchon, E. Engineering Powder Properties By Supercritical Fluid for Optimum Drug Delivery. *Bioprocess Int.* 54–60 (2005).

47. Reverchon, E. & Antonacci, A. Chitosan microparticles production by supercritical fluid processing. *Ind. Eng. Chem. Res.* **45,** 5722–5728 (2006).

48. Reighard, T. S., Lee, S. T. & Olesik, S. V. Determination of methanol/CO2 and acetonitrile/CO2 vapor-liquid phase equilibria using a variable-volume view cell. *Fluid Phase Equilib.* **123,** 215–230 (1996).

49. Newman, D. J. & Cragg, G. M. Natural products as sources of new drugs over the last 25

years. *J. Nat. Prod.* **70,** 461–477 (2007).

50. Bérdy, J. Bioactive microbial metabolites. *J. Antibiot. (Tokyo).* **58,** 1–26 (2005).

51. Drew, S. W. & Demain, a L. Effect of primary metabolites on secondary metabolism. *Annu. Rev. Microbiol.* **31,** 343–356 (1977).

52. Demain, A. . & Fang, A. The natural functions of secondary metabolites. *Adv. Biochem. Eng. Biotechnol.* **69,** 222 (2000).

53. Fenical, W. & Jensen, P. R. Developing a new resource for drug discovery: marine actinomycete bacteria. *Nat. Chem. Biol.* **2,** 666–673 (2006).

54. Subramani, R. & Aalbersberg, W. Marine actinomycetes: An ongoing source of novel bioactive metabolites. *Microbiol. Res.* **167,** 571–580 (2012).

55. Kuzuyama, T. & Seto, H. Diversity of the biosynthesis of the isoprene units. *Nat. Prod. Rep.* **20,** 171–183 (2003).

56. Gallagher, K. A., Fenical, W. & Jensen, P. R. Hybrid isoprenoid secondary metabolite production in terrestrial and marine actinomycetes. *Curr. Opin. Biotechnol.* **21,** 794–800 (2010).

57. Kawasaki, T. *et al.* Biosynthesis of a natural polyketide-isoprenoid hybrid compound, furaquinocin A: Identification and heterologous expression of the gene cluster. *J. Bacteriol.* **188,** 1236–1244 (2006).

58. Xiao, Y., Machacek, M., Lee, K., Kuzuyama, T. & Liu, P. Prenyltransferase substrate binding pocket flexibility and its application in isoprenoid profiling. *Mol. Biosyst.* **5,** 913–7 (2009).

59. Motohashi, K. *et al.* Studies on Terpenoids Produced by Actinomycetes: Oxaloterpins A, B, C, D, and E, Diterpenes from Streptomyces sp. KO-3988. 1712–1717 (2007).

60. Musmade, P. B., Tumkur, A., Trilok, M. & Bairy, K. L. Fusidic acid - Topical antimicrobial in the management of staphylococcus aureus. *Int. J. Pharm. Pharm. Sci.* **5,** 737–746 (2013).

61. Curbete, M. M. & Salgado, H. R. N. A Critical Review of the Properties of Fusidic Acid and Analytical Methods for Its Determination. *Crit. Rev. Anal. Chem.* (2016).

62. Howden, B. P. & Grayson, M. L. Dumb and dumber--the potential waste of a useful antistaphylococcal agent: emerging fusidic acid resistance in Staphylococcus aureus. *Clin.Infect.Dis.* **42,** 394–400 (2006).

63. Nagaev, I., Björkman, J., Andersson, D. I. & Hughes, D. Biological cost and compensatory evolution in fusidic acid-resistant Staphylococcus aureus. *Mol. Microbiol.* **40,** 433–439 (2001).

64. Fernandes, P. & Hill, C. Methods of treating bacterial infections through pulmonary delivery of fusidic acid. **1,** 16 (2013).

65. Turnidge, J. Fusidic acid pharmacology, pharmacokinetics and pharmacodynamics. *Int. J. Antimicrob. Agents* **12,** (1999).

66. Lapham, K. *et al.* Inhibition of Hepatobiliary Transport Activity by the Antibacterial

Agent Fusidic Acid: Insights into Factors Contributing to Conjugated Hyperbilirubinemia/Cholestasis. *Chem. Res. Toxicol.* **29,** 1778–1788 (2016).

67. Prieto-Davó, A. *et al.* The Madeira archipelago as a significant source of marine-derived actinomycete diversity with anticancer and antimicrobial potential. *Front. Microbiol.* **7,** 1–12 (2016).

68. Yoon, I. K. *et al.* Multifunctional forms of polyoxazoline copolymers and drug compositions comprasing the same. Patent US 8,501,899 B2. 35 (2013).

69. Gordo, J. *et al.* Convenient synthesis of 3-vinyl and 3-styryl coumarins. *Org. Lett.* **13,** 5112–5115 (2011).

70. Almeida, V. C. Dry powder formulations containing bioactive compounds from marine Actinobacteria. (2015).

71. Soria-Mercado, I. E., Jensen, P. R., Fenical, W., Kassel, S. & Golen, J. 3,4a-Dichloro-10a-(3-chloro-6-hydroxy-2,2,6-trimethylcyclohexylmethyl)-6,8-dihydroxy-2,2,7-trimethyl-3,4,4a,10a-tetrahydro-2 *H* -benzo[*g*]chromene-5,10-dione. *Acta Crystallogr. Sect. E Struct. Reports Online* **60,** o1627–o1629 (2004).

72. Soria-Mercado, I. E., Prieto-Davo, A., Jensen, P. R. & Fenical, W. Antibiotic terpenoid chloro-dihydroquinones from a new marine actinomycete. *J. Nat. Prod.* **68,** 904–910 (2005).

73. Rastrup-Andersen, N. & Duvold, T. Reassignment of the 1H NMR spectrum of fusidic acid and total assignment of 1H and 13C NMR spectra of some selected fusidane derivatives. *Magn. Reson. Chem.* **40,** 471–473 (2002).

Annex 1 – Extraction, Isolation and purification of PTM-029 Compounds

Materials

Isooctane (99.5% purity), methanol (98.5% purity), dichloromethane (>99.8% purity), water and acetonitrile (99.9% purity, HPLC grade) were purchased from ProLabo. Ethyl acetate (99.8% purity) and silica gel 60 were purchased from Merck. Sea sand washed was purchased from Scharlau and trifluoroacetic acid (99% purity) from Alfa Aesar. D-chloroform (99.8%) was purchased from Cambridge Isotope Laboratories, Inc.

Liquid-Liquid Extraction

The actinomycete strain PTM-029 was cultivated on A1 medium consisted by 750 mL of seawater, 250 mL of distilled water, 10 g of starch, 4 g of yeast extract and 2 g of peptone, incubated for 7 days at 30° C with shaking at 200 rpm.[67] After this period, the medium was extracted three times with ethyl acetate and then the solvent was removed by evaporation in a Büchi Rotavapor R-114 equipped with Büchi Waterbath B-480 at 40ºC to generate the crude extract. Then, the crude extract was dryed under vacuum for two days.

Flash Chromatography

The crude extract was fractionated in a silica chromatography column using ratios of isooctane/ethyl acetate (100:0, 80:20, 60:40, 40:60, 20:80 and 0:100) and ratios of methanol/ethyl acetate (10:90, 50:50 and 100:0) to produce nine fractions of increasing polarity. Each fraction was placed in a Büchi Rotavapor R-114 equipped with Büchi Waterbath B-480 at 40ºC to evaporate the small amounts of organic solvents and then were dryed under vacuum for two days.

Compounds isolation by HPLC

The fractions F2, F3, F4, F5 and F6 obtained by flash chromatography were fractionated in HPLC to obtain pure compounds that have high antimicrobial activity. HPLC compounds isolation was performed using a Dionex Ultimate 3000 system equipped with an Ultimate 3000 Diode Array Detector (DAD-3000), and a Phenomenex Luna silica C18 column (250 × 10 mm, 5 µm, 100 Å) at flow rate of 1.5 mL/ min with various gradients of ACN/H_2O (0,1%TFA).

Results

Flash Chromatography

Table 9 - Mass of the PTM-029 fractions obtained by flash chromatography

Fraction	Mass of the fraction (g)
F1	0.0280
F2	0.2883
F3	0.2598
F4	0.0637
F5	0.0444
F6	0.0468
F7	0.2293
F8	0.1945
F9	0.0580

HPLC

Table 10 - Mass of the PTM-029 fractions obtained by HPLC

Fraction of flash chromatography	Fraction of HPLC	Retention time (min)	Mass of the sample (g)
F2	F20	30.64	0.0137
	F29	37.86	0.0210
	F31	40.24	0.0282
F3	F47	42.48	0.0307
	F48	43.69	0.0030
	F61	73.66	0.0031
F4	F39	41.77	0.0068
F5	F34	41.58	0.0031
F6	F25	24.83	0.0017
	F26	25.47	0.0019
	F30	26.41	0.0022
	F31	28.46	0.0016
	F32	29.22	0.0024
	F33	30.17	0.0010
	F34	30.91	0.0036
	F35	31.27	0.0026
	F46	41.51	0.0011
	F55	57.66	0.0045
	F56	59.73	0.0018

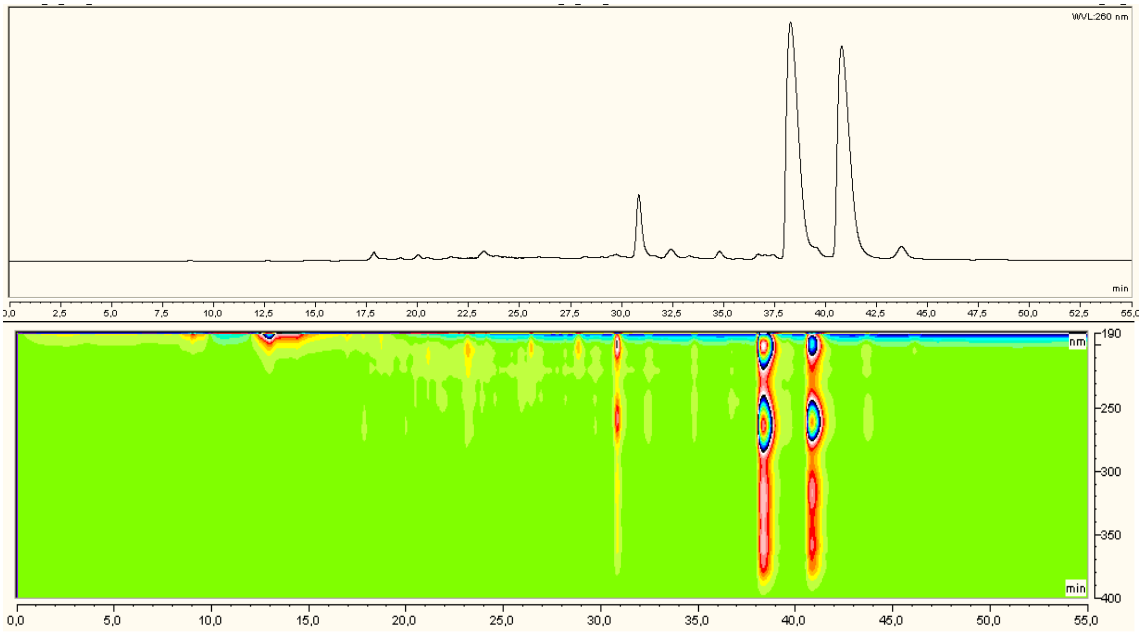

Figure 38 - Chromatographic profile at λ= 260 nm and DAD, respectively, of F2 from PTM-029 performed by HPLC

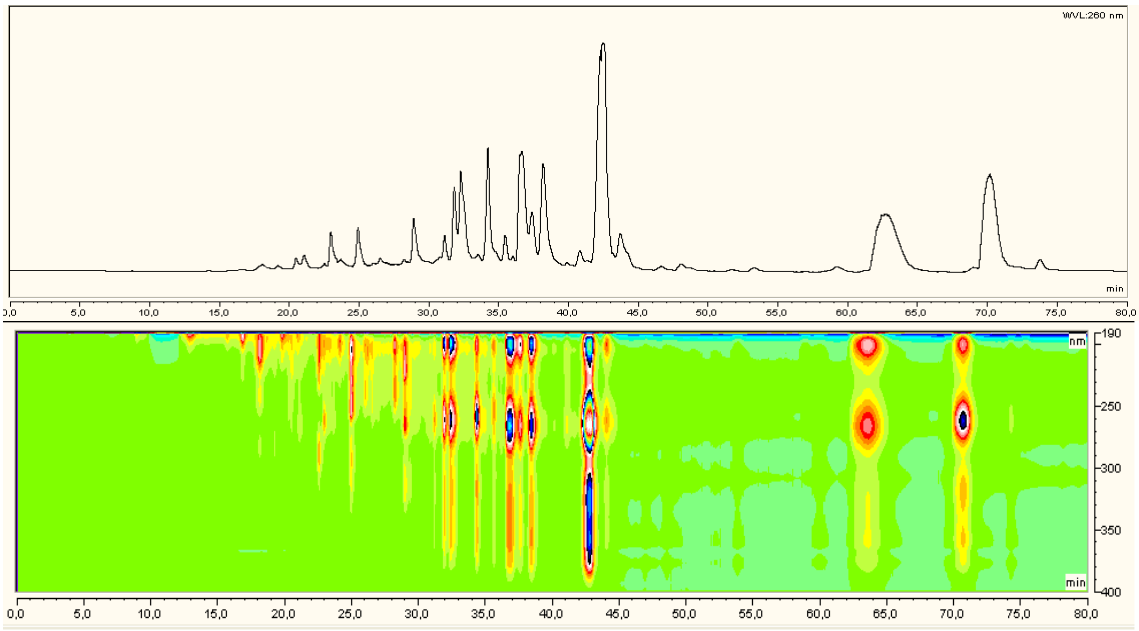

Figure 39 - Chromatographic profile at λ= 260 nm and DAD, respectively, of F3 rom PTM-029 performed by HPLC

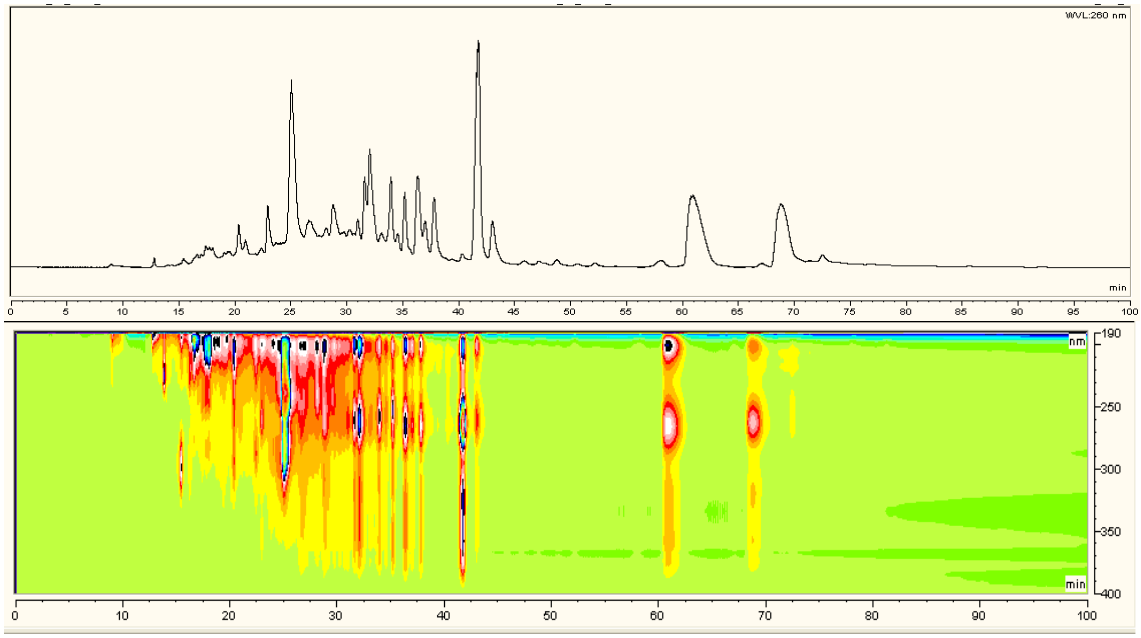

Figure 40 - Chromatographic profile at λ= 260 nm and DAD, respectively, of F4 from PTM-029 performed by HPLC

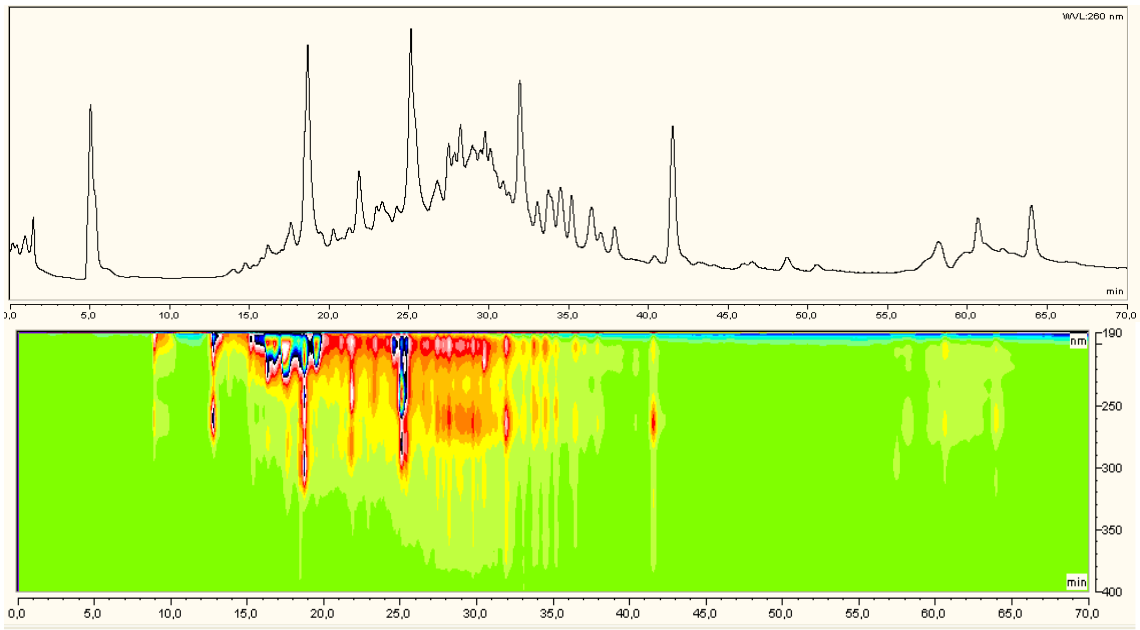

Figure 41 - Chromatographic profile at λ= 260 nm and DAD, respectively, of F5 from PTM-029 performed by HPLC

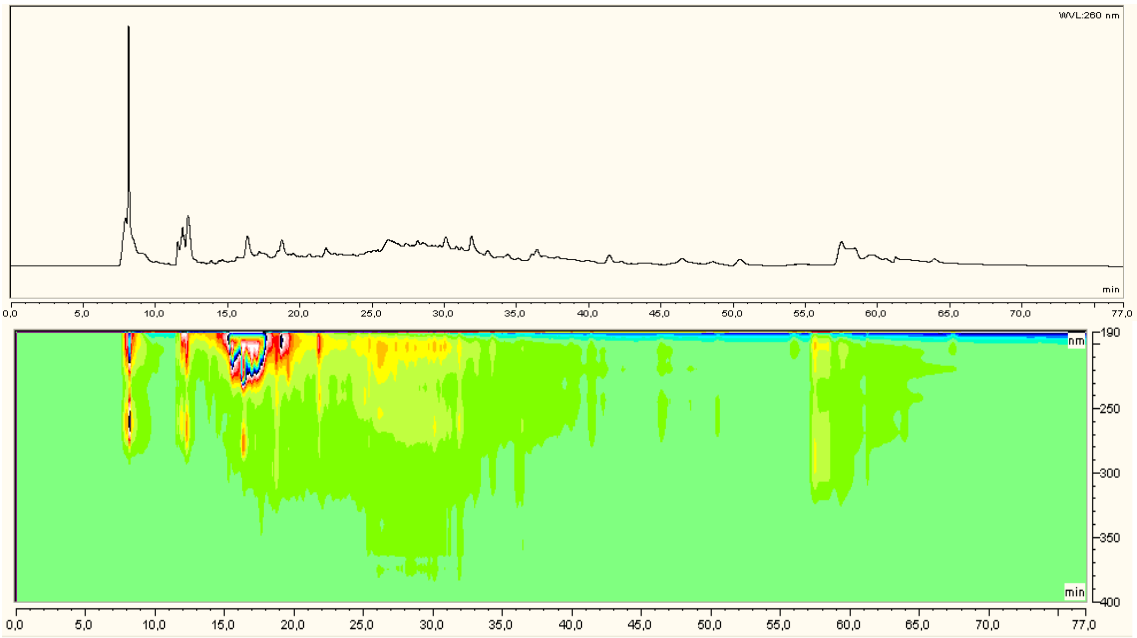

Figure 42 - Chromatographic profile at λ= 260 nm and DAD, respectively, of F6 from PTM-029 performed by HPLC

PTM-029, F4, F39 (yellow oil): **^{1}H NMR (400MHz, $CDCl_3$):** δ 12.30 (s, 3H), 7.84 (s, 3H), 6.37 (s, 3H), 4.57 (dd, 3H), 3.45 (dd, 3H), 2.65 – 2.43 (m, 10H), 2.23 (s, 9H), 2.17 – 1.74 (m, 16H), 1.64 – 1.61 (m, 11H), 1.57 (s, 3H), 1.47 – 1.41 (d, 6H), 1.36 – 1.31 (d, 21H), 1.24 (d, 12H), 0.98 – 0.77 (m, 3H), 0.77 – 0.73 (d, 3H), 0.51 – 0.43 (d, 3H).

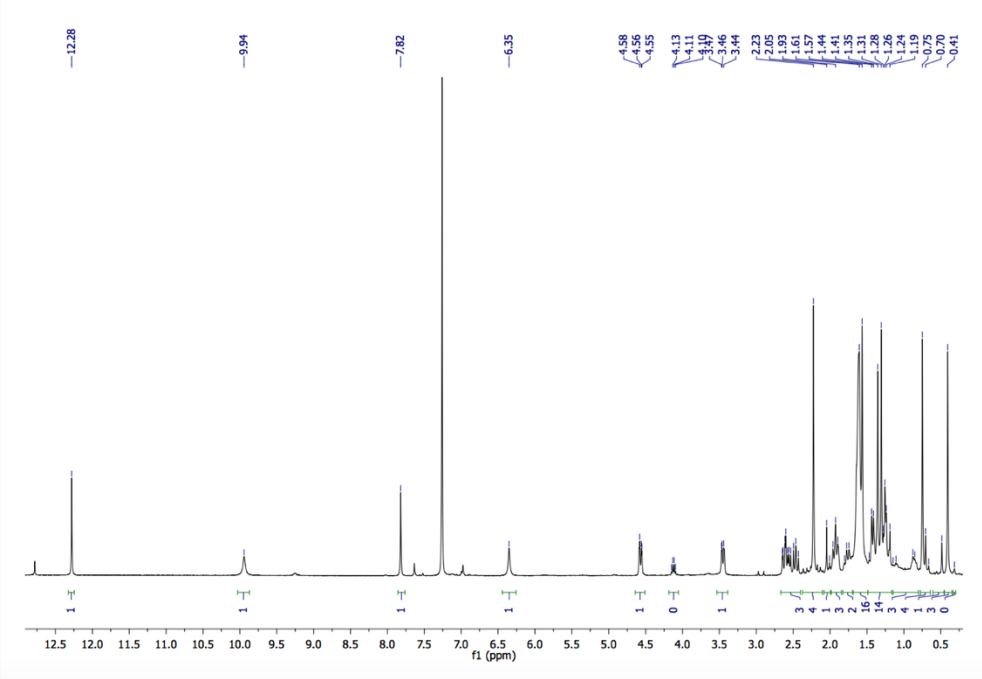

Figure 43- ^{1}H NMR spectrum of PTM-029, F4, F39 in $CDCl_3$

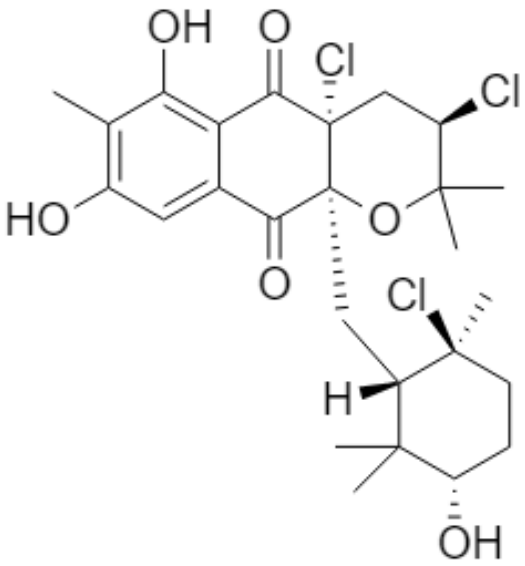

Figure 44 - Struture of the compound PTM-029, F4, F39 based in a previous work[70] and it has similuar NMR data with antibiotic A80915C[71,72]

Annex 2 – ^{13}C NMR Spectrum of Conjugation of Activated Fusidic Acid with Polymers

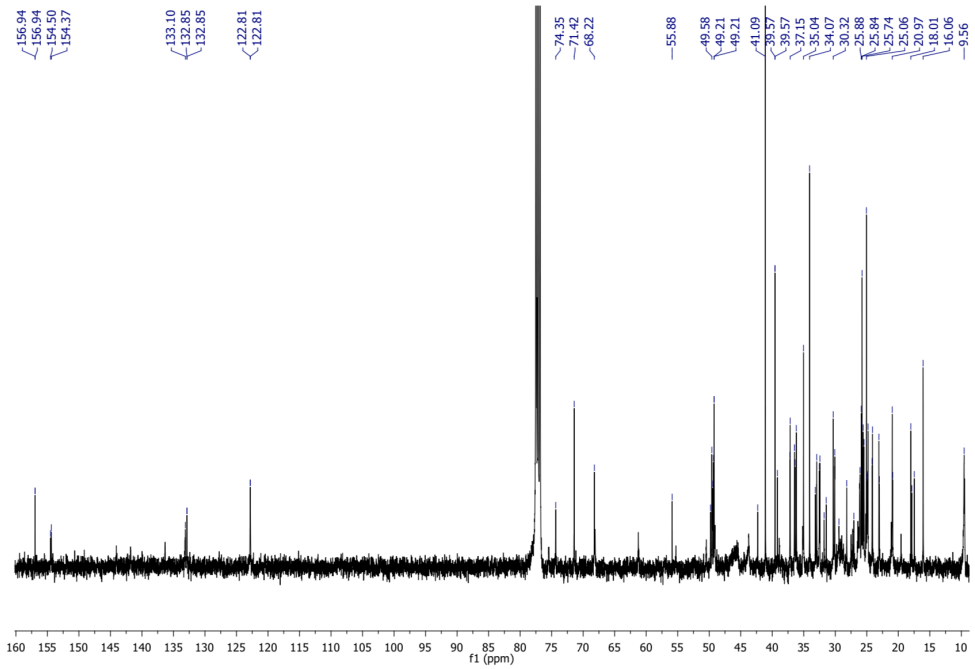

Figure 45 - ^{13}C NMR spectrum of conjugation reaction with PEtOx-NH_2 in $CDCl_3$

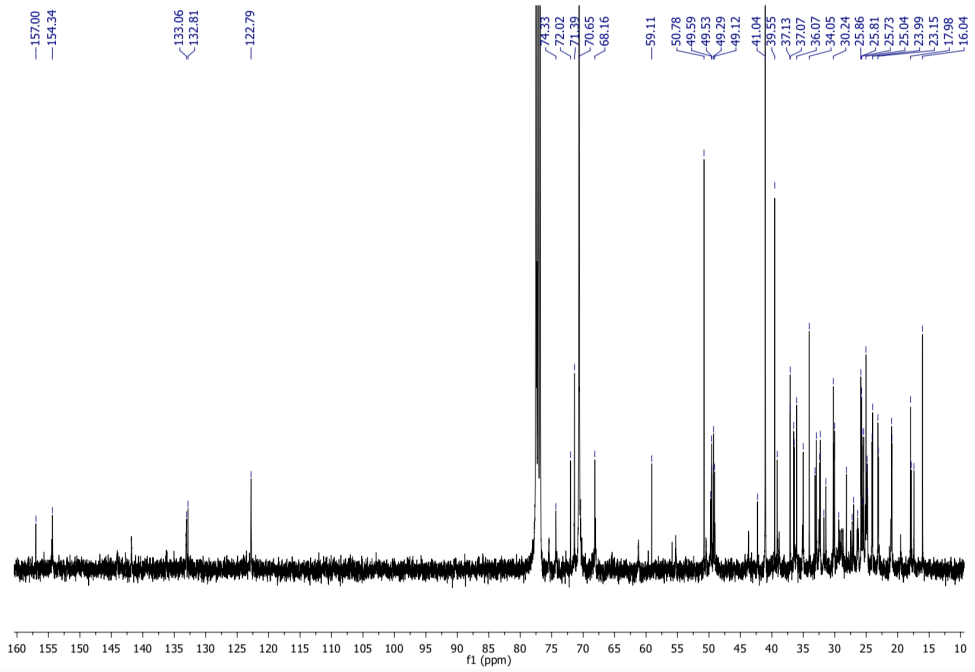

Figure 46 - ^{13}C NMR spectrum of conjugation reaction with PEG-NH_2 in $CDCl_3$

Annex 3 – Spectral Data of Fusidic Acid

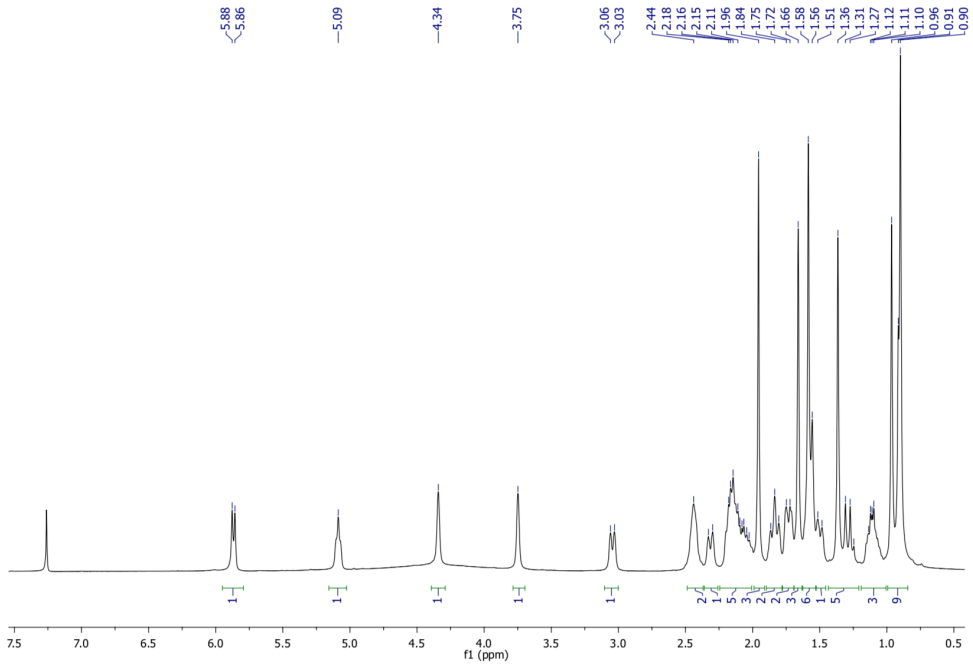

Figure 47 -^{1}H NMR spectrum of FA in $CDCl_3$

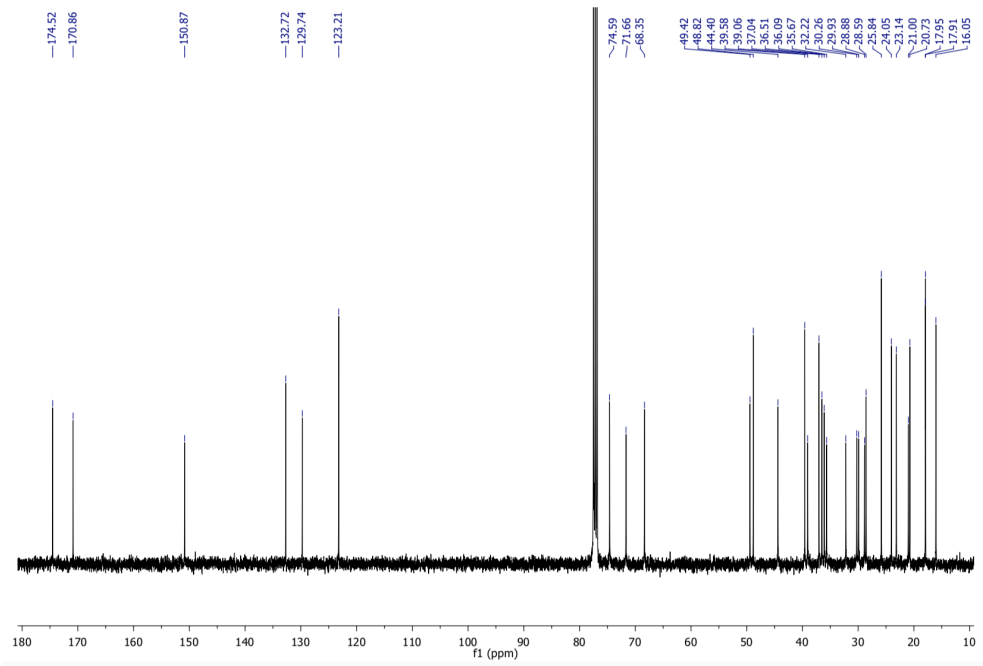

Figure 48 - ^{13}C NMR spectrum of FA in $CDCl_3$

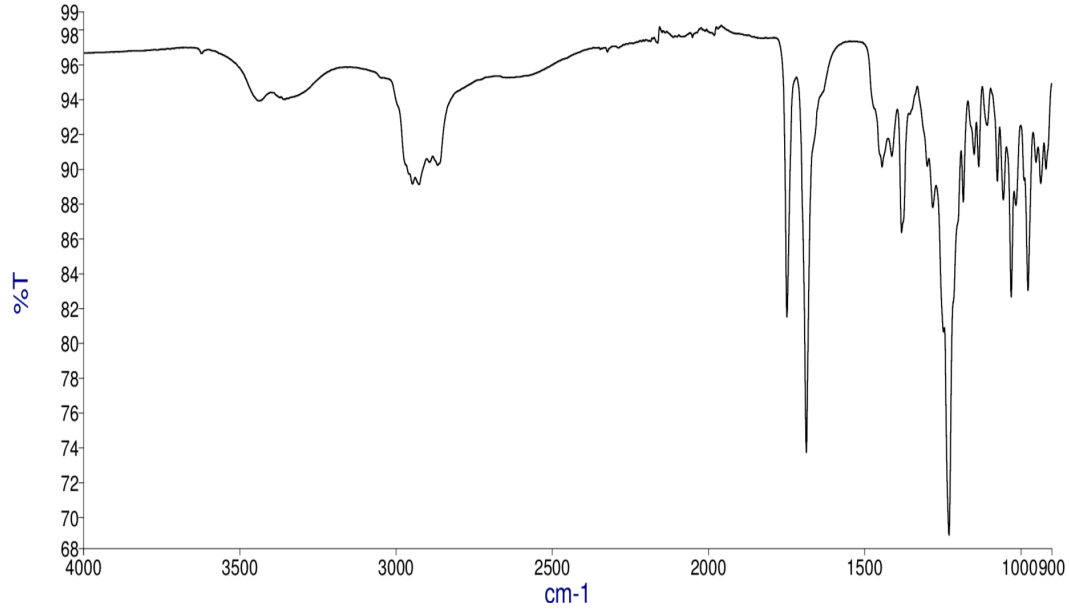

Figure 49 - FT-IR of fusidic acid

FA (white powder): ^{1}H NMR (400 MHz, $CDCl_3$): δ 5.87 (d, 1H, J = 8.27 Hz), 5.09 (s, 1H), 4.34 (s, 1H), 3.75 (s, 1H), 3.04 (d, 1H, J = 11.49 Hz), 2.44 (s, 2H), 2.31 (d, 1H, J = 12.73 Hz), 2.18-2.03 (m, 5H), 1.96 (s, 3H), 1.84 (t, 2H, J = 121.87 Hz), 1.74 (d, 2H, J = 11.00 Hz), 1.66 (s, 3H), 1.57 (d, 6H, J = 11.57 Hz), 1.50 (d, 1H, J = 12.53 Hz), 1.36-1.25 (m, 5H), 1.12 (dd, 3H, J = 5.59, 10.14 Hz), 0.96 (s, 3H), 0.90 (d, 6H, J = 6.08 Hz) ppm; **^{13}C NMR (400 MHz, $CDCl_3$):** δ 174.52, 170.86, 150.87, 132.72, 129.74, 123.21, 74.59, 71.66, 68.35, 53.53, 49.42, 48.82, 44.40, 39.58, 39.06, 37.04, 36.51, 36.09, 35.67, 32.22, 30.26, 29.93, 28.88, 28.59, 25.84, 24.05, 23.14, 21.00, 20.73, 17.95, 17.91, 16.05 ppm; **IR (ATR):** 3441 (O–H *stretching* of hydroxyl), 2927 (C–H *stretching*), 1748 (C=O *stretching* of acetyl), 1686 (C=O *stretching* of carboxylic), 1229 (C–O *stretching* of ether) cm^{-1}.

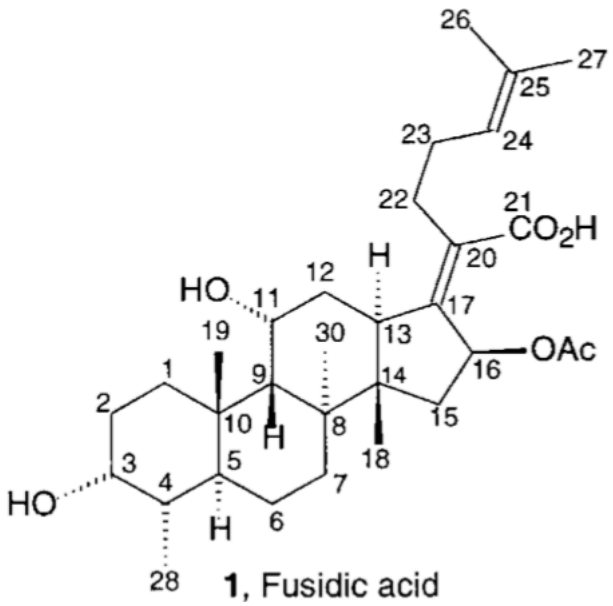

Figure 50 - Enumeration of the carbon and protons of fusidic acid, adapted from Rastrup-Andersen, N. & Duvold, T.[73]

Annex 4 – Spectral Data of PEG-NH_2

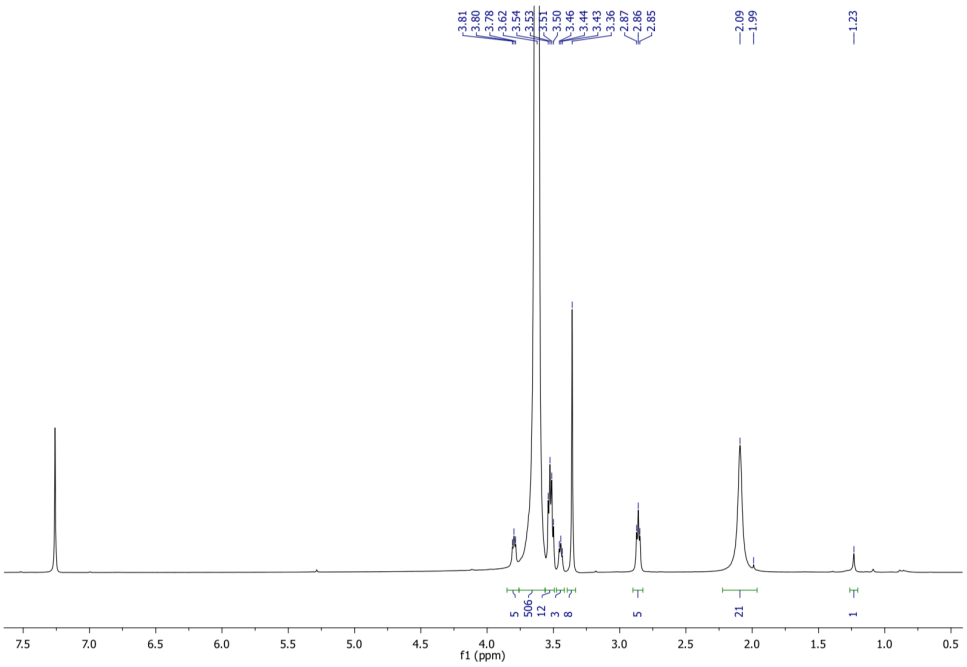

Figure 51 - ^{1}H NMR spectrum of PEG-NH_2 in $CDCl_3$

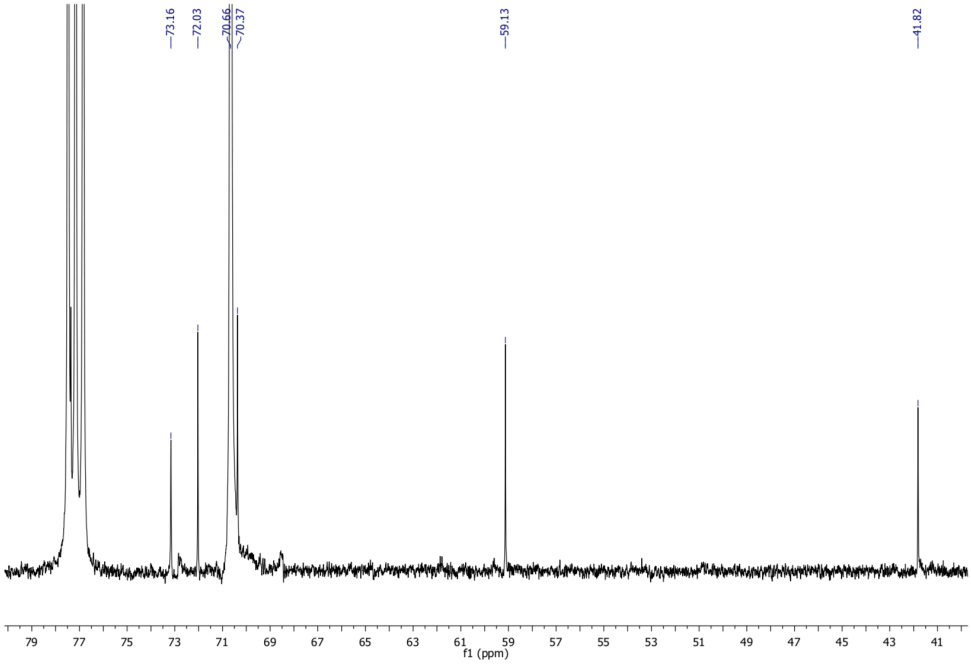

Figure 52 - ^{13}C NMR spectrum of PEG-NH_2 in $CDCl_3$

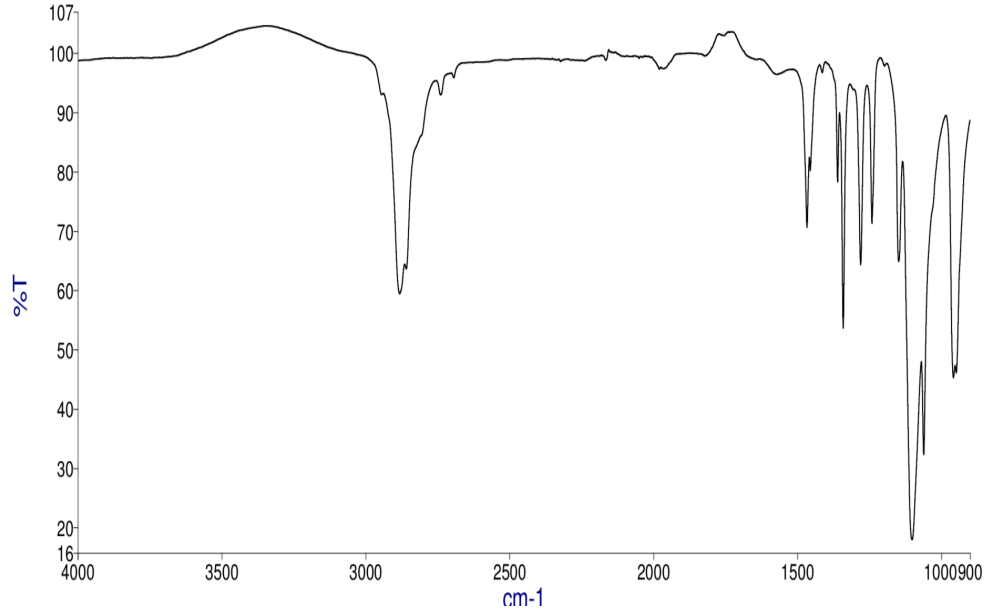

Figure 53 - FT-IR of PEG-NH_2

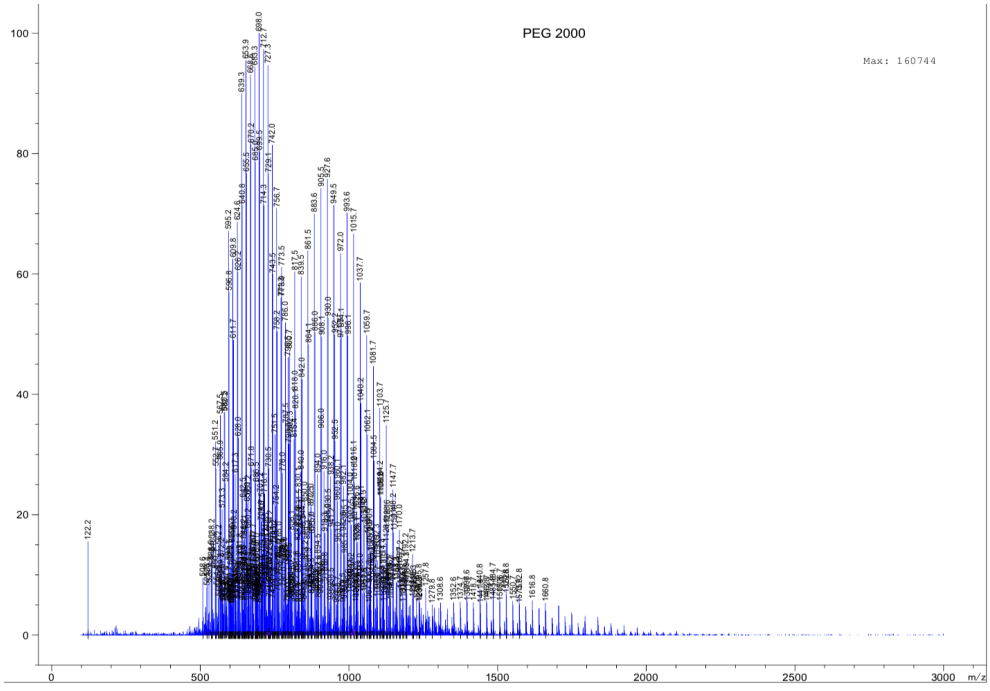

Figure 54 - Mass spectrum of PEG-NH_2 (positive mode)

PEG-NH_2 (yellow oil): ^{1}H NMR (400 MHz, $CDCl_3$): δ 3.81-3.78 (bs, 5H), 3.62 (bs, 506H), 3.54-3.50 (bs, 12H), 3.46-3.43 (bs, 3H), 3.36 (bs, 8H), 2.87-2.85 (bs, 5H), 2.09 (bs, 21H), 1.23 (bs, 1H) ppm; **^{13}C NMR (400 MHz, $CDCl_3$):** δ 73.16, 72.03, 70.66, 70.37, 59.13, 41.82 ppm; **IR (ATR):** 2884 (C–H *stretching*), 1341 (C–H *bending*), 1105 (C–O *stretching* of ether) cm^{-1}.

Annex 5 – Spectral Data of Benzylamine-Fusidic Acid

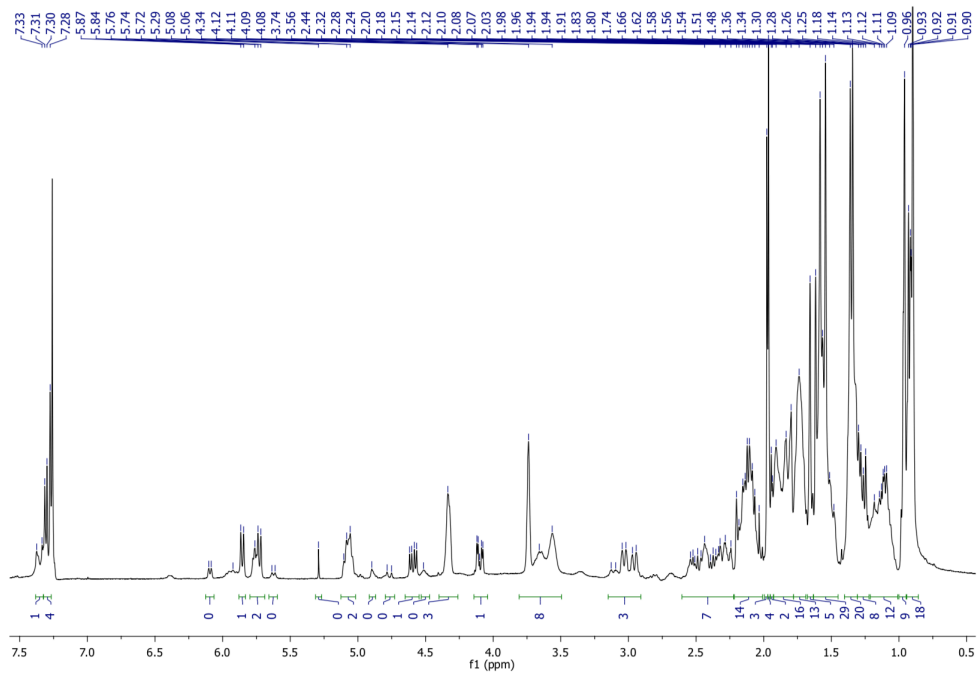

Figure 55 - ^{1}H NMR Spectrum of benzylamine-fusidic acid

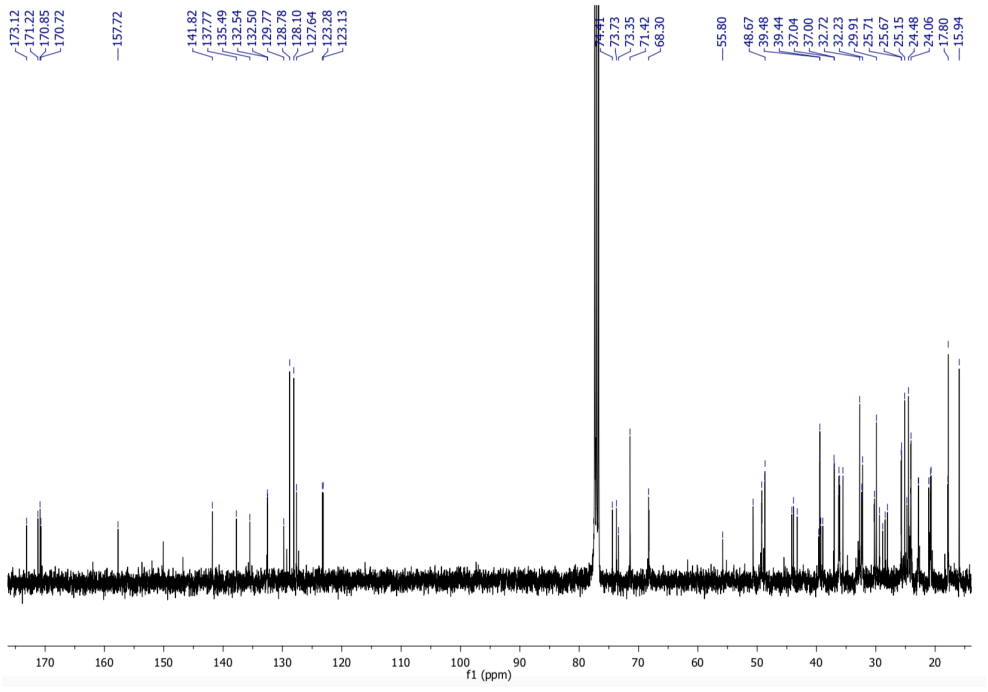

Figure 56 - ^{13}C NMR Spectrum of benzylamine-fusidic acid

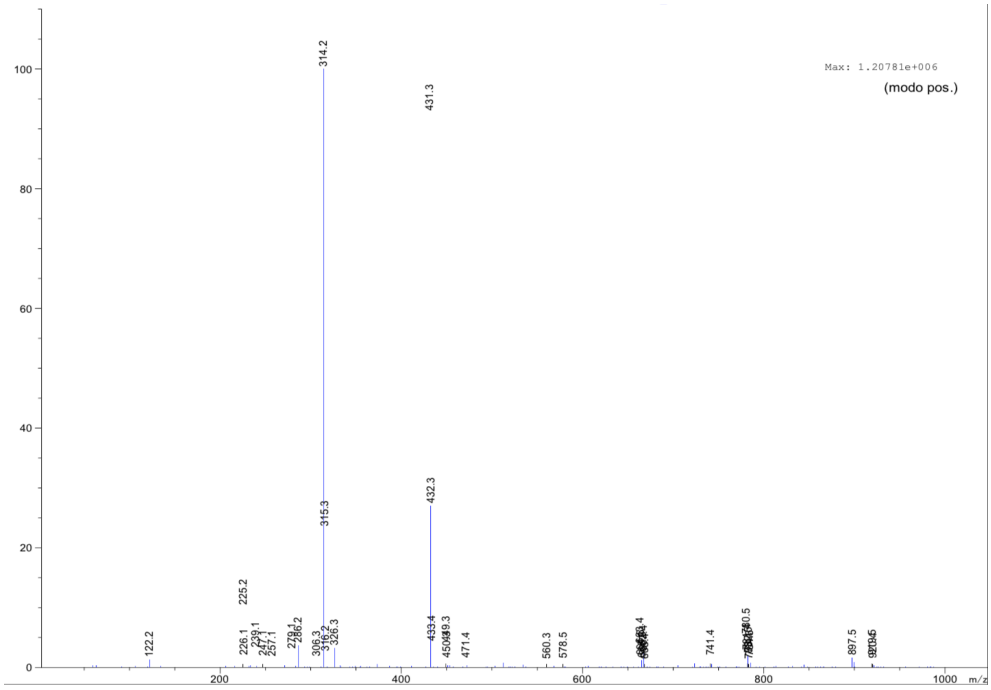

Figure 57 - Mass spectrum of benzylamine-fusidic acid (positive mode)

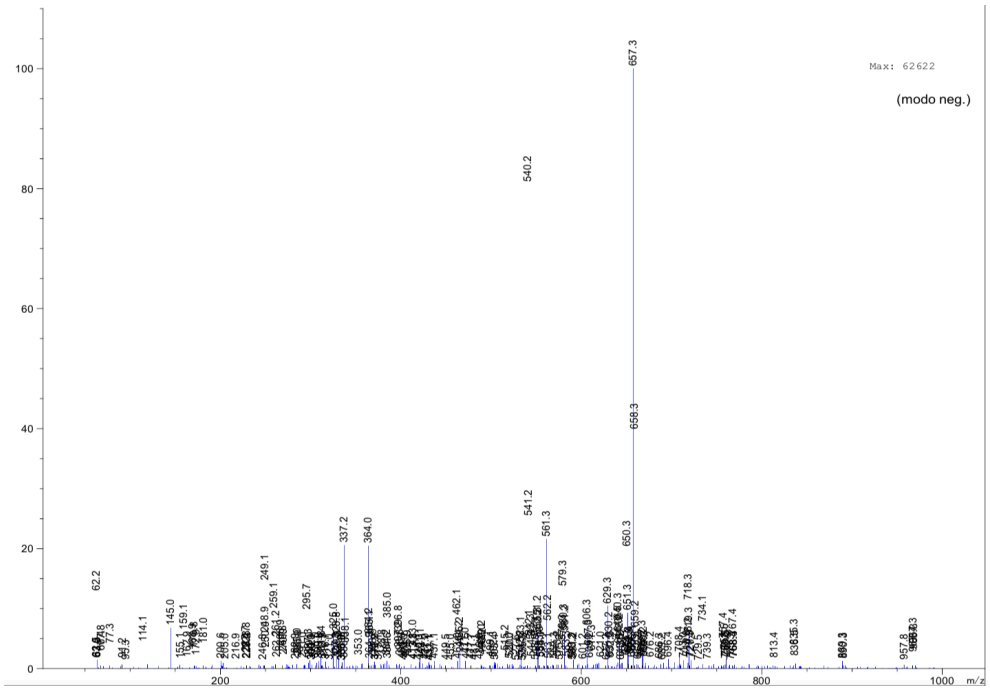

Figure 58 - Mass spectrum of benzylamine-fusidic acid (negative mode)

Benzylamine-fusidic acid (white powder): ^{1}H NMR (400 MHz, $CDCl_3$): δ 7.35 (d, 1H, J = 16.07 Hz), 7.33-7.28 (m, 4H), 6.09 (d, 1H, J = 7.46 Hz), 5.86 (d, 1H, J = 8.37 Hz), 5.76-5.72 (m, 2H), 5,62 (d, 1H, J = 9.29 Hz), 5.29 (s, 1H), 5.10-5.06 (m, 2H), 4.90 (s, 1H), 4.77 (d, 1H, J = 13.01 Hz), 4.59 (dd, 1H, J = 6.40, 14.44 Hz), 4.51 (s, 1H), 4.34 (s, 3H), 4.1210 (dd, 1H, J = 3.72, 13.95 Hz), 3.74-3.56 (m, 8H), 3.13-3.94 (m, 3H), 2.54-2.24 (m, 7H), 2.10-2.04 (ddd, 50H), 2.20-2.03 (m, 14H), 1.98 (s, 3H), 1.96 (s, 4H), 1.94 (d, 2H, J = 3.36 Hz), 1.91-1.80 (m, 16H), 1.74 (s, 13H), 1.66 (s, 5H), 1.55 (dt, 29H, J = 13.88, 24.64 Hz), 1.35 (d, 20H, J = 7.13 Hz), 1.27 (dd, 8H, J = 6.79, 14.05 Hz), 1.18-1.09 (m, 12H), 0.96 (s, 9H), 0.93-0.90 (dd, 18H, J = 5.05, 7.32 Hz) ppm; **^{13}C NMR (400 MHz, $CDCl_3$):** δ 173.12, 171.22, 170.85, 170.72, 157.72, 141.82, 137.77, 135.49, 132.54, 132.50, 129.77, 128.78, 128.10, 127.64, 123.28, 123.13, 74.41, 73.73, 73.35, 71.42, 68.30, 55.80, 50.69, 49.23, 48.72, 48.67, 44.16, 43.89, 43.24, 39.64, 39.48, 39.44, 39.26, 38.94, 37.04, 37.00, 36.27, 36.21, 36.13, 35.54, 32.72, 32.38, 32.30, 32.23, 30.22, 29.91, 29.40, 28.83, 28.43, 28.03, 25.71, 25.67, 25.15, 24.76, 24.48, 24.06, 22.85, 22.79, 21.08, 20.77, 20.68, 17.86, 17.80, 15.94 ppm; **MS (m/z):** 540.2, 657.3, 314.2 $[M+H]^+$, 431.3 $[M+H]^+$ Da.

Annex 6 – Spectral Data of PEtOx-FA

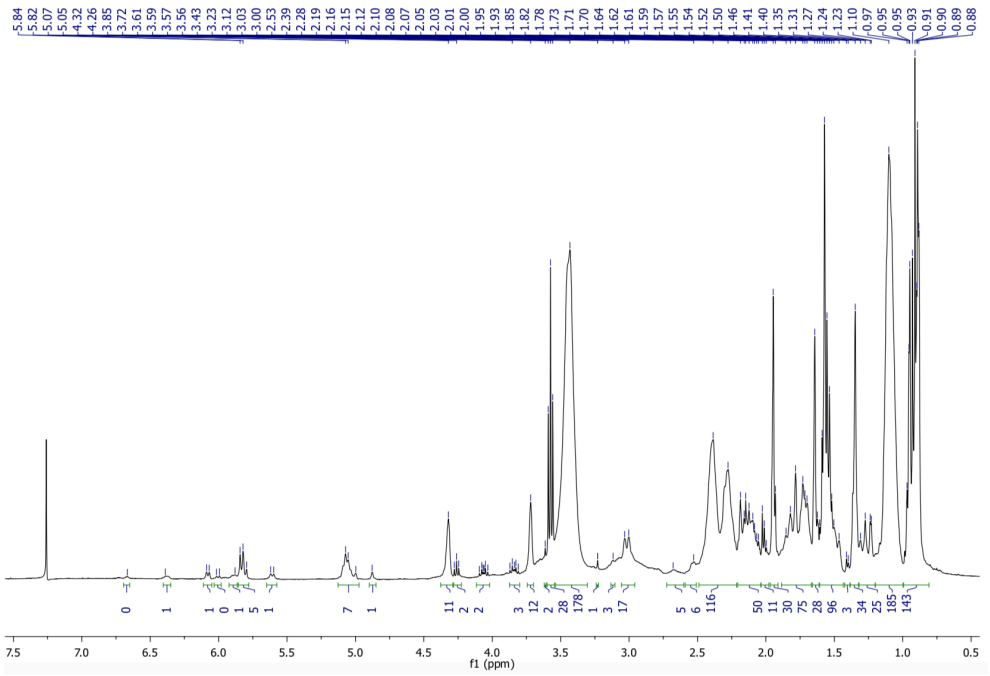

Figure 59 - ^{1}H NMR spectrum of PEtOx-FA in $CDCl_3$

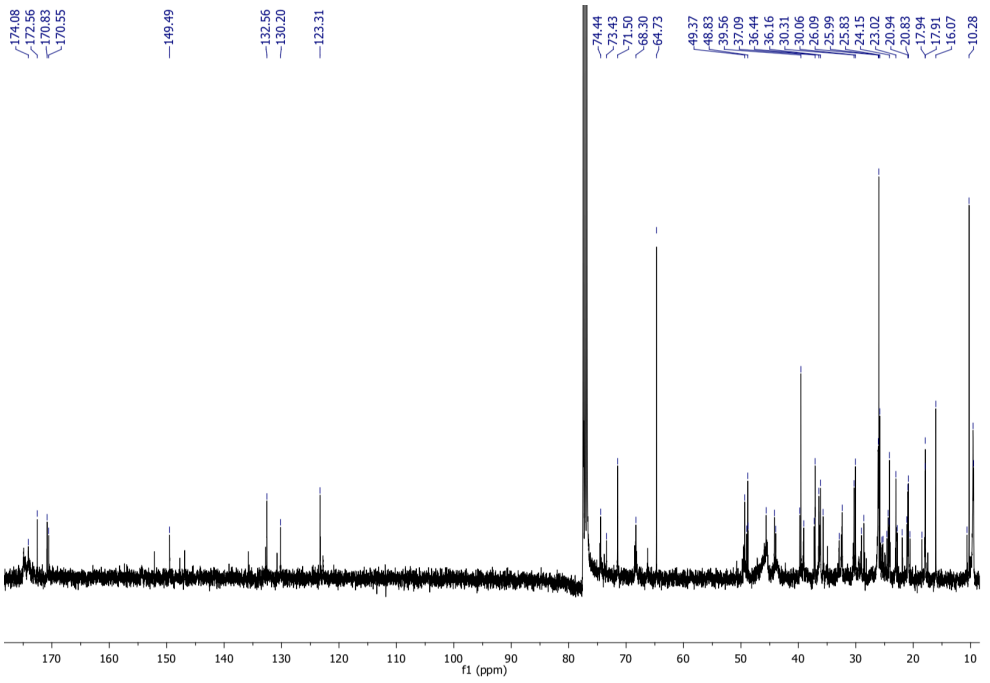

Figure 60 - ^{13}C NMR spectrum of PEtOx-FA in $CDCl_3$

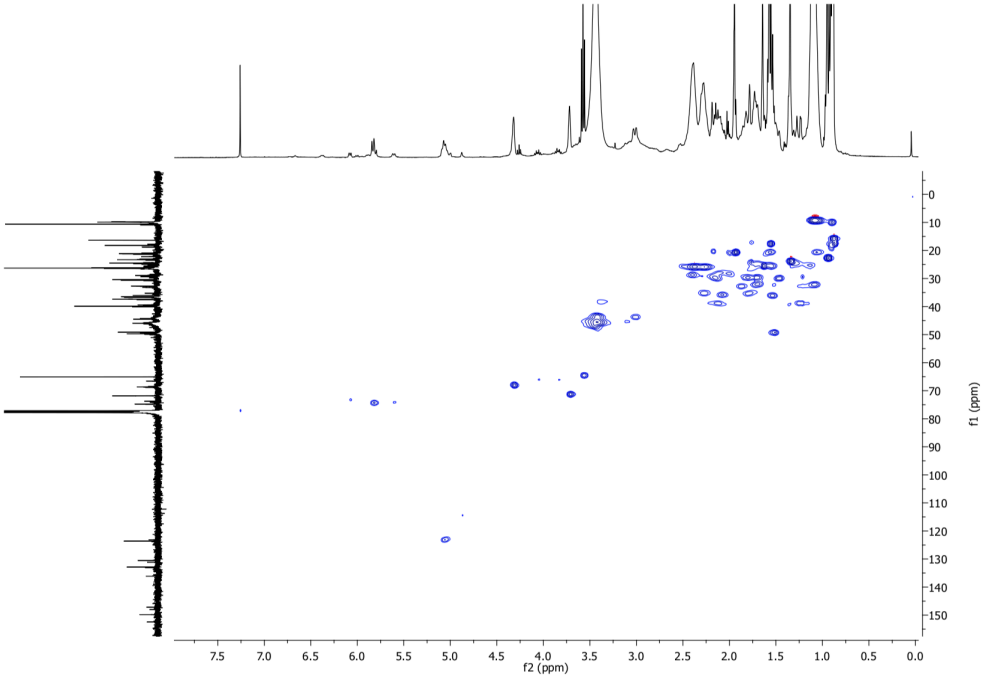

Figure 61 - HSQC spectrum of PEtOx-FA

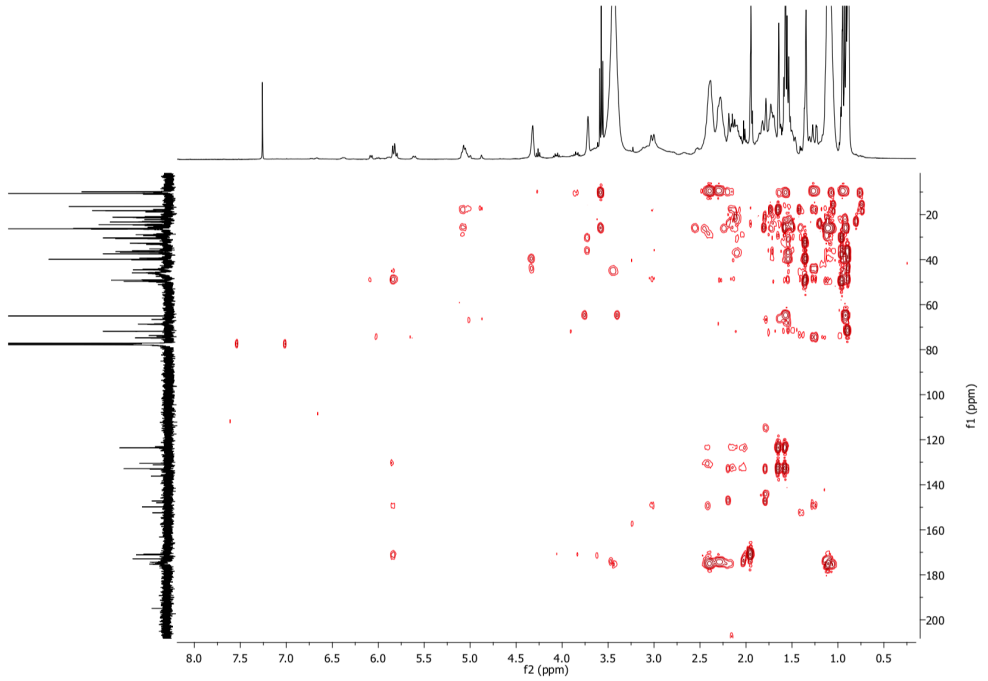

Figure 62 - HMBC spectrum of PEtOx-FA

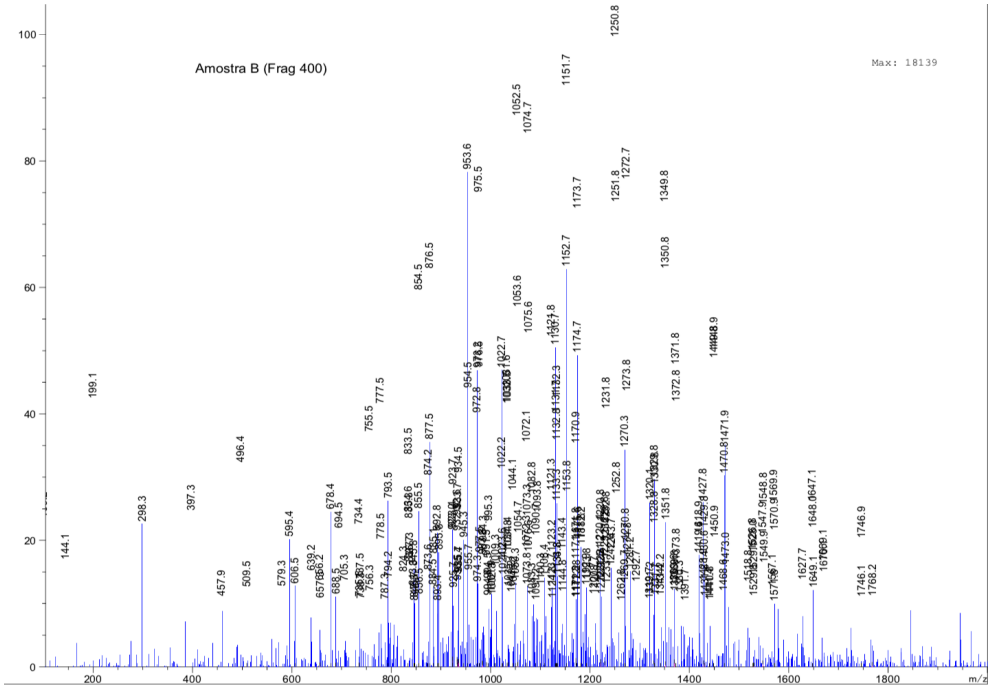

Figure 63 - Mass spectrum of PEtOx-FA (positive mode)

PEtOx-FA (clear yellow powder): ^{1}H NMR (400 MHz, $CDCl_3$): δ 6.35 (s, 1H), 6.08 (d, 1H, J = 7.67 Hz), 6.00 (d, 1H, J = 8.77 Hz), 5.88 (s, 1H), 5.82 (t, 5H, J = 9.42 Hz), 5.61 (d, 1H, J = 9.18 Hz), 5.07-5.00 (m, 7H), 4.88 (s, 1H), 4.32 (s, 11H), 4.26 (t, 2H, J = 6.66 Hz), 4.06 (dt, 2H, J = 6.98, 10.84 Hz), 3.85-3.83 (m, 3H), 3.72 (s, 12H), 3.61 (s, 2H), 3.57 (t, 28H, J = 6.67 Hz), 3.43 (bs, 178H), 3.23 (s, 1H), 3.12 (s, 3H), 3.02 (d, 17H, J = 11.70 Hz), 2.68 (s, 5H), 2.53 (s, 6H), 2.33 (d, 116H, J = 43.51 Hz), 2.10-2.04 (ddd, 50H, J = 8.37, 13.65, 16.71 Hz), 2.03-2.01 (m, 11H), 1.94 (d, 30H, J = 6.09 Hz), 1.85-1.70 (m, 75H), 1.63 (d, 28H, J = 7.83 Hz), 1.59-1.47 (m, 96H), 1.40 (d, 3H, J = 5.03 Hz), 1.34 (s, 24H), 1.31-1.23 (dd, 25H, J = 8.44, 23.26 Hz), 1.10 (bs, 158H), 0.97-0.88 (ddd, 143H, J = 4.75, 7.17, 11.49 Hz) ppm; **^{13}C NMR (400 MHz, $CDCl_3$):** δ 174.08, 172.56, 170.83, 170.55, 149.49, 132.56, 130.20, 123.31, 74.44, 73.43, 71.50, 68.30, 64.73, 49.37, 49.01, 48.83, 48.76, 45.61, 44.19, 43.95, 39.75, 39.56, 39.07, 37.25, 37.09, 36.44, 36.16, 35.70, 32.89, 32.37, 30.31, 30.06, 29.03, 28.61, 26.09, 25.99, 25.83, 24.15, 23.02, 20.94, 20.83, 18.49, 17.94, 17.91, 16.07, 10.64, 10.28, 9.59, 9.48 ppm;

Annex 7 – Spectral Data of PEG-FA

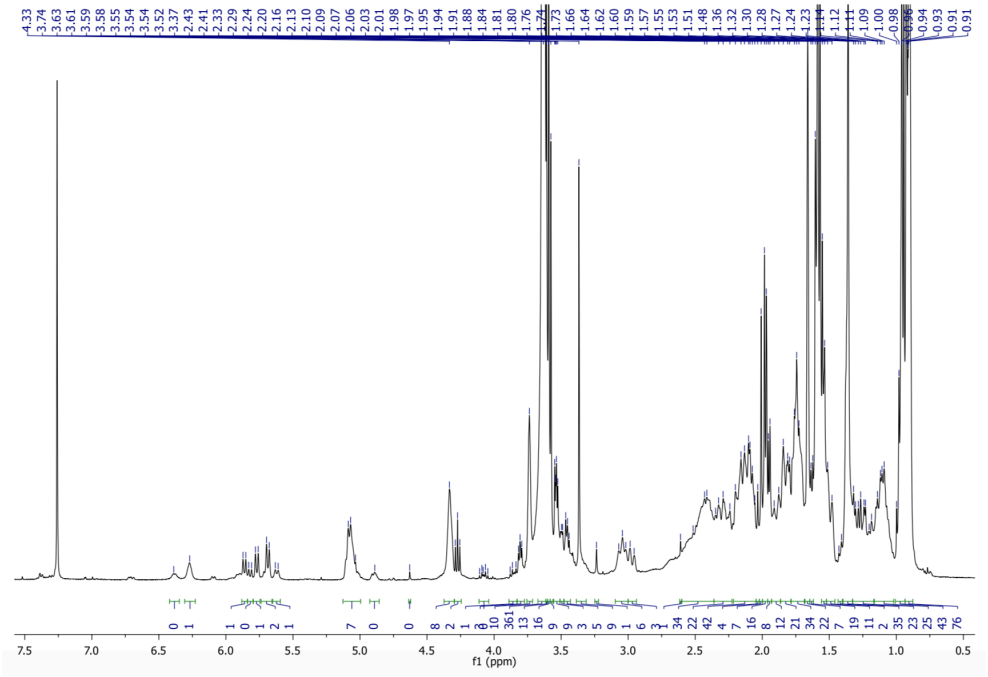

Figure 64 - ^{1}H NMR spectrum of PEG-FA in $CDCl_3$

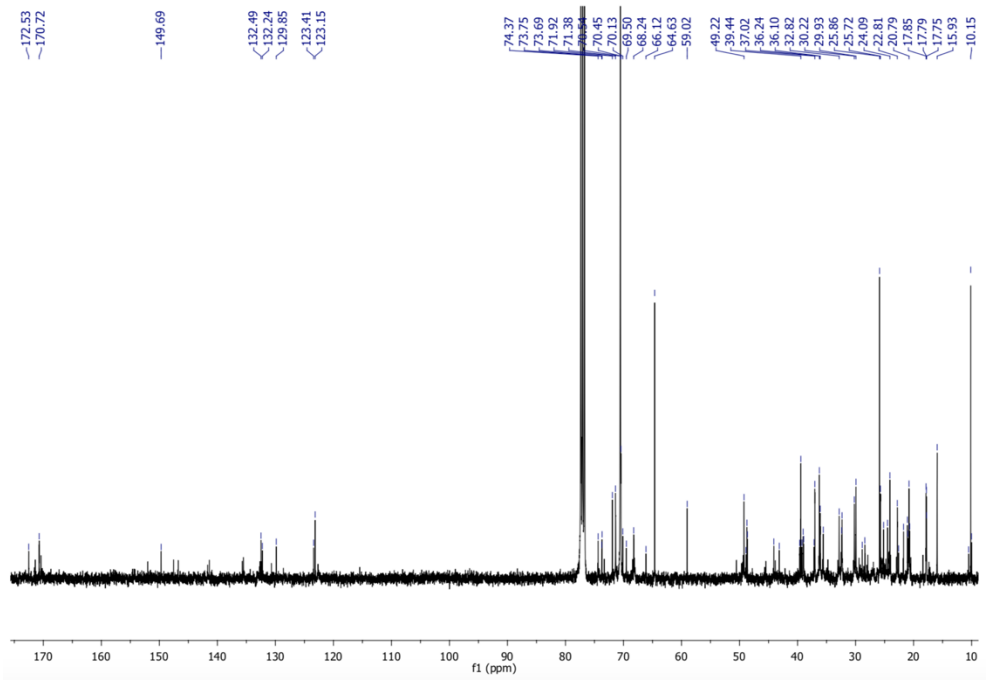

Figure 65 - ^{13}C NMR spectrum of PEG-FA in $CDCl_3$

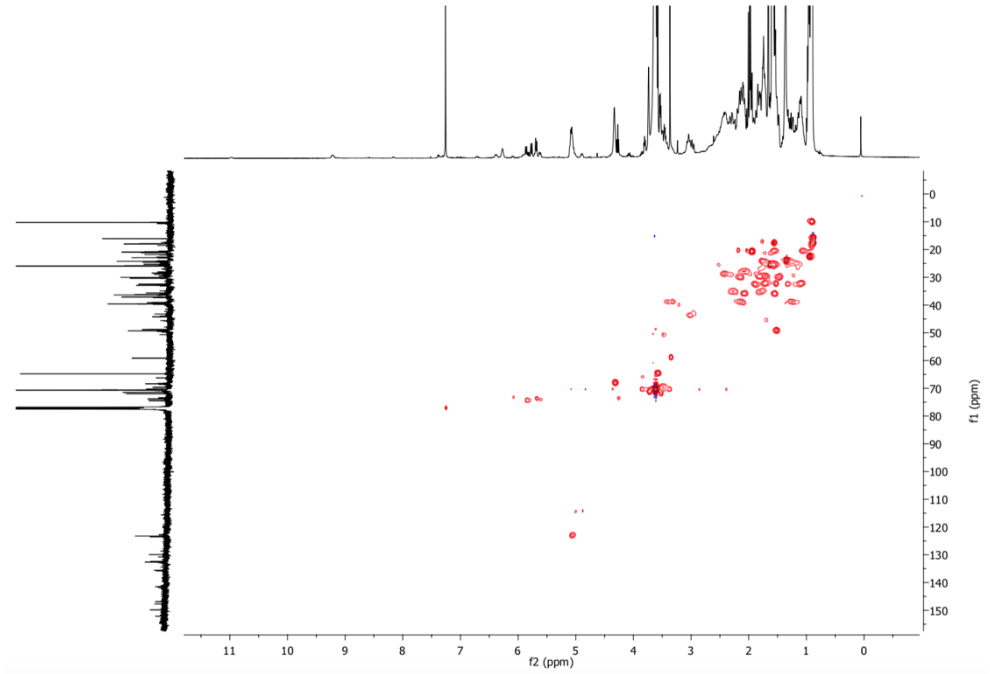

Figure 66 - HSQC spectrum of PEG-FA

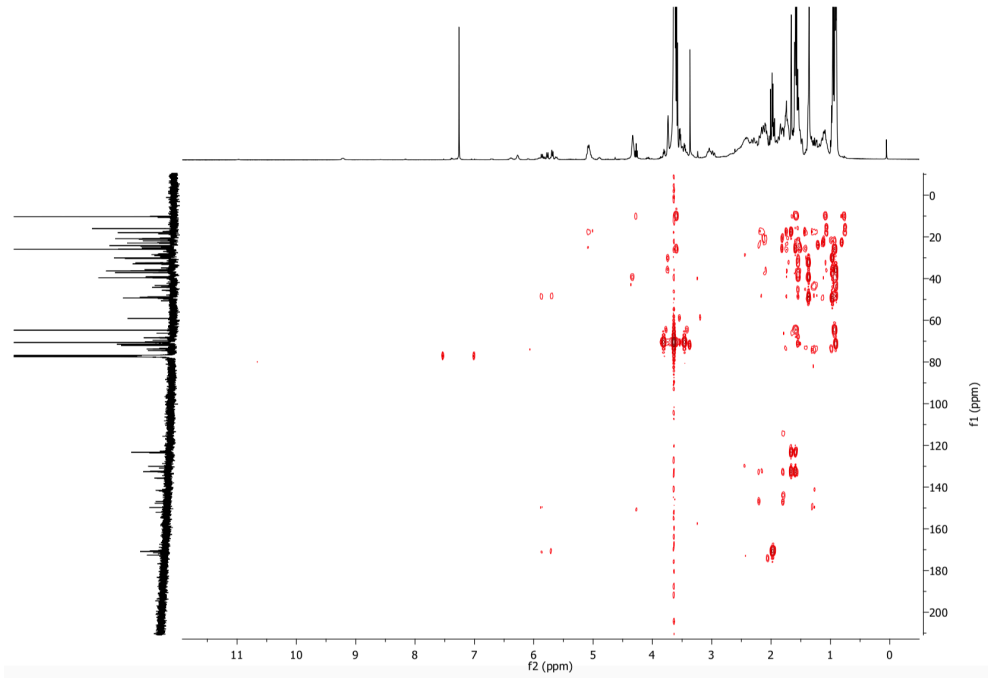

Figure 67 - HMBC spectrum of PEG-FA

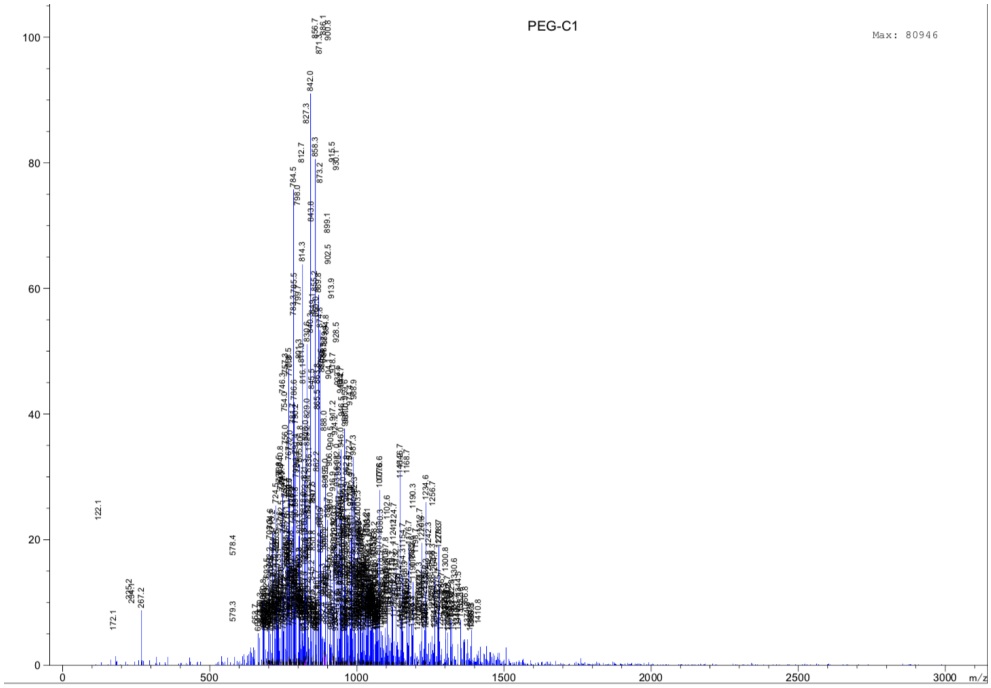

Figure 68 - Mass spectrum of PEG-FA (positive mode)

PEG-FA (yellow oil): ^{1}H NMR (400 MHz, $CDCl_3$): δ 6.27 (s, 1H), 5.86 (d, 1H, J = 8.33 Hz), 5.82 (d, 1H, J = 8.56 Hz), 5.77 (d, 1H, J = 8.22 Hz), 5.69 (d, 2H, J = 8.19 Hz), 5.62 (d, 1H, J = 8.46 Hz), 5.09-5.07 (d, 7H, J = 6.90 Hz), 4.89 (s, 1H), 4.33 (s, 8H), 4.27 (t, 2H, J = 6.66 Hz), 4.11-4.05 (m, 1H), 3.88-3.84 (m, 1H), 3.82-3.79 (m, 3H) 3.74 (bs, 10H), 3.63 (bs, 361H), 3.61 (bs, 13H), 3.59 (bs, 16H), 3.58 (bs, 9H), 3.54 (dd, 9H, J = 3.49, 5.79 Hz), 3.49 (d, 3H, J = 3.24 Hz), 3.47-3.43 (m, 5H), 3.37 (s, 9H), 3.24 (s, 1H), 3.07-3.02 (m, 6H), 2.97 (d, 3H, J = 11.91 Hz), 2.61 (s, 1H), 2.52-2.41 (d, 34H), 2.30 (dd, 22H, J = 14.64, 28.29 Hz), 2.16-2.06 (m, 42H), 2.03 (s, 4H), 2.01 (s, 7H), 1.98 (d, 16H, J = 5.64 Hz), 1.95 (d, 8H, J = 5.05 Hz), 1.89 (d, 12H, J = 13.76 Hz), 1.84-1.81 (m, 21H), 1.76-1.71 (m, 34H), 1.66 (s, 22H), 1.63 (d, 7H, J = 5.28 Hz), 1.59 (t, 58H, J = 6.99 Hz), 1.54 (d, 18H, J = 6.87 Hz), 1.50 (d, 11H, J = 12.82 Hz), 1.42 (d, 2H, J = 7.64 Hz), 1.36 (s, 36H), 1.25 (ddd, 23H, J = 6.40, 16.16, 32.42 Hz), 1.11 (dd, 25H, J = 7.71, 12.35 Hz), 0.97 (dd, 43H, J = 6.69, 14.72 Hz), 0.93-0.91 (m, 76H) ppm; **^{13}C NMR (400 MHz, $CDCl_3$):** δ 172.53, 170.73, 149.66, 132.49, 130.24, 129.85, 123.41, 123.15, 74.37, 73.75, 73.69, 71.92, 71.38, 70.54, 70.45, 70.13, 69.50, 68.24, 66.12, 64.63, 59.02, 49.22, 48.83, 48.89, 48.72, 48.64, 44.09, 43.15, 39.63, 39.44, 39.25, 39.03, 38.94, 37.16, 37.02, 36.24, 36.10, 35.55, 32.82, 32.39, 32.32, 30.22, 29.93, 28.85, 28.41, 25.86, 25.72, 25.17, 24.49, 24.09, 22.81, 22.59, 21.73, 21.06, 20.99, 20.79, 20.67, 17.85, 17.79, 17.75, 15.93, 10.64, 10.52, 10.15, 10.02 ppm;

Annex 8 – ACI Mesuaments of all the DPF

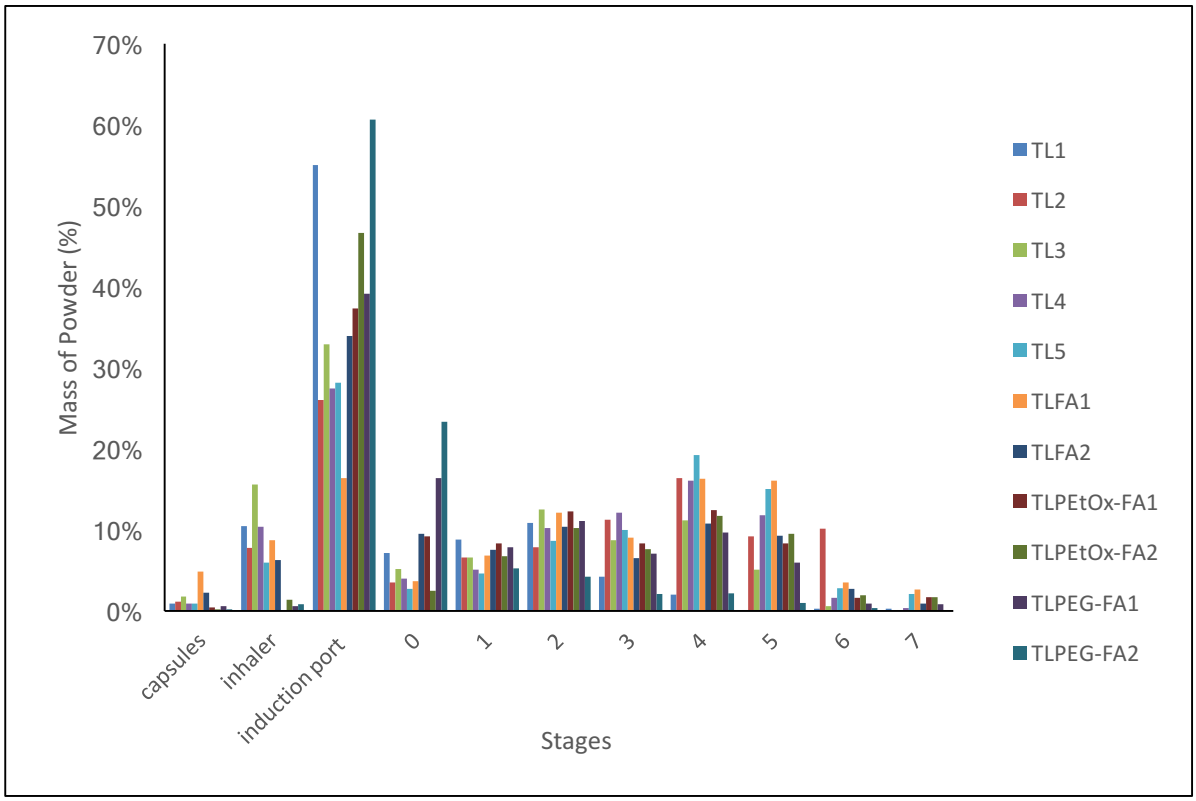

Figure 69 - Graphical representation of the powder distribution in the ACI stages for all DPF

Table 11 - Aerodynamic properties of all DPFs, determined by ACI and DUSA

Assay		FPF (%)	EF (%)	MMAD (µm)	GSD
1	TL	20.1	99.1	4.31	1.60
2		56.9	98.9	1.76	2.79
3		40.0	98.3	3.10	2.04
4		53.6	99.1	1.99	2.10
5		59 ± 1	99.0 ± 0.1	1.48 ± 0.38	2.25 ± 0.01
6	TLFA	61.7 ± 0.2	97.8 ± 2.3	1.64 ± 0.09	2.38 ± 0.02
7		42.7	97.8	2.93	2.64
8	TLPEtOx-FA	43 ± 4	99.3 ± 0.3	3.15 ± 0.13	2.48 ± 0.06
9		44.5	99.8	2.09	2.32
10	TLPEG-FA	35 ± 2	99.3 ± 0.1	3.85 ± 0.05	2.34 ± 0.02
11		10.9	99.8	6.88	1.53

Annex 9 – Additional Spectral Data (FT-IR)

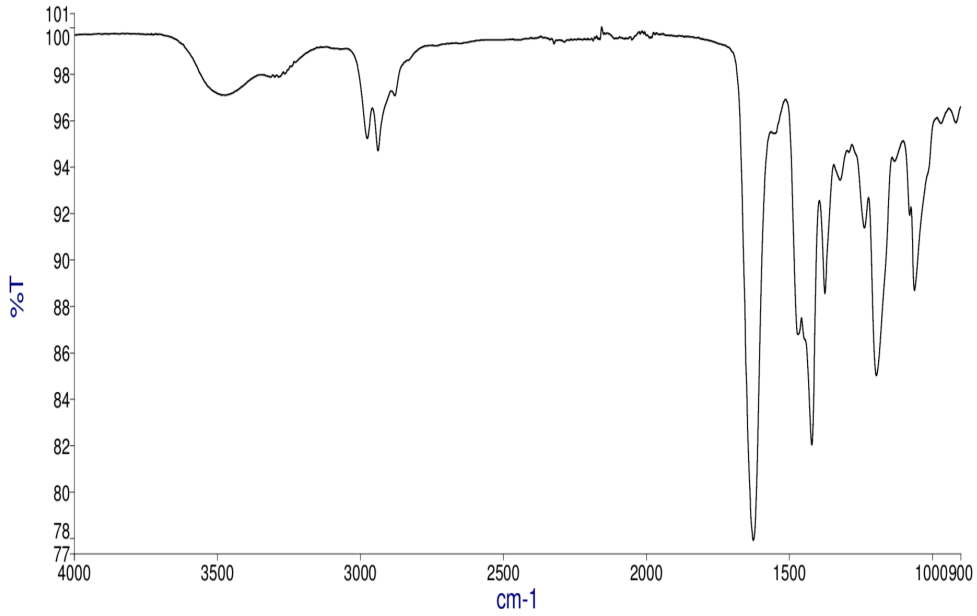

Figure 70 - FT-IR of PEtOx-NH_2

PEtOx-NH_2 (yellow oil): IR (ATR): 3474 (N–H *stretching* of amine group), 2939 (C–H *stretching* of ethyl group), 1626 (C=O *stretching* of the amide group), 1375 (C–H *stretching* of methylene groups) cm^{-1}.

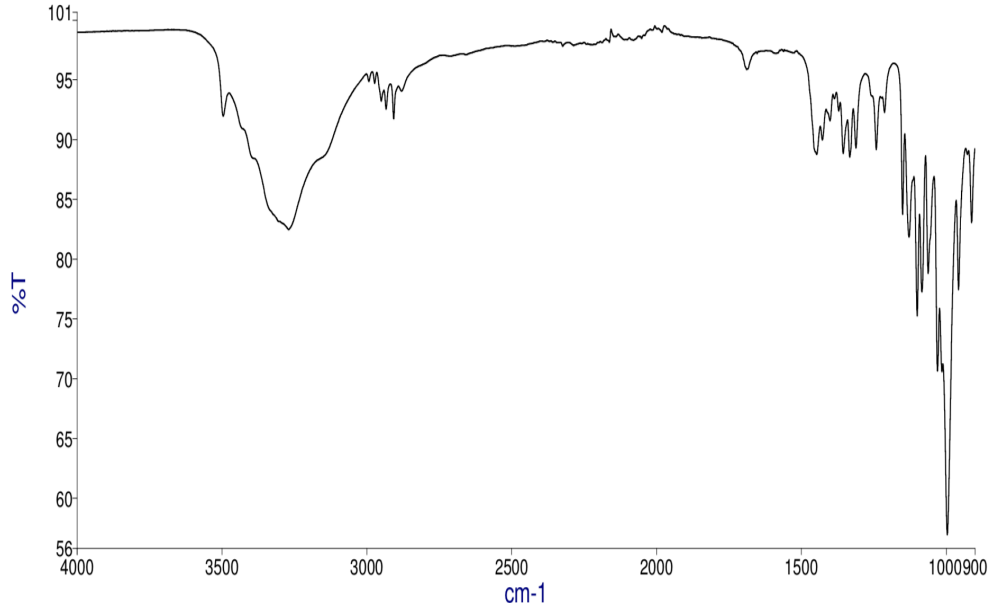

Figure 71 - FT-IR of trehalose

Trehalose (white powder): IR (ATR): 3271 (O–H *stretching* of hydroxyl), 1028/995 (C–O *stretching* of hydroxyl) cm^{-1}.

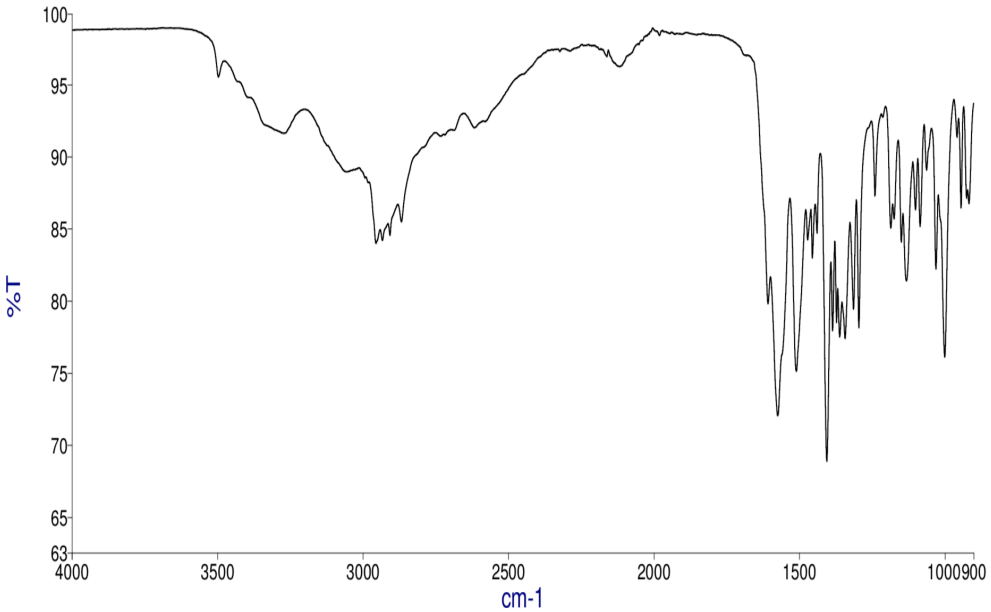

Figure 72 - FT-IR of leucine

L-leucine (white powder): IR (ATR): 3056 (NH_3^+ *stretching*), 2957 (C–H *stretching* of methyl), 1574 (C=O *stretching*), 1607/1510 (NH_3^+ *deformation*) cm^{-1}.

Annex 10 – Quantification Data of Fusidic Acid

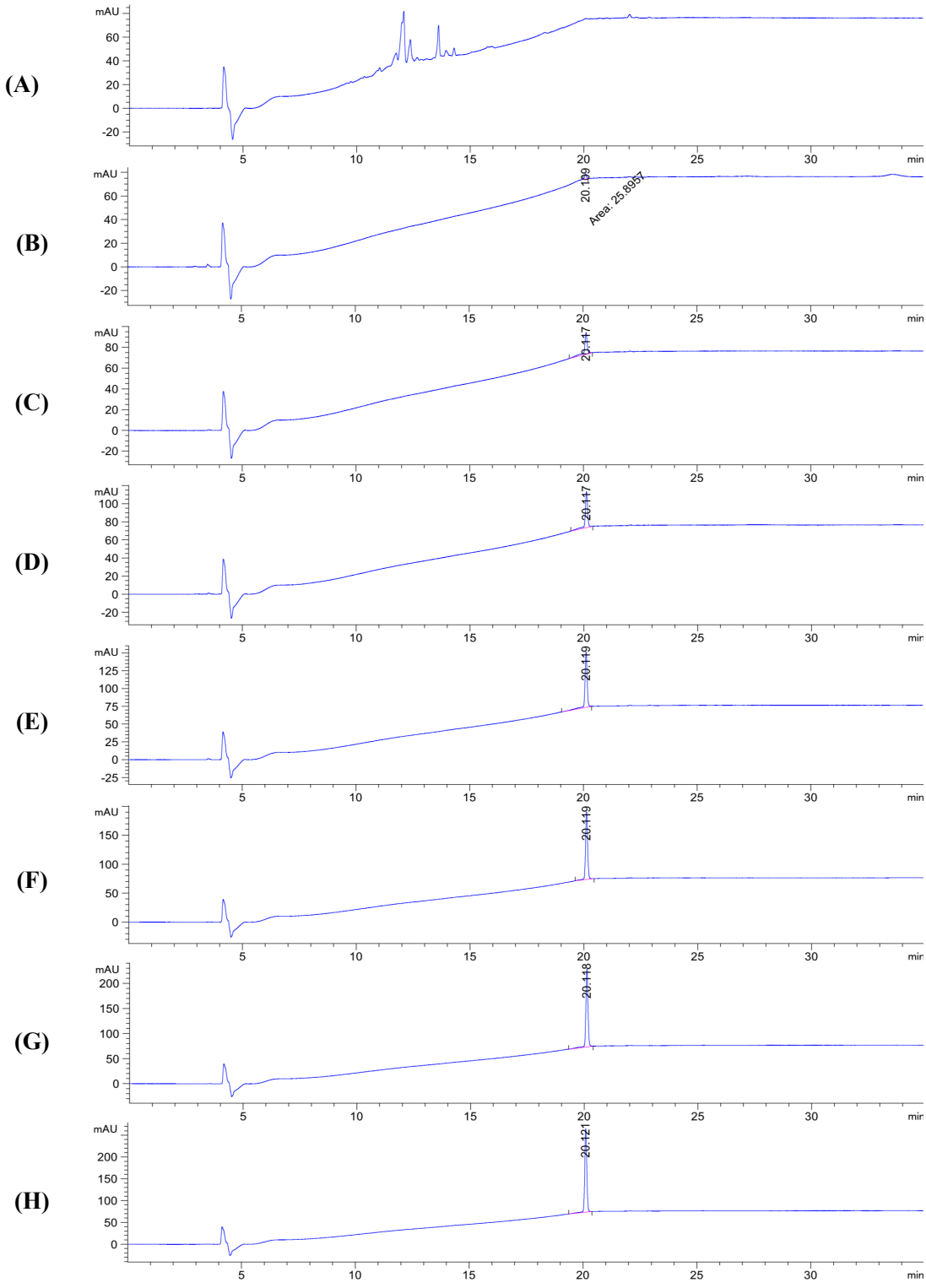

Figure 73 – Chromatogram profile at λ= 240 nm of fusidic acid solutions: (A) 0, (B) 1.103, (C) 5.064, (D) 10.128, (E) 20.256, (F) 30.384, (G) 40.512 and (H) 50.64 mg/l

Table 12 - Experimental data for the calibration line

Fusidic Acid Concentration (mg/l)	Retention time (min)	Peak Area
0	----	0
1.013	20.109	26
5.064	20.117	173
10.13	20.117	288
20.26	20.119	537
30.38	20.119	754
40.51	20.118	1008
50.64	20.212	1233

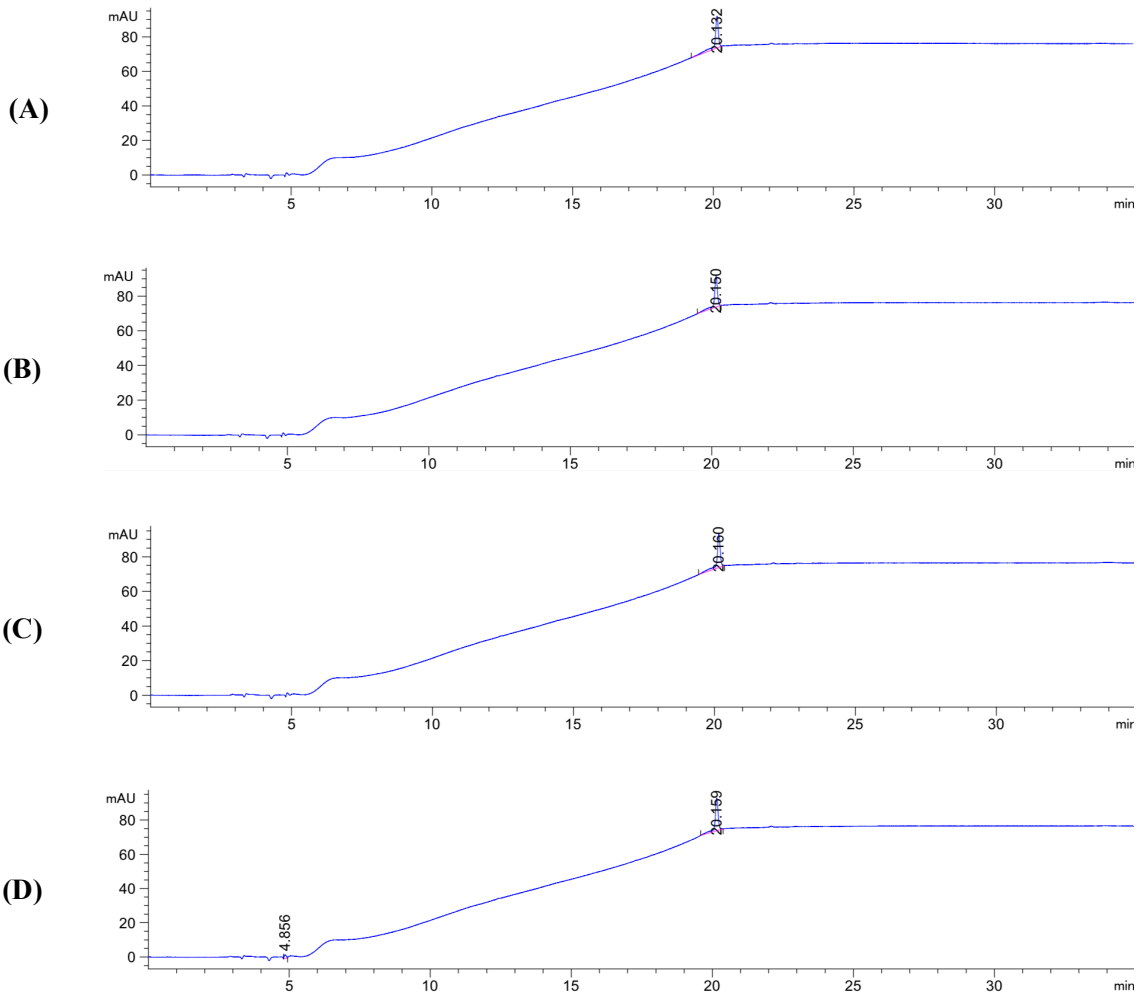

Figure 74 - Chromatogram profile at λ= 240 nm of sample solutions: (A) and (B) TLFA1; (C) and (D) TLFA2

Table 13 - Sample data for quantification

Sample	Retention time (min)	Peak Area
TLFA1	20.132	151
TLFA1 (B)	20.150	139
TLFA2	20.160	154
TLFA2 (B)	20.156	142